EVALUATION OF SENSITIVITY OF METU GAIT ANALYSIS SYSTEM

A THESIS SUBMITTED TO
THE GRADUATE SCHOOL OF NATURAL AND APPLIED SCIENCES
OF
MIDDLE EAST TECHNICAL UNIVERSITY

BY

PINAR KAFALI

IN PARTIAL FULFILLMENT OF THE REQUIREMENTS
FOR
THE DEGREE OF MASTER OF SCIENCE
IN
MECHANICAL ENGINEERING

MAY 2007

Approval of the Graduate School of Natural and Applied Sciences

_____

Prof. Dr. Canan Özgen
Director

I certify that this thesis satisfies all the requirements as a thesis for the degree of Master of Science.

_____

Prof. Dr. S. Kemal İder
Head of Department

This is to certify that we have read this thesis and that in our opinion it is fully adequate, in scope and quality, as a thesis for the degree of Master of Science.

_____   _____
Prof. Dr. S. Turgut Tümer   Asst. Prof. Dr. Ergin Tönük
Co-Supervisor   Supervisor

Examining Committee Members

Prof. Dr. M. Kemal Özgören   (METU, ME)   _____

Asst. Prof. Dr. Ergin Tönük   (METU, ME)   _____

Prof. Dr. S. Kemal İder   (METU, ME)   _____

Prof. Dr. Reşit Soylu   (METU, ME)   _____

Asst. Prof. Dr. Senih Gürses   (METU, ES)   _____

I hereby declare that all information in this document has been obtained and presented in accordance with academic rules and ethical conduct. I also declare that, as required by these rules and conduct, I have fully cited and referenced all material and results that are not original to this work.

Name, Last name : Pınar Kafalı

Signature   :

ABSTRACT

EVALUATION OF SENSITIVITY OF METU GAIT ANALYSIS SYSTEM

Kafalı, Pınar

M.Sc., Mechanical Engineering Department

Supervisor : Asst. Prof. Dr. Ergin Tönük
Co-Supervisor : Prof. Dr. S. Turgut Tümer

May 2007, 196 pages

Gait analysis is one of the primary applications of biomechanics and deals with scientific description of human locomotion, which is a qualitative concept as observed through the human eye. METU Gait Analysis Laboratory has been operating in various fields of gait and motion analyses since 1999. Although several studies have previously been undertaken about METU Gait Analysis System, until now, the effects of methodology and protocol related system parameters on kinematic analysis results have not been fully and exhaustively investigated.

This thesis presents an assessment on sensitivity and compatibility of METU Gait Analysis Protocol to variations in experimental methodology and implementation of various joint center estimation methods, performed through investigation of the resulting joint kinematics. It is believed that the performance and reliability of METU Gait Analysis System will be improved based on the findings of this study.

Keywords: Gait Analysis, Hip Joint Center, Knee Joint Center

ÖZ

ODTÜ YÜRÜYÜŞ ANALİZİ SİSTEMİNİN HASSASİYETİNİN DEĞERLENDİRİLMESİ

Kafalı, Pınar

Yüksek Lisans, Makina Mühendisliği Bölümü

Tez Yöneticisi   : Y. Doç. Dr. Ergin Tönük
Ortak Tez Yöneticisi : Prof. Dr. S. Turgut Tümer

Mayıs 2007, 196 sayfa

Yürüyüş analizi ana biyomekanik uygulamalarından biridir ve insan gözüyle bakıldığında nitel bir kavram olan insan yürüyüşünün bilimsel olarak açıklanmasıyla ilgilenir. ODTÜ Hareket Analizi Laboratuvarı yürüyüş ve hareket analizi alanlarında 1999 yılından bu yana çalışmaktadır. ODTÜ Hareket Analiz Sistemi'yle ilgili daha önce çeşitli çalışmalar yapılmış olmasına karşın, şimdiye kadar, sistemde kullanılan protokol ve metodolojiyle ilgili parametrelerin kinematik analiz sonuçlarına etkisi tam ve ayrıntılı olarak incelenmemiştir.

Bu tez, ODTÜ Hareket Analiz Protokolü'nün deneysel metodolojideki farklılıklar ve çeşitli eklem merkezi tahmin metodlarına gösterdiği hassasiyet ve uyum üzerine, elde edilen eklem kinematiği sonuçlarının incelenmesi yoluyla gerçekleştirilmiş bir değerlendirme sunmaktadır. Bu çalışmadan elde edilen sonuçlara dayalı olarak ODTÜ Hareket Analizi Sistemi'nin performans ve güvenilirliğinin artırılabileceğine inanılmaktadır.

Anahtar kelimeler: Yürüyüş Analizi, Kalça Eklem Merkezi, Diz Eklem Merkezi

To My Family

ACKNOWLEDGEMENTS

TABLE OF CONTENTS

LIST OF TABLES

TABLES

LIST OF FIGURES

FIGURES

xvi

CHAPTER 1

INTRODUCTION

Understanding human movement has been a subject that raised great interest of mankind since ancient times. Primarily being limited to qualitative observations, human motion studies have undergone a great progress throughout the decades in parallel with advances realized in technology. Today, qualitative and quantitative human movement analysis has become an important tool for identification of motion characteristics in humans, as well as providing aid in relevant clinical diagnosis and decision making situations.

1.1 Gait Analysis

Gait analysis deals with the scientific description of human locomotion, which is a qualitative concept as observed through the human eye. Davis (1988) defines gait analysis as "the systematic measurement, description, and assessment of those quantities thought to characterize human locomotion"; referring to a process in which kinematic and kinetic data are acquired, measured and analyzed, and from which an assessment is performed by means of interpretation of the obtained gait parameters.

According to Whittle (2002), the first study of human locomotion with a truly scientific approach was presented by Borelli in De Motu Animalum (1682), who estimated center of mass of the body and described how balance is maintained during walking. Later in 1867, Duchenne described functions of individual muscles of the human body in Physiologie des Mouvements, which is regarded as the first systematic evaluation of muscle functions (Banta, 1999). In 1836, the Weber Brothers reported the first quantitative study regarding

temporal and distance parameters of human locomotion (Andriacchi and Alexander, 2000). Pioneers of kinematic measurement, Marey (1873) and Muybridge (1887), employed photographic techniques to present human movement patterns (as cited in Whittle, 2002). In 1895, Braune and Fischer published Der Gang des Menschen. They placed fluorescent lights on limbs and determined three-dimensional trajectory, velocity and accelerations of segments as well as forces acting on the body during gait (Whittle, 2002). In the 20th century, progress in gait analysis studies was achieved further through implementation of force plates, and electromyography (EMG) measurements into kinematic data acquisition systems.

Improvements realized in data acquisition and processing technologies over the past few decades have transformed gait analysis, which was initially research-oriented due to technical limitations, into a tool that is utilized progressively more in clinical environment today. Clinical gait analysis provides an assisting method in applications such as diagnosis and monitoring of pathologies like cerebral palsy, spina bifida and neuromuscular disorders; in addition to development of orthoses and prostheses, clinical decision making and treatment planning activities. Gait research remains to be an important part of gait analysis studies, improving insight into mechanisms of normal and pathological gait with its outputs being utilized in a large variety of applications ranging from modeling and simulation of gait to clinical studies (Andriacchi and Alexander, 2000; Pandy, 2001; Simon, 2004; Baker, 2006; Best and Begg, 2006).

1.2 Gait Analysis Terminology

1.2.1 Gait Cycle

Human locomotion is realized through successive interchanging sequences of right and left limb movements. Gait cycle is defined as the single sequence of functions performed by one limb during gait (Perry, 1992). Due to cyclic nature of walking, any two successive identical events performed by the same limb can designate initiation and termination of the gait cycle. In general clinical practice, however, gait cycle is defined based on heel strike (initial contact) events since they are more easily identifiable, with the aid of force plates, compared to other events of gait.

Each gait cycle consists of two main periods, namely, stance and swing. Stance denotes the interval where foot is in contact with the ground, starting with initial contact and ending with toe-off. In stance period, foot contact with the ground provides the support needed during forward movement of the remaining limb. The term toe-off is employed to indicate the instance when foot leaves the ground, which is the beginning of swing period for the foot. The limb progresses forward during swing period and finally foot contacts the ground again (second heel strike) which completes one gait cycle. Stance and swing periods constitute approximately 60% and 40% of the gait cycle in a normal gait pattern.

Stance and swing periods can further be divided into subgroups. The interval where both feet are on the ground is termed as double support period, which occurs twice in the gait cycle, one in the beginning (initial double stance) and one in the end (terminal double stance) of the cycle. Single support period covers the interval when only one foot is in contact with the ground, which corresponds to swing phase of the other limb (Figure 1.1).

3
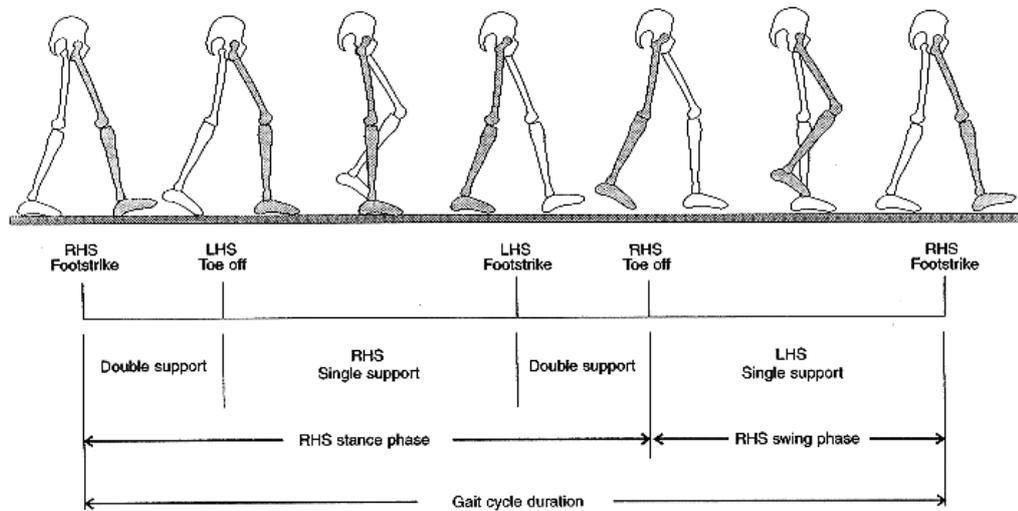
Figure 1.1 Gait Cycle (Adapted from Gill et al., 1997)

1.2.2 Phases of Gait

The stance period is divided into five phases as initial contact, loading response, midstance, terminal stance and preswing (Perry, 1992). Stance begins with initial contact of the foot on the ground. Loading response phase comprises initial double-limb support period, during which body weight is transferred fully onto the stance limb. Midstance and terminal stance phases comprise single limb support period. Midstance begins with toe-off of the opposite foot and continues until body weight is aligned over the forefoot. Terminal stance is initiated and terminated by heel rise of the stance limb and initial contact of the swing limb on the ground, respectively. Body weight moves head of the forefoot within this period. The final phase of stance period, preswing phase, is the terminal double stance period; beginning with initial contact of opposite foot and ending with toe-off of the stance limb. Weight is transferred onto the opposite foot in this phase of gait cycle.

4

Swing period is comprised of three phases, namely initial swing, midswing and the terminal swing phases. Initial swing phase begins with toe-off and continues until maximum knee flexion. Midswing phase starts at this instant, and ends when tibia becomes vertical. In the final phase, which is the terminal swing, limb advancement takes place until second foot contacts the ground.

1.2.3 Temporal Gait Parameters

Temporal parameters such as stride length, step length, cadence and speed enable quantitative assessment of characteristics of human gait, together with kinematic and kinetic parameters (i.e. joint angles, moments and powers).

Stride length is defined as the distance traveled between two successive heel strikes of the foot. Stride period or cycle is the period of time elapsed between these two successive gait events. Commonly misused in place of stride length, step length is the distance between successive floor contacts of originating and opposite feet. Step period, again, is the time elapsed between these two events. Another parameter, cadence, is used to denote the number of steps taken per minute. Finally, average speed defines the rate of change of forward progression with time (Whittle, 2002).

1.3 Gait Analysis Systems

A typical gait analysis system performs three main types of measurements: Motion data of the subject is recorded via a motion measurement system; ground reaction forces and moments are recorded by force plates, and an electromyography (EMG) unit is utilized for acquisition of muscle activation information. Diverse equipments have been employed in human movement analysis applications; which include footswitches, electrogoniometers,

gyroscopes, accelerometers, force platforms and pressure mats for acquisition of temporal, spatial and kinetic data during experiments (Best and Begg, 2006).

Most clinical gait analysis systems employ light-reflecting passive markers attached on the skin, which are tracked by cameras for acquisition of 3-D movement information of body segments. Force platforms are used for measurement of ground reaction forces and moments, as well as providing aid in determination of gait events. Temporal gait parameters, joint kinematics and joint kinetics are then calculated from motion data and force measurements via utilization of biomechanical models.

Biomechanical models employed by gait analysis systems define lower extremities as an open chain of rigid segments, connected by joints with 1 to 5 degrees of freedom. Reference frames that are constructed from three non-collinear markers on each segment are employed for estimation of instantaneous segment positions and orientations in space. These segmental reference frames can be divided into two main groups as technical and anatomical reference frames. Technical frames are constructed from markers that are specifically positioned to comply with technical requirements such as visibility to cameras, being located sufficiently distant from each other and minimization of relative movement between them and the bony segment; and need not have any repeatable reference to the segment morphology (Cappozzo et al., 2005). Anatomical reference frames, on the other hand, are defined in compliance with the anatomy of the segment; their planes approximating sagittal, transverse and frontal planes. Since these frames are utilized in joint kinematics calculations, their construction in a repeatable manner is important for reliability of the calculations.

Anatomical landmarks that cannot be identified by direct marker placement due to technical and morphological limitations are located via anatomical

landmark calibration (Cappozzo, 1984; Cappozzo et al., 1995). This procedure basically involves determination of anatomical landmarks which are not directly accessible with respect to a group of markers that are more easily identifiable. In general the instrumentation (i.e. centering devices, wands, etc.) employed for anatomical landmark calibration do not permit their application to walking, therefore two separate trials are performed. In the static trial, desired anatomical landmarks are located relative to segment technical frames. Relative position between located point and the technical reference frame is assumed to be constant at all times since segments are modeled as rigid. Then, desired anatomical landmarks are re-located in dynamic (gait) trial relative to the technical frames constructed from technical markers.

1.4 Motivation and Scope

Middle East Technical University (METU) Gait Analysis Laboratory has been operating in various fields of gait and motion analyses since 1999. Several studies on METU Gait Analysis System have been performed in past years. However, until now, effects of methodology and protocol related system parameters on kinematic analysis results have not been fully and exhaustively investigated.

This thesis aims to evaluate the sensitivity and compatibility of METU Gait Analysis protocol, **Kiss** (**Ki**nematic **S**upport **S**ystem/**K**as **İs**kelet **S**istemi) to variations in experimental methodologies and implementation of various joint center estimation methods to the analysis protocol, by means of an investigation on joint kinematics results provided by the system. It is further aimed to investigate the relationship between the selected joint center estimation methods through this thesis work. It is believed that enhancements in system performance and reliability can be realized in the light of the results obtained from this study.

7

1.5 Outline

Chapter 1 gives the introduction to this thesis, presenting scope and motivation of the study as well as a brief discussion on gait analysis applications and systems.

Chapter 2 presents a survey of literature regarding estimation of hip and knee joint centers, in addition to previous studies performed at METU Gait Analysis Laboratory.

Chapter 3 presents a discussion on METU Gait Analysis System. Laboratory hardware and software are presented, and the standard experimental protocol of Kiss is explained from the performer point of view.

In **Chapter 4**, current joint kinematics calculation procedure of METU Gait Analysis System is presented. Kinematic analysis procedure is explained in steps, and results of the re-generated computer code for kinematic analysis calculations are compared to results of Kiss-GAIT software.

In **Chapter 5**, an assessment of effects of thigh and shank marker relocation on resulting joint kinematics is performed. Theoretical background is presented together with the experimental procedure, and a discussion on resulting joint kinematics is presented.

Performances of various hip and knee joint center estimation methods in Kiss protocol are investigated in **Chapter 6**, through adaptation of these methods in the system. Algorithms of each employed method, as well as the experimental procedures are presented. Effects of these adapted methods on joint kinematics results are also discussed.

Chapter 7 presents a brief summary of the thesis work and conclusions derived from results obtained in the study. Several suggestions for future research are also presented in this chapter.

CHAPTER 2

LITERATURE SURVEY

2.1 Joint Center Estimation Methods

Estimation of internal anatomical landmarks from surface marker locations constitutes an important part of gait analysis calculations. Joint centers have special importance since they are directly employed in anatomical reference frame construction; therefore joint kinematics and kinetics are directly influenced from locations of estimated joint centers (Della Croce et al., 2005).

2.1.1 Hip Joint Center Estimation Methods

Among all other joint centers, hip joint center estimation methods receive special attention in literature; since accurate and precise estimation of the hip joint center is critical in terms of error propagation to joint kinematics and kinetics (Kadaba, 1990; Stagni et al., 2000; Della Croce et al., 2005).

Two major approaches are adopted in literature for estimation of hip joint centers from surface marker coordinates. First method is the predictive approach, which employs anthropometric and pelvis measurements taken from subjects together with regression equations obtained from a number of either radiologic or cadaveric studies, to estimate hip joint center coordinates.

Bell et al. (1989) proposed a method that combined two previous approaches of Andriacchi et al. (1980) and Tylowski, reporting hip joint center could be predicted in adults within 2.6 cm of true joint center location. One year later, Bell et al. revised the method by locating hip joint center from ASIS by 30%

distal, 14% medial and 19% posterior of inter-ASIS distance; estimating hip joint center approximately 1.5 cm from true location (Bell et al., 1990). Experiments of this study were conducted with 7 male subjects.

Another predictive method proposed by Davis et al. (1991) locates hip joint center by use of regression equations; together with pelvic width, leg length, marker radius values and regression coefficients. The relations and coefficients are obtained from radiographic hip studies of 25 subjects.

Seidel et al. (1995) estimated hip joint center by a predictive method as 14% of pelvic width in medial direction, 34 % of pelvic depth in posterior direction and 79% of pelvic height inferior as located to ASIS. Measurements were obtained from cadaver studies of 35 females and 30 males. The method requires measurement of inter-ASIS distance as well as pelvic height and pelvic depth.

Among the presented predictive methods, most widely used are those proposed by Bell et al. (1990) and Davis et al. (1991). However, since predictive methods are based on small populations of subjects, their validity for clinical applications is still controversial (Della Croce et al., 2005).

Second approach for locating hip joint center is the functional approach. Due to the geometry of the femoral head, hip joint is modeled as a spherical joint in gait analysis applications. Using this assumption, functional methods utilize relative motion between thigh and pelvis segments to determine hip joint center locations.

The functional approach for determination of hip joint center location was first proposed by Cappozzo (1984). In the conducted experiments, subjects performed a special trial consisting of abduction/adduction of the thigh

11

followed by flexion/extension. Reconstructed thigh markers were afterwards utilized in a least squares algorithm to determine the hip joint center.

Several functional methods are developed in recent years for estimation of hip joint center. Piazza et al. (2001) proposed a functional method utilized with a mechanical linkage and evaluated the performance of the proposed method with limited range of motion. The authors concluded that an adequate hip motion range is more important than the type of motion for performance of the employed method.

The method of Piazza et al. (2001) was then adapted to clinical setting (Piazza et al., 2004). Several tasks were performed by subjects; which are walking, sit-to-stand, stair ascend/descend and a varied hip motion trial consisting of circumduction, flexion/extension and abduction/adduction of the hip. Worst-case hip joint center location errors of 26 mm were obtained for limited range of special hip motion trial, whereas errors of approximately 70 mm were encountered for commonly performed tasks where motion is restricted to sagittal plane. The authors state that large errors are obtained in walking trials and a special hip motion trial is needed for accurate estimation of hip joint center locations with the proposed algorithm.

Hicks and Richards (2005) compared performances of three different sphere fitting algorithms by employing computer simulated data with artificially introduced random noise. One linear least squares and two iterative sphere fitting methods were employed in calculations. The algorithm providing the best results, which employed Newton's method, was further utilized in clinical assessment. Hip joint center coordinates were computed for walking and special hip motion trials employing different marker sets. Furthermore, hip joint center coordinates were also computed using a predictive method. The

sphere fitting algorithm provided more accurate results in special hip motion trial as compared to walking trial data.

Another "pivoting algorithm" is presented by Siston and Delp (2006). A mechanical linkage with a ball-and-socket joint was employed in the experiments. Smallest mean errors of 2.2 ± 0.2 mm were obtained for a motion pattern resembling circumduction, whereas largest mean errors of 4.2 ± 1.3 mm occurred for single plane motion.

Performances of functional and predictive methods are evaluated and compared in several studies. A study by Bell et al. (1990) employs regression equations of Andriacchi et al. (1980) and Bell et al. (1990) together with the functional method. Results reveal that mean error of functional method is larger than both predictive methods.

On the other hand, results of another study by Leardini et al. (1999), where predictive methods suggested by Bell et al. (1990) and Davis et al. (1991) are compared with the functional method, reveal that performance of the functional method is found to be superior to both of the employed predictive methods

In their study, Hicks and Richards (2005) also evaluated predictive method results relative to the functional method utilized for clinical assessment. Significantly smaller mean errors in hip joint center estimates were obtained from functional method with special hip motion trial as compared to predictive method.

Considering the results provided by the recent studies, functional methods appear to provide more accurate estimates of hip joint centers with a special hip motion trial as compared to predictive methods. Employment of functional method in walking trial data, on the other hand, has not provided desirable

results yet. Functional methods may be preferred when the subject can perform a special trial covering an adequate range of hip motion in sagittal and frontal planes. On the contrary, predictive methods are straightforward and commonly employed in commercial gait analysis systems. However, their applicability in clinical settings is arguable since they are obtained from a relatively small number of healthy subjects. Hence, each approach has its advantages and disadvantages; and their selection should be performed by careful consideration of the needs of the system.

2.1.2 Knee Joint Center Estimation Methods

A common method employed in literature for determination of knee axis and joint center is identification of knee joint center from lateral and medial femoral epicondyle coordinates by use of anatomical landmark calibration techniques (Cappozzo et al., 1995).

Another method, described by Davis et al. (1991) and commonly employed by commercial gait analysis systems such as Vicon® (Vicon Motion Systems Ltd., Oxford, UK) locates knee joint center from walking data, in thigh frontal plane relative to knee marker attached on the lateral femoral epicondyle (Civek, 2006).

Helical axis concept is also adapted to knee for estimation of knee axis and joint center (Shiavi et al., 1987; Besier et al., 2003). However, difficulty in interpretation of helical axis representation by clinicians is a problem for clinical gait analysis applications.

2.2 Previous Studies on METU Gait Analysis System

Several studies regarding performance evaluation and enhancement of METU Gait Analysis System have been performed in recent years as briefly presented below.

Development of mathematical formulations and hardware employed in establishment of METU Gait Analysis Laboratory was originally presented by Güler (1998). In addition to development of the gait analysis system for clinical applications and validation of system outputs, Güler also developed a model for forward dynamics simulation of the foot.

Shafiq (1998) developed software for marker tracking and 3-D marker trajectory reconstruction from recorded camera data to be employed by METU Gait Analysis System.

Accuracy and resolution of kinematic data acquisition system of METU Gait Analysis Laboratory was evaluated by Karpat (2000), who also developed and implemented camera calibration and linearization algorithms into the system.

Afşar (2001) investigated effects of skin movement artefacts on reconstructed surface marker coordinates; proposing an experimental and analytical joint kinematics calculation procedure that utilizes double static calibration technique for compensation of errors associated with soft tissue movement.

Söylemez (2002) evaluated reliability and repeatability of METU Gait Analysis System by investigating effects of hip joint center location and centering device placement on joint kinematics results of the system. A new dynamic gait analysis protocol for joint kinematics calculations, which

eliminates the need of centering device placement for determining knee and ankle joint axes, was also proposed in this study.

CHAPTER 3

METU GAIT ANALYSIS SYSTEM

3.1 METU Gait Analysis Laboratory

METU Gait Analysis Laboratory is the first gait analysis laboratory founded in Turkey, by using off-the-shelf equipment and utilizing its own locally developed data acquisition and analysis software for motion analysis. In the laboratory, clinical gait analysis studies are performed in cooperation with medical doctors, as well as research projects carried out in various fields of motion analysis and biomechanics (Figure 3.1)

Figure 3.1 METU Gait Analysis Laboratory

3.1.1 Laboratory Hardware

Kinematic data acquisition is performed with six charged-coupled device (CCD) cameras (Ikegami Electronics, Inc., Maywood, NJ, USA) positioned around the laboratory, with a sampling frequency of 50 Hz. These cameras are equipped with infrared light emitting diodes (LED) and infrared-pass filters, tracking light reflecting passive markers placed on the subject (Figure 3.2). Synchronization and storage of camera data is performed by a video triggering unit designed by TÜBİTAK – Bilten (Ankara, Turkey) and produced by ODESA Inc. (Ankara, Turkey).

Figure 3.2 Camera with Infrared LED's and Filter

Modified Helen Hayes marker set is used in experiments. Markers are 12.7 mm (1/2") radius wooden balls coated with 3M® (St. Paul, MN, USA) retro-reflective material. Three types of markers are present in the marker set, as shown in Figure 3.3:

Figure 3.3a Marker on Wand, on Triangular Base (Type 1)

Figure 3.3b Marker on Wand, on Rectangular Base (Type 2)

Figure 3.3c Marker on Circular Base (Type 3)

Force measurement unit consists of two force plates, two amplifiers and a data acquisition card. Force plates of type 4060 HT (Bertec Corporation, Columbus, OH, USA) are embedded in staggered form in the 4.6 m walkway for acquisition of ground reaction forces and moments. Two 6-channel amplifiers

(type AM6-3, Bertec Corporation, Columbus, OH, USA) are employed for amplification of voltage output from the force plates. The data acquisition card NI AT-MIO-64E-3 (National Instruments, Austin, TX, USA) converts analog signals to digital data.

An 8-channel electromyography (EMG) unit (type Octopus AMT-8, Bortec Biomedical Ltd., Alberta, Canada) is used to record muscle activity during the gait trial (optional). Force plate, EMG and camera data are synchronized and stored in the computer.

At the beginning of each experiment, camera calibration is performed by aid of calibration rods. To correct lens distortion errors in camera images, a linearization grid is employed (Figure 3.4).

Figure 3.4 Calibration Rods (Front) and Linearization Grid (Back)

A more detailed discussion on laboratory hardware is presented in the Ph.D. dissertation by H. Cenk Güler (1998).

3.1.2 Laboratory Software

METU Gait Analysis System is named as **Kiss**, as an abbreviation of "**Ki**nematic **S**upport **S**ystem" in English and "**K**as **İs**kelet **S**istemi" in Turkish. Two programs, **Kiss-DAQ** and **Kiss-GAIT** constitute the software part of Kiss.

Data acquisition during gait trials is performed by **Kiss-DAQ** program. The software performs calibration and linearization of the cameras, as well as synchronous recording of camera images with force plate and EMG data. In addition, Kiss-DAQ performs off-line processing of image data for identification of markers and generation of marker trajectories.

Kiss-GAIT software calculates time-distance parameters, joint angles, joint moments and joint powers from an input file that combines marker trajectories and force plate data, along with anthropometric measurements taken on the subject during gait trial.

3.2 Experimental Procedure

A standard gait experiment at METU Gait Analysis Laboratory is comprised of several steps. At the beginning of each experiment, Kiss-DAQ creates a new folder with subject's name, which is going to contain camera, force plate and EMG data (optional) from each trial, as well as calibration and linearization parameters.

3.2.1 Linearization

Due to camera lens distortions, marker image coordinates recorded by the cameras are different from real marker coordinates. Therefore, a correction must be performed on recorded coordinates before the calibration process. For this purpose, a linearization grid is employed (Figure 3.4). The 15x20 grid consists of circles formed of retro-reflective material. A stick with retro-reflective material at its tip is mounted in the middle of the grid. First, each camera is positioned perpendicularly in front of the grid so that the points and the tip of the stick in the middle are seen by the camera (Figure 3.5). Then, stick is removed and image of the grid is recorded with 1 second duration. A linearization algorithm is then utilized, which corrects lens distortion errors by employing a mapping between distorted images and the original grid, and calculating related linearization parameters (Karpat, 2000).
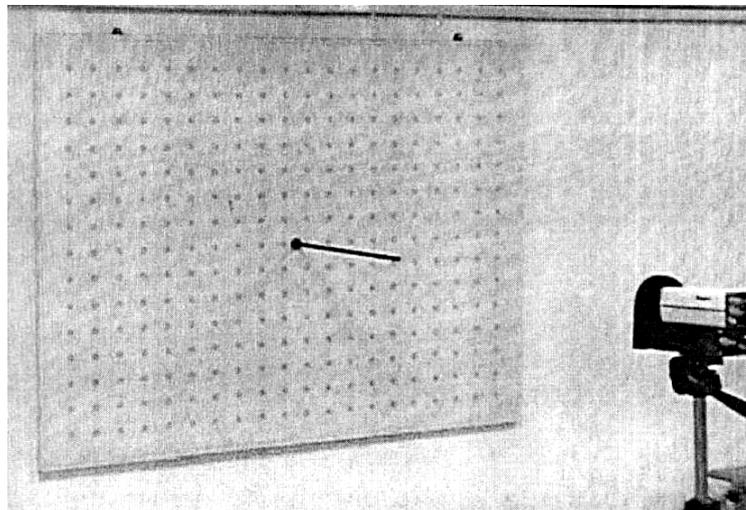
Figure 3.5 Linearization Grid and Camera (Karpat, 2000)

Linearization procedure should to be performed periodically, preferably every six month, to avoid errors due camera image distortions. Since, unless camera focal length and aperture are not changed during experiments, linearization parameters do not change considerably in time; and since this procedure is relatively time consuming and is not practical to apply before each experiment, previously identified linearization parameters are generally employed in the experiments.

3.2.2 Camera Calibration

The cameras need to be calibrated before each gait experiment session. The purpose of this calibration process is to relate 2-D marker image data on each camera image plane to its 3-D counterpart, performing calculations based on known 3-D marker coordinates within the calibration volume enclosed by four calibration rods. Motion analysis results are expected to yield valid results only within this calibration volume (Shafiq, 1998). Calibration rods, each with six light-reflecting markers are suspended from the ceiling as shown in Figure 3.1. Markers are positioned differently on each rod to ease automatic identification of the rods.

A surveyor's telescope (Figure 3.6) is used to adjust the height of suspended calibration rods so that coordinates of markers on the rods are same as the 3-D marker coordinates known by Kiss-DAQ program. Images are recorded for 1 second and related calibration parameters are calculated using known coordinates of the 24 markers on the calibration rods.

Figure 3.6 Surveyor's Telescope

During calibration, all markers on the rods should be visible to all cameras. Re-calibration may be needed if cameras are touched or moved during trials.

3.2.3 Static Trial

Calibration rods are removed after calibration and subject is prepared for static trial. Kiss gait analysis protocol requires 19 markers to be attached on the lower extremity of the subject during static trial. Since marker positions are coupled to the biomechanical model employed by the system, utmost care should be taken when anatomical landmarks are determined and markers are placed on these locations. Markers are attached on the skin of the subject with double sided adhesive bands and secured by plasters in order to minimize marker movement relative to the skin during trials.

Main purpose of static trial is to perform anatomical landmark calibration. By the use of this procedure, certain anatomical landmarks like the joint centers, which cannot be identified by direct marker attachment, can be located relative to markers that can easily be tracked by the cameras, as discussed in Chapter 1.

In static trial, ankle and knee centering devices are utilized for locating ankle and knee joint axes. Each centering device has two reflective markers attached at a distance, line connecting the markers passing through the circular edges of the centering device (Figure 3.7).
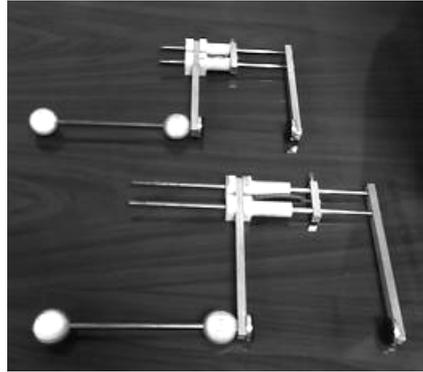
Figure 3.7 Ankle and Knee Centering Devices

Knee centering device (KCD) is placed on the knee with its two circular edges positioned on medial and lateral femoral epicondyles; through which the knee axis is assumed to pass at erect posture. With this technique, knee axis can easily be located from positions of markers on the centering device. In a similar manner, ankle axis is located by use of the ankle centering device (ACD), ends of the ACD being positioned at medial and lateral malleoli on the ankle.

In addition to centering devices, heel markers are also attached on the subject during static trial, and removed in dynamic trial in order to minimize the number of markers attached on the foot segment during gait. Again, position of heel marker can be reconstructed in dynamic trial if needed, employing marker coordinate information obtained from static trial.

Figure 3.8 shows markers attached on subject during static trial. In the front view, heel marker attached on the posterior segment of foot is not visible. Heel markers can be viewed in Figure 3.9.
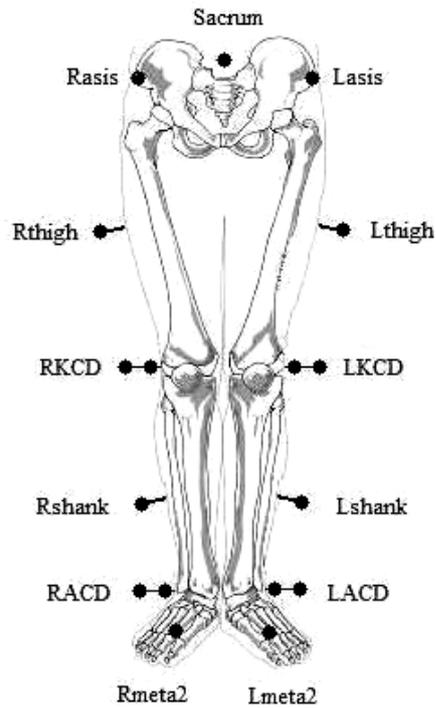
Figure 3.8 Marker Placements in Static Trial

List of markers employed in static trial is provided in Table 3.1, together with their types and positions on body segments.

Table 3.1 Markers Used in Static Trial

Marker Name	Marker Position	Marker Type
Rasis	Anterior Superior Iliac Spine, Right	3
Lasis	Anterior Superior Iliac Spine, Left	3
Sacrum	Mid-point between Posterior Superior Iliac Spines	1
Rthigh	Lateral mid-thigh (position not critical), Right	2
Lthigh	Lateral mid-thigh (position not critical), Left	2
Rshank	Lateral mid-shank (position not critical), Right	2
Lshank	Lateral mid-shank (position not critical), Left	2
Rheel	Heel, Right	3
Lheel	Heel, Left	3
Rmeta2	Second Metatarsal, Right	3
Lmeta2	Second Metatarsal, Left	3
RIKCD	Inner Marker of Right Knee Centering Device	-
ROKCD	Outer Marker of Right Knee Centering Device	-
LIKCD	Inner Marker of Left Knee Centering Device	-
LOKCD	Outer Marker of Left Knee Centering Device	-
RIACD	Inner Marker of Right Ankle Centering Device	-
ROACD	Outer Marker of Right Ankle Centering Device	-
LIACD	Inner Marker of Left Ankle Centering Device	-
LOACD	Outer Marker of Left Ankle Centering Device	-

After markers and centering devices are placed, the subject is instructed to take natural upright position on one of the force plates, facing forward and standing stationary. Static shot is taken for 1 second (Figure 3.9).
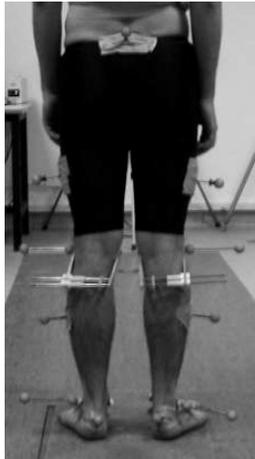
Figure 3.9 Static Shot

3.2.4 Dynamic Trial

Dynamic trial is the second part in the experiment. Heel markers and centering devices are removed from the subject after static shots are taken. Type 3 markers are placed on lateral femoral epicondyles and lateral malleoli (Figure 3.10). Positions of all other markers remain identical in both static and dynamic trials.
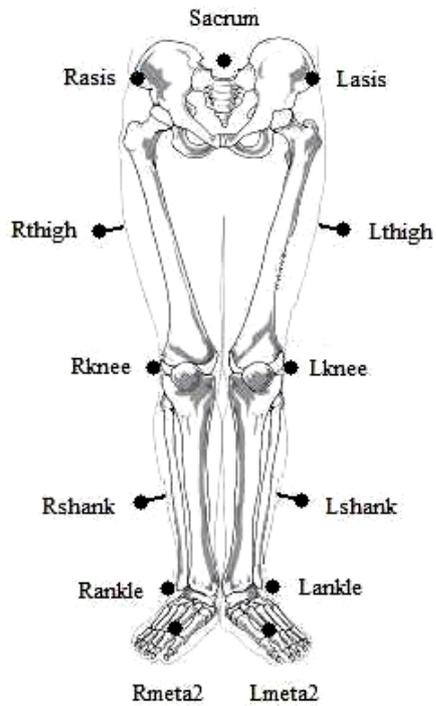
Figure 3.10 Marker Placements in Dynamic Trial

List of markers used in dynamic trial is provided in Table 3.2, together with their types and locations on body segments.

Table 3.2 Markers Used in Dynamic Trial

Marker Name	Marker Location	Marker Type
Rasis	Anterior Superior Iliac Spine, Right	3
Lasis	Anterior Superior Iliac Spine, Left	3
Sacrum	Midpoint Between Posterior Superior Iliac Spines	1
Rthigh	Lateral Mid-Thigh (Position Not Critical), Right	2
Lthigh	Lateral Mid-Thigh (Position Not Critical), Left	2
Rknee	Lateral Femoral Epicondyle, Right	3
Lknee	Lateral Femoral Epicondyle, Left	3
Rshank	Lateral Mid-Shank (Position Not Critical), Right	2
Lshank	Lateral Mid-Shank (Position Not Critical), Right	2
Rankle	Lateral Malleolus, Right	3
Lankle	Lateral Malleolus, Left	3
Rmeta2	Second Metatarsal, Right	3
Lmeta2	Second Metatarsal, Left	3

Following marker placement, the subject performs a number of gait trials to get used to walking normally with the attached markers, along the walkway positioned at the center of the laboratory. During gait, the subject must step on first force plate with right foot and second force plate with left foot, and step on only one plate at a time to be able to record ground reaction forces and moments acting on each foot (Figure 3.11). Starting point of the subject is thus determined based on the observation of the performer so that the above criteria

will be satisfied. Usually, the subject is not informed about force plates since trying to step on them will affect normal gait of the subject. As the subject walks, camera and force plate data are recorded for a period of 5-6 seconds.

Figure 3.11 Dynamic Trial

3.2.5 EMG Measurements

Electromyography (EMG) is employed to record the electrical activity of muscles, in order to collect information about muscle activity times. Although EMG data is not used in kinematic and kinetic calculations, EMG measurements may be taken during gait trials if demanded by medical doctors since it may help identification of sources of observed deviations from normal (healthy) gait pattern.

3.2.6 Anthropometric Measurements

Anthropometric data of the subject is used together with marker coordinates in estimation of joint centers, segment mass centers, and mass moment of inertias of segments for kinematic and kinetic calculations. Following anthropometric measurements are taken in a regular gait experiment:

- <u>ASIS-ASIS Distance:</u> Distance between right and left anterior superior iliac spines
- <u>Leg Length:</u> Leg length, measured from ASIS to medial malleolus, passing through medial femoral epicondyle. Leg length is measured for both sides.
- <u>Knee Width:</u> Distance between medial and lateral femoral epicondyles. Knee width is measured for both sides.
- <u>Ankle Width:</u> Distance between medial and lateral malleoli. Ankle width is measured for both sides.
- <u>Mass:</u> Body mass of the subject
- <u>Height:</u> Height of the subject

In addition to above anthropometric data; age, gender and medical condition of the subject are also recorded and stored in the database of the system.

3.3 Processing Experimental Data

Several software packages are employed in METU Gait Analysis Laboratory for processing and analyzing image data collected in experiments. Raw image data obtained from six cameras are first processed by the **Motion Tracking** program embedded in **Kiss-DAQ** (Figure 3.12); which, as a first step, performs grouping of pixels, identification of markers and construction of 3-D marker coordinates (Shafiq, 1998). Afterwards, marker images are interactively labeled by user and marker trajectories are constructed (Figures 3.13 and 3.14).

Figure 3.12 Main Window of Motion Tracking Program

Figure 3.13 Marker Labeling
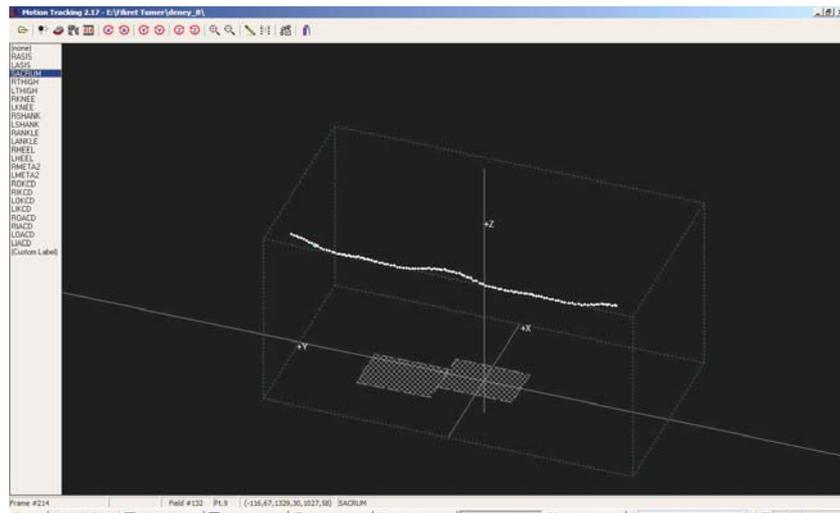
Figure 3.14 Constructed Marker Trajectories

In the next step, **Bvd Filer** program combines the following information into a single file (Figure 3.15):

- Marker trajectories from static shot
- Marker trajectories from dynamic trial
- Force plate data of the related dynamic trial
- EMG records (if available)
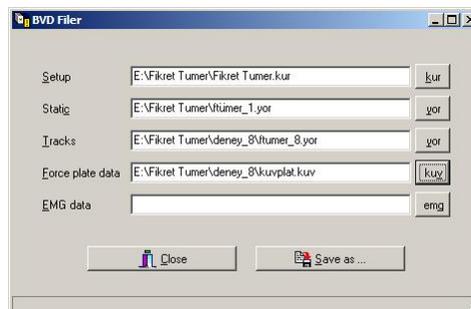
Figure 3.15 Bvd Filer

Kiss-GAIT program accepts the created .bvd file along with anthropometric measurements from the subject, and calculates temporal, kinematic and kinetic gait parameters via utilization of a biomechanical model. Gait events such as heel strike and toe off are identified interactively by user (Figure 3.16), which enables the determination gait cycles for right and left lower extremities, and calculation of the following time-distance parameters: Step length, stride length, step time, stride time and cadence (Figure 3.17).
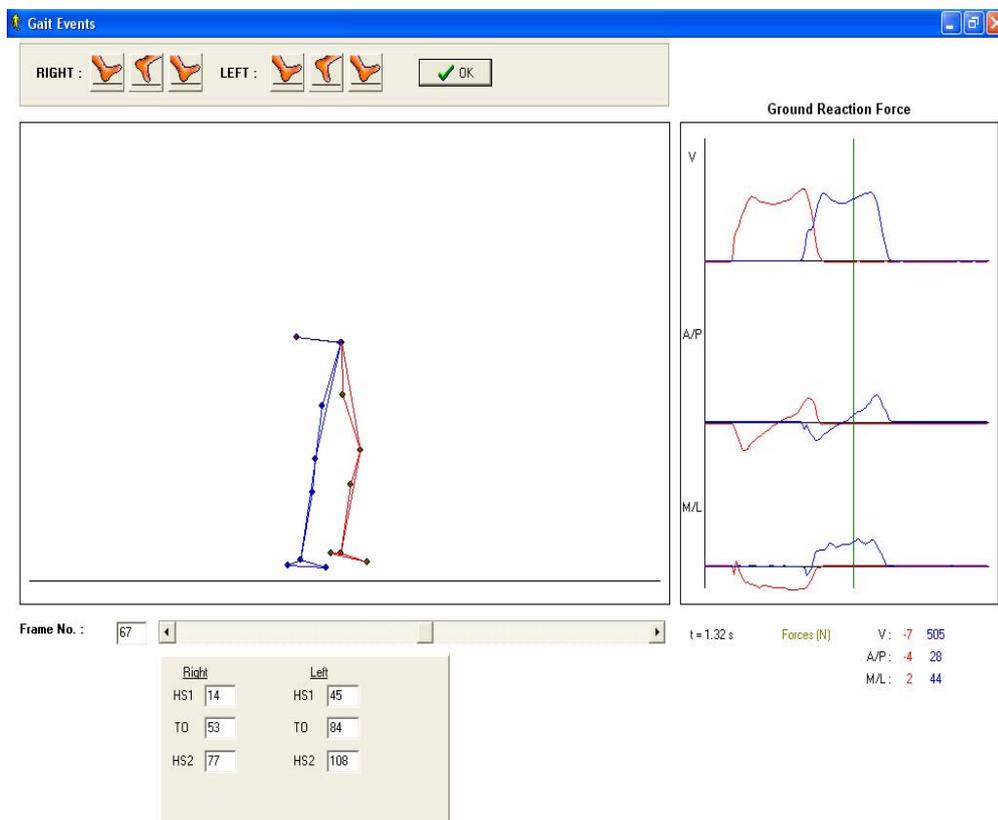
Figure 3.16 Determination of Gait Events in Kiss-GAIT
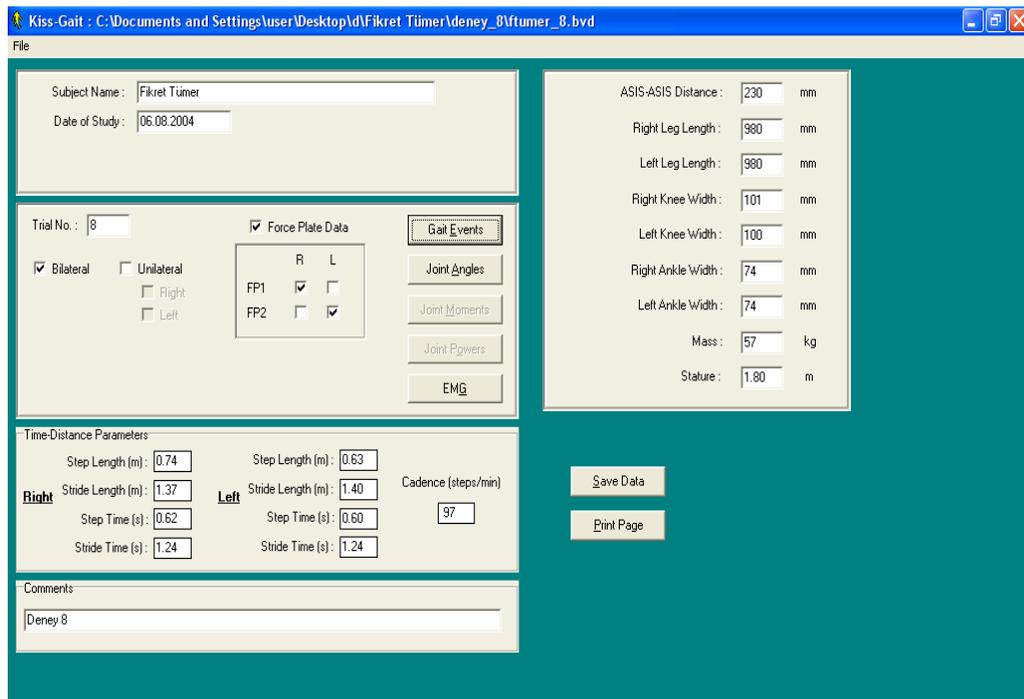
Figure 3.17 Kiss-GAIT Main Window

Following joint angles are calculated after determination of gait events:

Joint Angles:

- Pelvic tilt, rotation, obliquity
- Hip flexion/extension, abduction/adduction, internal/external rotation
- Knee flexion/extension, varus/valgus, internal/external rotation
- Dorsi/plantar flexion, foot internal/external rotation
- Foot alignment (with respect to laboratory frame)

Kiss-GAIT also calculates joint moments and powers from camera and force plate data. Computed kinematic and kinetic parameters can then be plotted as a function of percentage of gait cycle. Joint angle plots of Kiss-GAIT program

36

are presented in Figure 3.18. If EMG records are taken during experiments, raw EMG data is also presented on joint angle and moment graphs, although it is not employed within the calculation procedure of these parameters.
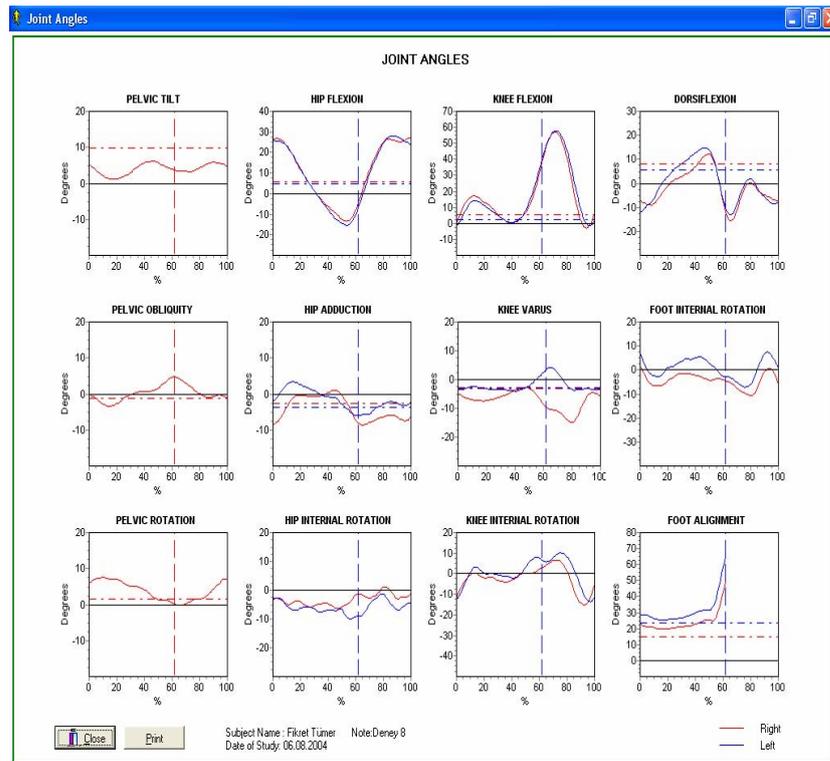
Figure 3.18 Joint Angle Plots of Kiss-GAIT

Kiss-GAIT program furthermore enables the user to save computed gait parameters such as static angles, raw and smoothed joint angles, joint moments, joint powers, etc. in text format.

CHAPTER 4

RE-GENERATION OF
JOINT KINEMATICS CALCULATIONS

4.1 Introduction

Calculation of gait parameters from stereophotogrammetric data entails utilization of methods of classical mechanics together with biomechanical models that enable representation of human body as a mechanical system. Evidently, procedures employed in these calculations are directly associated with the experimental protocol.

Adaptation of various joint center estimation methods to Kiss protocol and investigation of joint center location effects on kinematic results undoubtedly require modifications to be introduced to the experimental protocol, and consequently, to the calculation methodology. In the current gait analysis protocol, kinematics calculations are performed by Kiss-GAIT software developed in Delphi® environment (Delphi Corporation, Troy, MI, USA). However, this program can not provide the flexibility needed to perform modifications on the calculation procedure. Hence, the necessity of development of a new computer code for joint kinematics calculations is evident.

Primary step in the undertakings of this thesis study was therefore the re-generation of current joint kinematics calculations employed by Kiss protocol. Having successfully re-generated kinematic results of current protocol with the new computer code, modifications on calculation procedure could then be performed in order to investigate resulting joint kinematics.

Joint kinematics calculations of Kiss-GAIT software was previously re-formulated by Afşar (2001) and Söylemez (2002), since no written documentation was available on the subject. In this study, methodology and formulations presented by Söylemez (2002) were employed for computer code re-generation of joint kinematics calculations.

In the following sections the joint kinematics calculation procedure of Kiss-GAIT is discussed, together with its theoretical background. Detailed formulations will not be presented here since they are provided in the dissertation of Söylemez (2002).

4.2 Procedure for Joint Kinematics Calculations

Main steps of the joint kinematics calculation procedure utilized in the current gait analysis protocol are presented in Figure 4.1:
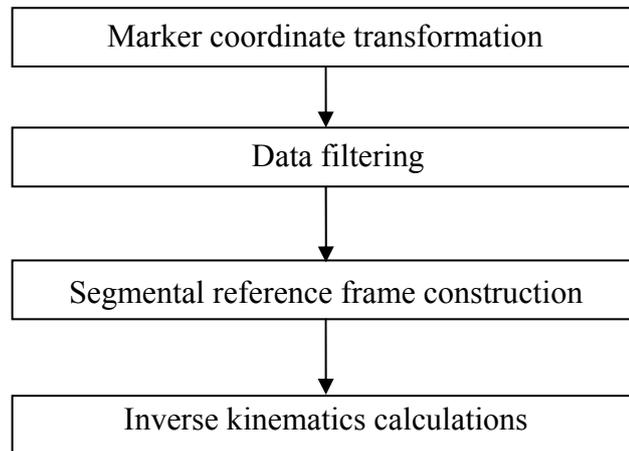
Figure 4.1 Joint Kinematics Calculation Procedure

4.3 Marker Coordinate Transformation

Marker coordinates reconstructed from raw camera data are defined in Kiss-DAQ coordinate system. Since reference frames employed by Kiss-DAQ and Kiss-GAIT are different, these marker coordinates should first be transformed into Kiss-GAIT coordinate system to be able to perform kinematic calculations.

Kiss-DAQ and Kiss-GAIT reference frames are shown in Figure 4.2, where D and G stand for Kiss-DAQ and Kiss-GAIT, respectively. Kiss-GAIT reference frame is defined such that it complies with International Society of Biomechanics (ISB) recommendations; in which, x-axis is in direction of travel, y-axis is upward and parallel with the field of gravity, and z-axis is perpendicular to x- and y- axes; constructing a right-handed coordinate system (Wu and Cavanagh, 1995).
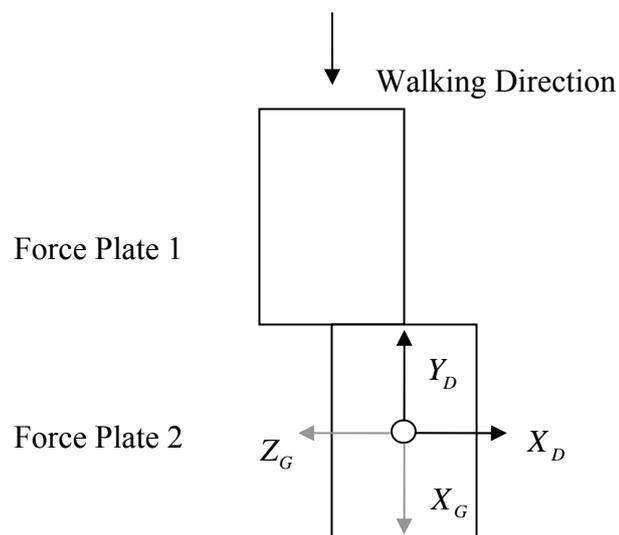
Figure 4.2 Kiss-DAQ and Kiss-GAIT Reference Frames

Governing equation of this coordinate transformation process is:

$$\bar{r}^{(G)} = \hat{C}^{(G,D)} \bar{r}^{(D)}$$ (4.1)

where $\bar{r}^{(G)}$ and $\bar{r}^{(D)}$ are Kiss-GAIT and Kiss-DAQ reference frame representations, respectively, of position vector $\vec{r}$ of any point at any time instant. $\hat{C}^{(G,D)}$ is the 3x3 transformation matrix between Kiss-GAIT and Kiss-DAQ reference frames and is defined as:

$$\hat{C}^{(G,D)} = \begin{bmatrix} 0 & -1 & 0 \\ 0 & 0 & 1 \\ -1 & 0 & 0 \end{bmatrix}$$ (4.2)

4.4 Data Filtering

Prior to kinematic calculations, three-dimensional marker data must be filtered in order to eliminate noise contained in the data. A second order Butterworth type filter is used for this purpose, whose equation is given as

$$X^*_n = a_0 X_n + a_1 X_{n-1} + a_2 X_{n-2} + b_1 X^*_{n-1} + b_2 X^*_{n-2}$$ (4.3)

where X^*_n and X_n denote filtered and raw data, respectively, at n^{th} time instant. The filter is applied once forward and once backward on data to eliminate the phase lag introduced by this sort of filter.

Constant coefficients of the above equation can be obtained from the following relations (Winter, 1990):

41

$$\omega_c = \tan\left(\frac{\pi f_c}{f_s}\right) \tag{4.4}$$

$$K_1 = \sqrt{2}\omega_c \quad , \quad K_2 = \omega_c^2 \tag{4.5}$$

$$a_0 = \frac{K_2}{1 + K_1 + K_2} \quad , \quad a_1 = 2a_0 \quad , \quad a_2 = a_0 \tag{4.6}$$

$$K_3 = \frac{2a_0}{K_2} \tag{4.7}$$

$$b_1 = -2a_0 + K_3 \quad , \quad b_2 = 1 - 2a_0 - K_3 \tag{4.8}$$

Since cut off frequency (f_c) is reduced when multiple passes of a filter is used, adjustments should be performed according to the desired cut-off frequency (f_d) for multiple uses of the filter as presented below (Robertson and Dowling., 2003):

$$f_c = \frac{f_d}{(\sqrt{2}-1)^{1/4}} \tag{4.9}$$

Following coefficients of Equation (4.3) are obtained with 25 Hz sampling frequency (f_s) and a desired cut-off frequency (f_d) of 6 Hz (Güler, 1998):

$$a_0 = a_2 = 0.389651 \quad , \quad a_1 = 0.779303$$
$$b_1 = -0.363569 \quad , \quad b_2 = -0.195035$$

Although the above values are those provided by Güler (1998) and Söylemez (2002), Kiss-GAIT software employs a different set of coefficients, as extracted from source code of the program:

$$a_0 = a_2 = 0.34202 \quad , \quad a_1 = 0.68405$$
$$b_1 = -0.19012 , \quad b_2 = -0.17796$$

Coefficients provided by Güler (1998) were calculated for 25 Hz, which was the sampling rate of cameras in primary system setup. It is believed that current coefficients of Kiss-GAIT software were determined after camera sampling rate was adjusted to 50 Hz. Albeit there is no written documentation available about calculation procedure of these new coefficients, still they were used in re-generation of kinematics calculations in order to enable comparison of obtained results with Kiss-GAIT outputs.

4.5 Construction of Segmental Reference Frames

In Kiss protocol, lower extremity is modeled as an open kinematic chain composed of seven rigid segments, connected by 3 degree-of-freedom joints. Instantaneous positions and orientations of these segments are calculated by the use of segment-fixed reference frames, which are constructed from coordinates of markers attached on the segment. Subsequent calculations for joint kinematics employ information obtained from these segment-based frames.

As stated by Cappozzo et al., (2005), joint kinematics calculations require utilization of anatomical segment reference frames. Kiss protocol employs joint coordinate system definitions proposed by Grood and Suntay (1983). Anatomical reference frames are defined such that their planes approximate anatomical planes of segments. In this way, utilization of the anatomical frames in joint angle calculations yield results in terms of clinically meaningful joint angles.

Construction of these anatomical frames entails determination of certain anatomical landmark positions such as knee and ankle joint centers, which are located in static trial by use of anatomical landmark calibration methods.

For each segment, technical and anatomical reference frames are constructed from static shot data. Transformation between these two frames is assumed to remain constant at all times, since segments are considered as rigid. This information proves to be useful in dynamic trial calculations, where only technical reference frames can be constructed from recorded data. Anatomical reference frames at each time instant can then be obtained in dynamic trial, from technical frames constructed using dynamic trial data, and the constant transformation between anatomical and technical frames. Following the same methodology, joint axes and centers can also be located in dynamic trial by expressing them in the relevant technical reference frame in static trial, and assuming this expression remains constant at all times due to rigidity of the segments.

4.5.1 Static Trial Calculations

Pelvis: Three markers are attached on pelvis during static trial, as shown in Figure 4.3:
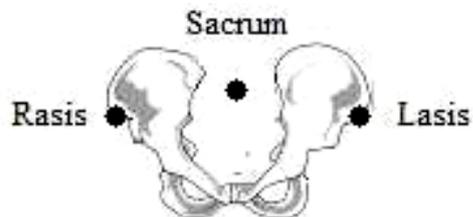
Figure 4.3 Markers on Pelvis

44

For pelvis segment, technical and anatomical frames are coincident, and denoted as pelvis reference frame (Figure 4.4).

Pelvis reference frame

- Origin: Midway between Rasis and Lasis (Pelvic Center)
- Axes:
  - z_p: Along the line connecting Rasis and Lasis; towards right hand side
  - y_p: Normal to the plane defined by Sacrum, Rasis and Lasis; directed superiorly
  - x_p: Perpendicular to z_p and y_p; forming a right-handed triad

Pelvis reference frame is expressed in fixed laboratory (Kiss-GAIT) coordinate system as:

$$\hat{C}^{(G,p)} = \begin{bmatrix} \vec{i}_p^{(G)} & \vec{j}_p^{(G)} & \vec{k}_p^{(G)} \end{bmatrix} \tag{4.10}$$

where $\vec{i}_p$, $\vec{j}_p$, $\vec{k}_p$ are unit vectors of pelvis reference frame.
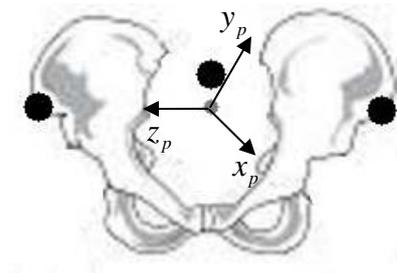
Figure 4.4 Pelvis Reference Frame

Thigh: For thigh segment, technical and anatomical reference frames are defined separately. Figure 4.5 shows anatomical landmarks that are used in constructing these frames. In the figure, knee centering device markers are shown in grey. Empty circles denote joint centers. Since they are internal to the body, joint centers cannot directly be tracked by markers and therefore their positions are calculated from markers attached on the surface of the segment.
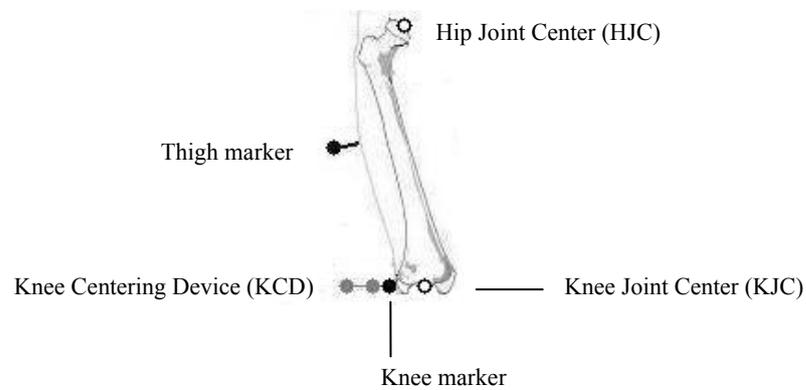
Figure 4.5 Anatomical Landmarks Used in Construction of Thigh Frames

Location of *hip joint center (HJC)* is calculated by means of a regression equation that employs pelvis marker coordinates and anthropometric parameters such as leg length and ASIS-ASIS distance (Davis et al., 1991).

Knee axis and *knee joint center* are determined by aid of the knee centering device (KCD). *Knee axis* is located by a vector that is defined from outer knee centering device marker (OKCD) to inner knee centering device marker (IKCD). *Knee joint center (KJC)* position is then determined by traveling a distance of half knee width plus marker radius, from knee marker along the knee axis (Figure 4.6).

Knee axis ($\vec{u}_k$) $\longrightarrow$ KJC
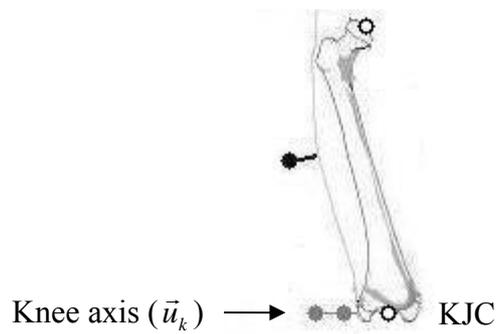
Figure 4.6 Knee Axis and Knee Joint Center

Knee marker is not present in static trial. However, by aid of the KCD, it can virtually be located. Defining knee centering device offset (KCDO) as the distance between knee marker in dynamic trial and inner marker of the centering device in static trial (Figure 4.7), "virtual" knee marker position can be determined such that it will be apart from IKCD marker by a distance of KCDO, in medial direction along the knee axis.
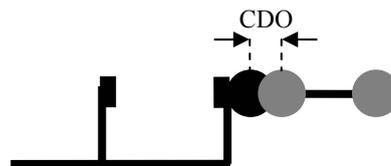
Figure 4.7 Centering Device Offset

Technical and anatomical reference frames of thigh are then constructed as follows (Figures 4.8 and 4.9):

Thigh technical reference frame

- Origin: *Knee marker*
- Axes:

  - x_t^*: Normal to the plane defined by *hip joint center*, *thigh marker* and *knee marker*; directed anteriorly

  - y_t^*: Along the line connecting *knee marker* and *hip joint center*; towards *hip joint center*

  - z_t^*: Perpendicular to x_t^* and y_t^*; forming a right-handed triad
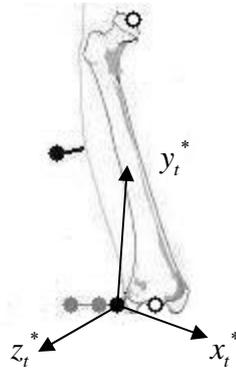
Figure 4.8 Thigh Technical Reference Frame

Thigh technical frame is expressed in fixed laboratory frame as:

$$\hat{C}^{(G,t^*)} = \begin{bmatrix} \vec{i}_t^{*(G)} & \vec{j}_t^{*(G)} & \vec{k}_t^{*(G)} \end{bmatrix} \tag{4.11}$$

where $\vec{i}_t^*$, $\vec{j}_t^*$, $\vec{k}_t^*$ are unit vectors of the reference frame.

Thigh anatomical reference frame

- Origin: *Knee joint center*
- Axes:
  - x_t: Normal to the plane defined by *hip joint center, knee joint center* and *knee axis*; directed anteriorly
  - y_t: Along the line connecting *knee joint center* and *hip joint center*; towards *hip joint center*
  - z_t: Perpendicular to x_t and y_t; forming a right-handed triad
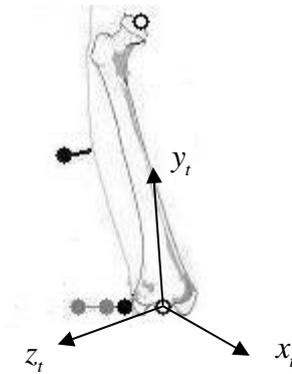
Figure 4.9 Thigh Anatomical Reference Frame

Thigh anatomical reference frame is expressed in fixed laboratory frame as:

$$\hat{C}^{(G,t)} = \begin{bmatrix} \vec{i}_t^{(G)} & \vec{j}_t^{(G)} & \vec{k}_t^{(G)} \end{bmatrix} \qquad (4.12)$$

where $\vec{i}_t$, $\vec{j}_t$, $\vec{k}_t$ are unit vectors of the frame.

Once technical and anatomical frames of thigh are constructed, their relative orientation can be found by use of the following relation:

49

$$\hat{C}^{(t^*,t)} = \hat{C}^{(t^*,G)}\hat{C}^{(G,t)} = \hat{C}^{(G,t^*)^T}\hat{C}^{(G,t)} \tag{4.13}$$

This transformation is assumed to remain constant at all times, and is employed for construction of thigh anatomical frame in dynamic trial calculations.

Shank: Similar to thigh segment, technical and anatomical reference frames are defined for shank in static trial. Anatomical landmarks used in construction of these frames are shown in Figure 4.10:
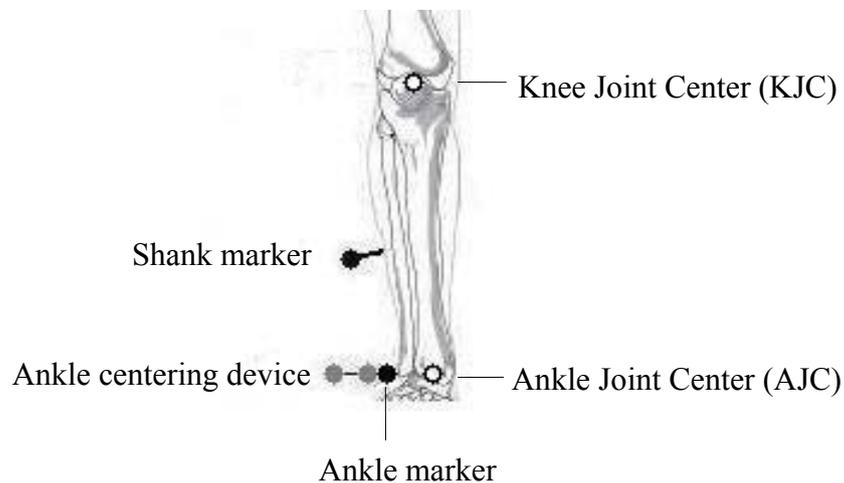
Figure 4.10 Anatomical Landmarks Used in Construction of Shank Frames

Similar to knee, *ankle axis* and *ankle joint center* are located with the aid of the ankle centering device (ACD) as follows: *Ankle axis* is identified by the vector defined from outer marker of ankle centering device (OACD) to inner marker of ankle centering device (IACD). *Ankle joint center* location is then determined such that it will be located at a distance of half ankle width plus marker radius, from ankle marker along ankle axis (Figure 4.11).

Ankle axis ($\vec{u}_a$) $\longrightarrow$ ●●● ○ AJC
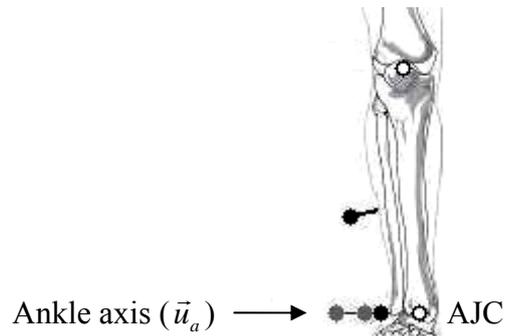
Figure 4.11 Ankle Axis and Ankle Joint Center

In static trial, *ankle marker* location is determined such that the distance between constructed ankle marker and IACD will be equal to ankle centering device offset (ACDO), ankle marker being medially positioned with respect to the IACD along the ankle axis.

Shank technical and anatomical reference frames (Figures 4.12 and 4.13) are then constructed as follows:

Shank technical reference frame
- Origin: *Ankle marker*
- Axes:
  - x_s^*: Normal to the plane defined by *knee joint center, shank marker* and *ankle marker*; directed anteriorly
  - y_s^*: Along the line connecting *ankle marker* and *knee joint center*; towards *knee joint center*
  - z_s^*: Perpendicular to x_s^* and y_s^*; forming a right-handed triad

51
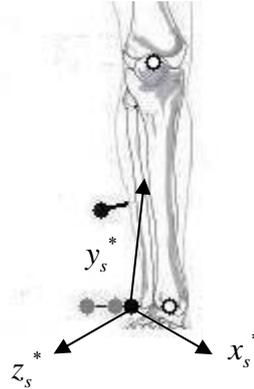
Figure 4.12 Shank Technical Reference Frame

Shank technical reference frame is expressed in fixed laboratory coordinate system as:

$$\hat{C}^{(G,s^*)} = \begin{bmatrix} \vec{i}_s^{*(G)} & \vec{j}_s^{*(G)} & \vec{k}_s^{*(G)} \end{bmatrix}$$ (4.14)

where $\vec{i}_s^{*}$, $\vec{j}_s^{*}$, $\vec{k}_s^{*}$ are unit vectors of shank technical reference frame.

Shank anatomical reference frame

- Origin: *Ankle joint center*
- Axes:
  - x_s: Normal to the plane defined by *knee joint center, ankle joint center* and *ankle axis*; directed anteriorly
  - y_s: Along the line connecting *ankle joint center* and *knee joint center*; towards *knee joint center*
  - z_s: Perpendicular to x_s and y_s; forming a right-handed triad

Shank anatomical reference frame is expressed in fixed laboratory coordinate system as:

$$\hat{C}^{(G,s)} = \begin{bmatrix} \vec{i}_s^{(G)} & \vec{j}_s^{(G)} & \vec{k}_s^{(G)} \end{bmatrix} \tag{4.15}$$

where $\vec{i}_s$, $\vec{j}_s$, $\vec{k}_s$ are unit vectors of shank anatomical frame.
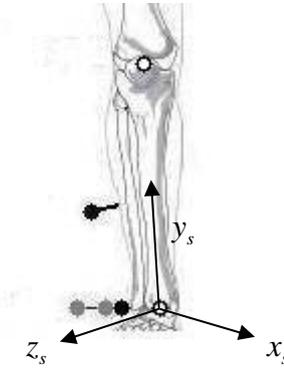
Figure 4.13 Shank Anatomical Reference Frame

Transformation matrix between technical and anatomical shank reference frames is defined as:

$$\hat{C}^{(s^*,s)} = \hat{C}^{(s^*,G)}\hat{C}^{(G,s)} = \hat{C}^{(G,s^*)^T}\hat{C}^{(G,s)} \tag{4.16}$$

This transformation is assumed to remain constant at all times, and is employed for shank anatomical frame construction in dynamic trial calculations.

4.5.2 Dynamic Trial Calculations

Pelvis: Markers attached on pelvis are identical in static and dynamic trials. Therefore, calculation procedure of pelvis frame in dynamic trial is same as the static trial case.

Thigh and Shank: In dynamic trials, only technical reference frames can be constructed since centering devices are not employed. However, by utilization of the constant transformations between segment-based anatomical and technical frames obtained in static trial calculations, anatomical reference frames may be obtained at each time instant as follows:

For thigh segment:

$$\hat{C}^{(G,t)} = \hat{C}^{(G,t^*)}\hat{C}^{(t^*,t)} \tag{4.17}$$

For shank segment:

$$\hat{C}^{(G,s)} = \hat{C}^{(G,s^*)}\hat{C}^{(s^*,s)} \tag{4.18}$$

4.6 Joint Angle Calculations

In Kiss protocol, each joint is modeled to be consisting of a proximal and distal segment, and two intermediate segments in between, being connected with revolute joints having perpendicular axes (Figure 4.14). This joint model enables representation of relative joint angles in terms of three independent clinically meaningful angle definitions; which are flexion/extension, abduction/adduction and internal/external rotation.
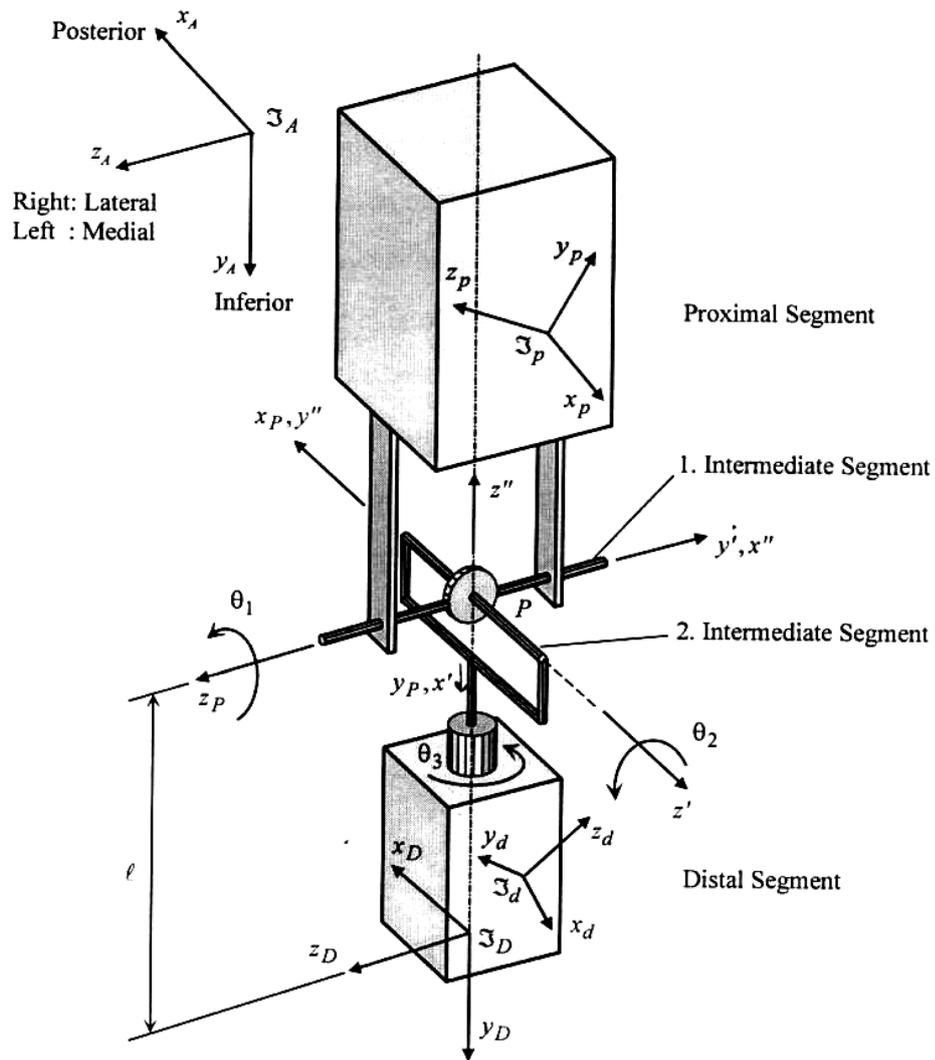
Figure 4.14 Mechanical Joint Model Employed By Kiss Protocol

(Güler, 1998)

Each segment employs its own coordinate system. For proximal and distal segments, anatomical reference frame of the related segment is selected as the coordinate system. Hartenberg-Denavit convention is employed for definition of segment parameters, which are summarized in Table 4.1:

Table 4.1 Hartenberg-Denavit Parameters

Joint (i)	Joint angle at reference position (θ_i)	Twist angle (α_i)	Link length (a_i)	Offset (d_i)
1	90°	−90°	0	0
2	90°	−90°	0	0
3	90°	−90°	0	−l

Rotation about z-axis of the proximal segment is denoted by θ_1, which corresponds to flexion/extension of the joint. Abduction/adduction of the joint is about z-axis of the first intermediate segment, and is represented by θ_2. Finally, θ_3 denotes the internal/external rotation of the joint, which takes place about z-axis of the second intermediate segment (Güler, 1998).

Joint angles are calculated from transformations between segment-based frames via implementation of inverse kinematics approach. Employing Hartenberg-Denavit convention, rotation matrix between proximal and distal segments can be expressed as:

$$\hat{C}^{(P,D)} = \hat{R}_3(\theta_1)\hat{R}_1(\alpha_1)\hat{R}_3(\theta_2)\hat{R}_1(\alpha_2)\hat{R}_3(\theta_3)\hat{R}_1(\alpha_3) \tag{4.19}$$

where $\hat{R}_1$ and $\hat{R}_3$ are elementary rotation matrices in x and z directions with the expressions

$$\hat{R}_1(\alpha) = \begin{bmatrix} 1 & 0 & 0 \\ 0 & \cos(\alpha) & -\sin(\alpha) \\ 0 & \sin(\alpha) & \cos(\alpha) \end{bmatrix} \tag{4.20}$$

$$\hat{R}_3(\theta) = \begin{bmatrix} \cos(\theta) & -\sin(\theta) & 0 \\ \sin(\theta) & \cos(\theta) & 0 \\ 0 & 0 & 1 \end{bmatrix} \tag{4.21}$$

Substituting Equations (4.20) and (4.21) in Equation (4.19) and simplifying yields

$$\hat{C}^{(P,D)} = \begin{bmatrix} (c_1 c_2 c_3 + s_1 s_3) & c_1 s_2 & (-c_1 c_2 s_3 + s_1 c_3) \\ (s_1 c_2 c_3 - c_1 s_3) & s_1 s_2 & (-s_1 c_2 s_3 - c_1 c_3) \\ -s_2 c_3 & c_2 & s_2 s_3 \end{bmatrix} = \begin{bmatrix} c_{11} & c_{12} & c_{13} \\ c_{21} & c_{22} & c_{23} \\ c_{31} & c_{32} & c_{33} \end{bmatrix} \tag{4.22}$$

In Equation (4.22), c_i and s_i denote $\cos(\theta_i)$ and $\sin(\theta_i)$, respectively. Right hand side of this equation contains direction cosines representation of elements of the transformation matrix.

Once $\hat{C}^{(P,D)}$ is calculated as the transformation between proximal and distal segment anatomical frames, related joint angles can be obtained from expressions of transformation matrix elements as follows:

$$\theta_2 = \cos^{-1}(c_{32}) \tag{4.23}$$

$$\theta_1 = \text{atan2}\left(\text{sign}(\sin(\theta_{12})) \cdot c_{22}, \text{sign}(\sin(\theta_{12})) \cdot c_{12}\right) \tag{4.24}$$

$$\theta_3 = \text{atan2}\left(\text{sign}(\sin(\theta_{12})) \cdot c_{33}, \text{sign}(\sin(\theta_{12})) \cdot c_{31}\right) \tag{4.25}$$

Equation (4.23) yields two values. Obtained θ_2 value should satisfy the following criteria:

$$0 \le \theta_2 \le \pi/2 \text{ for } c_{32} > 0$$
$$\pi/2 \le \theta_2 \le \pi \text{ for } c_{32} < 0 \tag{4.26}$$

The inverse kinematics solution yields a singularity for $\theta_2 = 0, \pi$. In this position, flexion/extension and internal/external rotation axes become parallel. However, for level walking this singular configuration is never realized (Güler, 1998)

Identification of θ_1, θ_2 and θ_3 is followed by determining clinically meaningful joint angles from the obtained angles. For each segment, anatomical angles are calculated as follows:

<u>Pelvis:</u> Pelvis angles are defined relative to fixed laboratory coordinate frame. Therefore, transformation between proximal and distal segments becomes

$$\hat{C}^{(P,D)} = \hat{C}^{(G,p)} \tag{4.27}$$

where $\hat{C}^{(G,p)}$ is the transformation matrix between pelvis and laboratory reference frames. Employing inverse kinematics solution procedure, pelvis angles are obtained via the following relations:

- Pelvic tilt $= 90° - \theta_1$ (4.28)
- Pelvic obliquity $= 90° - \theta_2$ (4.29)
- Pelvic rotation $= 90° - \theta_3$ (4.30)

<u>Hip Joint</u>: Proximal and distal segments of the hip joint are pelvis and thigh, respectively. Transformation between anatomical reference frames of these segments is:

$$\hat{C}^{(P,D)} = \hat{C}^{(p,t)} = \hat{C}^{(G,p)T} \hat{C}^{(G,t)} \tag{4.31}$$

In static trial calculations, $\hat{C}^{(G,p)}$ and $\hat{C}^{(G,t)}$ can directly be constructed from marker coordinates. For dynamic trial, Equation (4.17) is employed to obtain anatomical frame of thigh.

Hip joint angles are calculated as:

- Hip flexion/extension $= \theta_1 - 90°$ (4.32)

- Hip abduction/adduction $= \sigma(\theta_2 - 90°)$ (4.33)

- Hip internal/external rotation $= \sigma(90° - \theta_3)$ (4.34)

In the above equations, $\sigma = +1$ for the right extremity and $\sigma = -1$ for the left extremity.

<u>Knee Joint</u>: For knee joint, proximal and distal segments become thigh and shank, respectively. Transformation between thigh and shank anatomical frames is obtained from the following relation:

$$\hat{C}^{(P,D)} = \hat{C}^{(t,s)} = \hat{C}^{(G,t)T}\hat{C}^{(G,s)} \tag{4.35}$$

Similar to the previous case, anatomical reference frame of shank is estimated from Equation (4.18) in dynamic trial calculations.

Knee joint angles are then calculated as:

- Knee flexion/extension $= 90° - \theta_1$ (4.36)

- Knee varus/valgus $= \sigma(\theta_2 - 90°)$ (4.37)

- Knee internal/external rotation $= \sigma(90° - \theta_3)$ (4.38)

where $\sigma = +1$ for the right extremity and $\sigma = -1$ for the left extremity.

Foot: Foot angles are obtained through a different procedure than other joint angles calculations. First, a static plantar flexion angle is calculated from static shot data, which is defined as the angle between the vector from second metatarsal to heel and the vector from second metatarsal to ankle joint center (Figure 4.15). During gait trial, dorsiflexion angle of foot is calculated by adding this static plantar flexion angle to the angle that the vector from ankle joint center to second metatarsal makes with x-axis of shank anatomical coordinate system. Foot rotation angle, which is the rotation of foot about y-axis of shank anatomical coordinate system, is the angle that the foot vector makes with x-axis of shank anatomical reference frame in transverse plane. Finally, foot alignment is calculated, which is rotation of foot around y-axis of fixed laboratory frame (Güler, 1998).
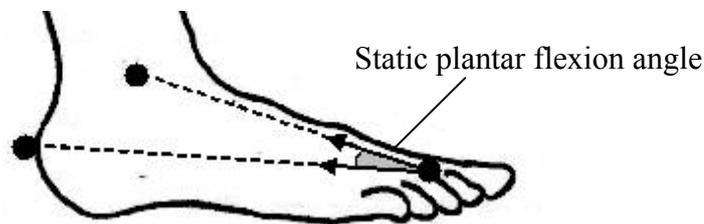
Figure 4.15 Static Plantar Flexion Angle

4.7 Computer Code for Kinematic Calculations Re-generation

A computer code was developed in Matlab® (Version 7.1.0.246 R14, The MathWorks Inc., MA, USA) for re-generation of the above discussed joint kinematics calculations of current gait analysis protocol. In order to realize

interactive and user-friendly operation of the computer code, a graphical user interface was also developed.

The developed program accepts text files containing static and dynamic trial marker trajectories, which can interactively be browsed and selected with the graphical user interface. Anthropometric data of the subject is also inputted by the user in the main program window (Figure 4.16).
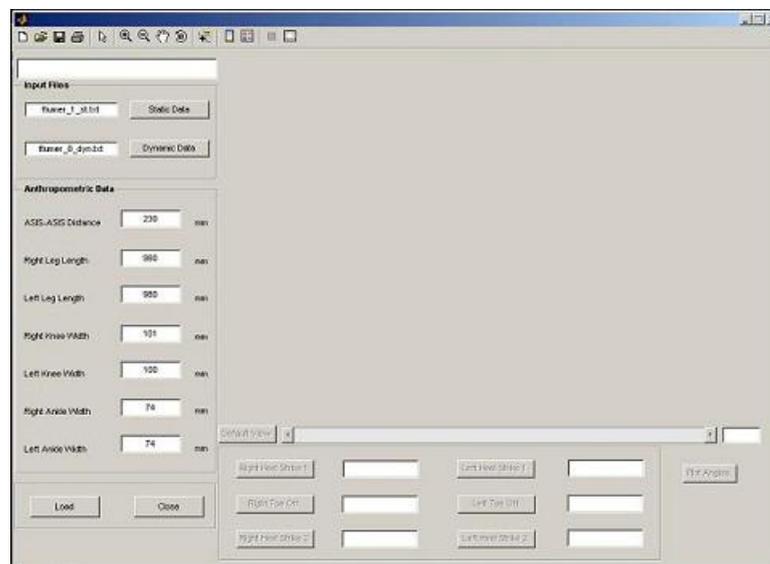
Figure 4.16 Main Window

After specification of input files and anthropometric data, markers for dynamic trial are plotted by pressing *Load* button. Red and blue markers denote right and left legs, respectively. Gait events (heel strike and toe off frames) are identified interactively by the user. This information is utilized in identification of the gait cycle (Figure 4.17). Joint angles are calculated when *Plot Angles* button is pressed. Smoothed joint angles are presented in degrees, in terms of percentage of gait cycle (Figure 4.18). In the plots, red and blue curves

represent right and left sides, respectively. Dashed lines denote static angles, which are calculated from static shot data.
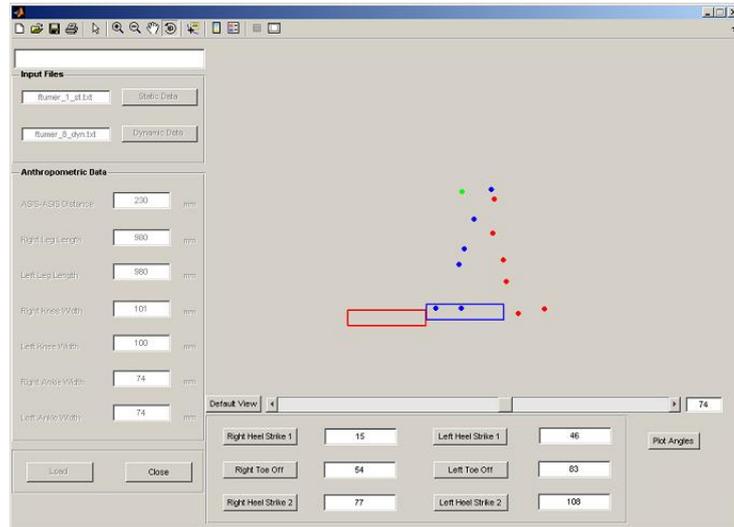
Figure 4.17 Specification of Gait Events
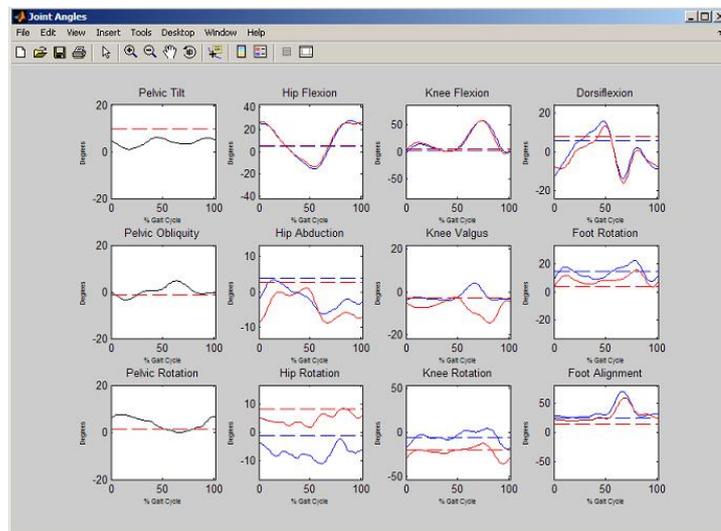
Figure 4.18 Joint Angles

Validation of the re-generated code was performed via comparison of program analysis results of with those of Kiss-GAIT, for one trial of subject FT.

Re-generated raw angles were plotted together with related Kiss-GAIT outputs within one gait cycle and presented in *Appendix A*. As observed from the graphs, results of both programs agreed significantly. Slight vertical shifts in angle values were present in internal/external rotation angle graphs. However, these variations may be considered negligible since they were relatively small in magnitude when compared to nominal values of angles. Therefore, it was concluded that joint kinematics calculations were successfully re-generated.

Re-generated smoothed joint angles, expressed as a function of percentage of gait cycle, were also plotted together with Kiss-GAIT results, as presented in *Appendix B.* Kiss-GAIT program performs a smoothing and differentiation procedure on raw angles prior to joint kinetics calculations. However, there is no written documentation available on this smoothing procedure applied on the angles. In the code re-generated for this study, a polynomial of 9th degree was fitted on raw angle data. In addition, smoothed angles were expressed as a function of percentage of gait cycle, which is a commonly employed normalization procedure for kinematic and kinetic gait parameters.

Examining smoothed angle graphs, it is observed that variations were present in outputs of two programs, especially again in internal/external rotation graphs. However, since raw angle plots overlapped, it was evident that these differences arose from the smoothing process applied on raw angles. In addition, evaluated angles followed the same trend through the gait cycle, which suggested that expressing angles in terms of percentage of gait cycle did not yield differences in program outputs. Since the smoothing procedure of Kiss-GAIT is not known, further inquiries and comparisons on effects of smoothing processes could not be performed. However, from the point of view

of joint kinematics, it was concluded that comparison of both raw and smoothed angles yielded satisfactory results and joint kinematics calculations of Kiss protocol was therefore successfully re-generated.

CHAPTER 5

"FREE" THIGH AND SHANK MARKERS:
EFFECTS OF THEIR RELOCATION ON JOINT KINEMATICS

5.1 Introduction

In gait analysis systems, determination of body segment motions is realizable through utilization of surface markers attached on each segment. Bony landmark coordinates needed for subsequent kinematic and kinetic calculations are thus obtained from these markers attached on corresponding locations on the segments. Therefore, position of each marker is directly related to the calculation methodology employed by the gait analysis system, and misplacement of markers evidently yields errors in gait parameters that are calculated from marker data.

Locations of thigh and shank markers are considered not to be critical in Kiss protocol. Unlike other markers which correspond to certain bony landmarks (e.g. ASIS, sacrum, etc.), these "free" markers can arbitrarily be placed on the relevant segment, provided they satisfy certain other technical requirements such as visibility to the cameras or non-collinearity with other markers of the segment.

This special condition of thigh and shank markers follows from their role in the joint kinematics calculation procedure. These markers are only used for construction of relevant segmental technical reference frames. As discussed in Chapter 1, technical frames need not have any repeatable reference to segment geometry; their absolute position and orientation being insignificant to the calculation procedure. A technical reference frame merely provides a basis for

construction of the anatomical reference frame of the segment in conditions where the anatomical frame cannot be directly determined. With the assumption that surface markers define rigid segments, the constant transformation between anatomical and technical frames obtained from static shot can be used together with technical reference frame in dynamic trial to reconstruct the anatomical frame (Figure 5.1). Therefore, possible effects of changes in absolute orientation of the technical frame should be compensated by this transformation process.
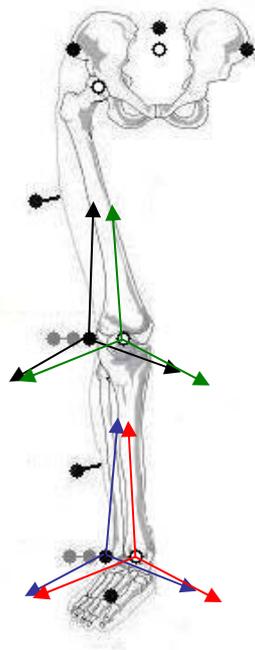
Figure 5.1a	Figure 5.1b
Thigh and Shank	Thigh and Shank
Reference Frames	Reference Frames
in Static Shot	in Dynamic Trial

(Solid lines denote anatomical and technical frames directly constructed from marker data, dashed lines denote anatomical frames constructed relative to technical reference frames in dynamic trial)

It follows from the above discussed hypothesis that, for two cases in which thigh and shank markers are located differently, calculated joint kinematics should be the same. This chapter, therefore, aims to investigate whether changes in thigh and shank marker locations impose differences on the resulting joint kinematics of Kiss protocol. For this purpose, gait experiments were conducted with necessary methodological modifications and results obtained for both cases were evaluated, which are discussed in detail in the following sections.

5.2 Experiments

Gait experiments were performed with 3 able-bodied volunteers (ED, GK, and KU) with no history of musculoskeletal injury or illness. For every subject, data were collected in a single experiment session; therefore each session consisted of a number of different trials which also involved collection of data needed for the second part of the study (i.e. implementation of different joint center estimation methods). However, in order to avoid confusion, only the relevant trials will be mentioned in each chapter.

Camera calibrations were carried out at the beginning of first session of each experiment day and repeated whenever necessary. One experiment session was performed for each subject. In each session, static and dynamic trials were performed and anthropometric data of the subject was recorded in compliance with general of gait experiment guidelines of METU Gait Analysis Laboratory which was discussed in Chapter 3.

A comparison on joint kinematics, resulting from different positioning of thigh and shank markers, could only be meaningful if coordinates of these markers were the only difference between the compared data sets. Evaluation of "free" marker location effects through successive trials, in which these markers were

placed in different locations on thigh and shank, might not yield reliable results due to intra-subject variability. Therefore, different positions of thigh and shank markers had to be recorded simultaneously in a single trial, which called for modifications to be performed on the standard marker placement methodology employed by METU Gait Analysis System. The adopted marker placement method was developed accordingly, thus providing ease in selecting the desired thigh and shank marker positions for analysis, without any change in trajectories of other markers.

Two different locations for each thigh and shank marker were selected to evaluate and compare resulting joint kinematics. In standard experiments performed at the laboratory, thigh and shank markers are placed on the lateral aspects of each segment, lying in segment frontal plane. First location for thigh and shank markers was thus selected to be the same as in a regular experiment; and these markers will be denoted as "side" markers from now on.

Several parameters were considered in determining locations of the additional thigh and shank markers. Markers had to be placed as far as possible from each other in order to be able to distinguish the markers. Visibility of these markers to cameras throughout gait was another important technical requirement. Furthermore, to select a marker location which could be identified in different subjects in a repeatable manner was essential. When all these requirements were considered, it was concluded that best location for additional thigh and shank markers were the frontal (most anterior) aspects of related segments. These markers are denoted as "front" markers in the following discussions.

Type 2 markers were employed as thigh and shank markers in the experimental protocol. Since these markers are positioned on a wand, their movement relative to underlying bones is more than Type 3 markers which are directly attached on the skin. This behavior is especially prominent in gait trials, where

acceleration of segments result in vibrations in the wand combined with soft tissue movement. Therefore, front and side markers were selected to be of the same type (Type 2) so that both would be affected from the above discussed conditions to the same extent.

Except for utilization of front markers, experiments were carried out according to the standard experimental procedure. In static trial, a total number of 23 markers were placed on the subject; 19 of them being markers employed in a regular static trial, and 4 of them being the front markers. Side thigh and shank markers were positioned so that they lay on the frontal segment planes. Side thigh markers were located sufficiently distal on their segments to avoid being hit and obstructed by the arms. Front markers were located at the same horizontal level with the side markers of the relevant segments. After placement of markers, one static shot with 1 second duration were recorded while subject stood with an upright posture on the left force plate, facing forward (Figure 5.2).

Figure 5.2 Static Shot with Front and Side Markers

For dynamic trial part of the experiments, centering devices were removed and Type 3 markers were attached on lateral femoral epicondyles and malleoli. A total number of 17 markers were placed on the subject for dynamic trials; 13 of them being markers employed in a regular gait trial, and 4 of them being front markers. The subject performed 3 gait trials along the walkway at a self-selected pace which were recorded for a duration of 5 seconds (Figure 5.3).

Figure 5.3 Dynamic Trial with Front and Side Markers

5.3 Data Sets

Recorded raw camera data was firstly processed with Motion Tracking program for identification and reconstruction of marker trajectories. From static shot and each dynamic trial, four different data sets were then extracted as presented in Table 5.1, to investigate effects of thigh and shank marker location variations on joint kinematics. Evidently, Set-1 corresponds to marker trajectories that would be obtained from a regular gait experiment. As noted previously, the only difference between constructed data sets were selected

70

combinations of thigh and shank marker locations; coordinates of the remaining markers were common to all data sets for each trial.

Table 5.1 Front/side data sets constructed for each trial

Data Set	Thigh	Shank
Set-1	Side	Side
Set-2	Front	Front
Set-3	Side	Front
Set-4	Front	Side

Each data set couple, consisting of static shot and one dynamic trial, were then analyzed. Evaluation of resulting joint kinematics is presented in the following section for one selected trial of subject KU (Trial 18).

5.4 Results and Discussion

5.4.1 Evaluation of Set-1 and Set-2 Results

As the primary step in investigation and comparison of joint angles obtained from side and front markers, analyses were performed with data sets 1 and 2, which contained side and front markers, respectively, of both thigh and shank. These data sets were separately analyzed with the re-generated user-interactive Matlab® program (Figures 5.4 and 5.5).
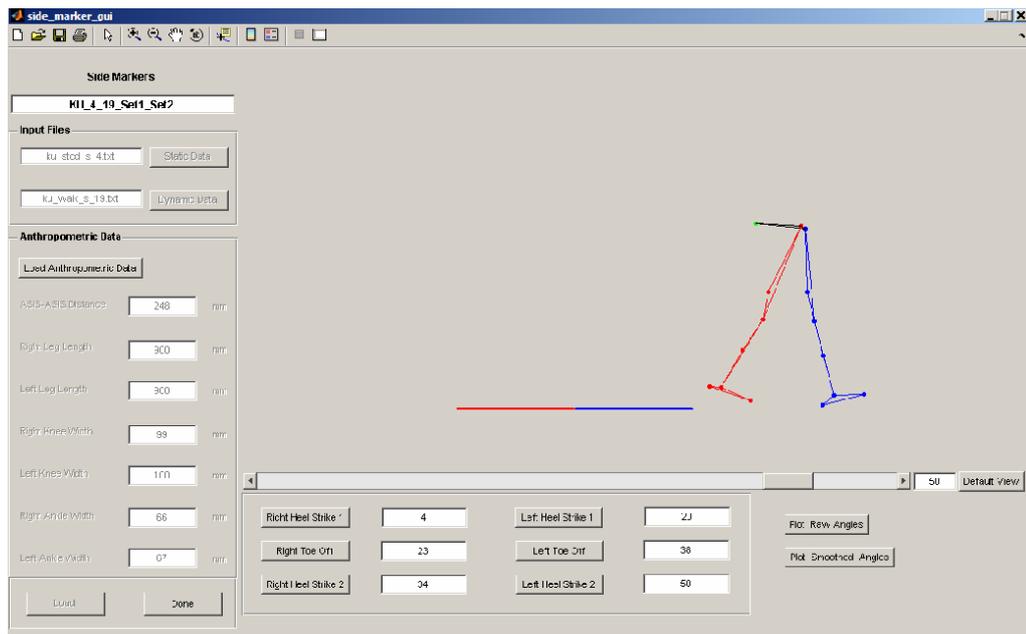
Figure 5.4 Analysis of Set-1 with Matlab® Code
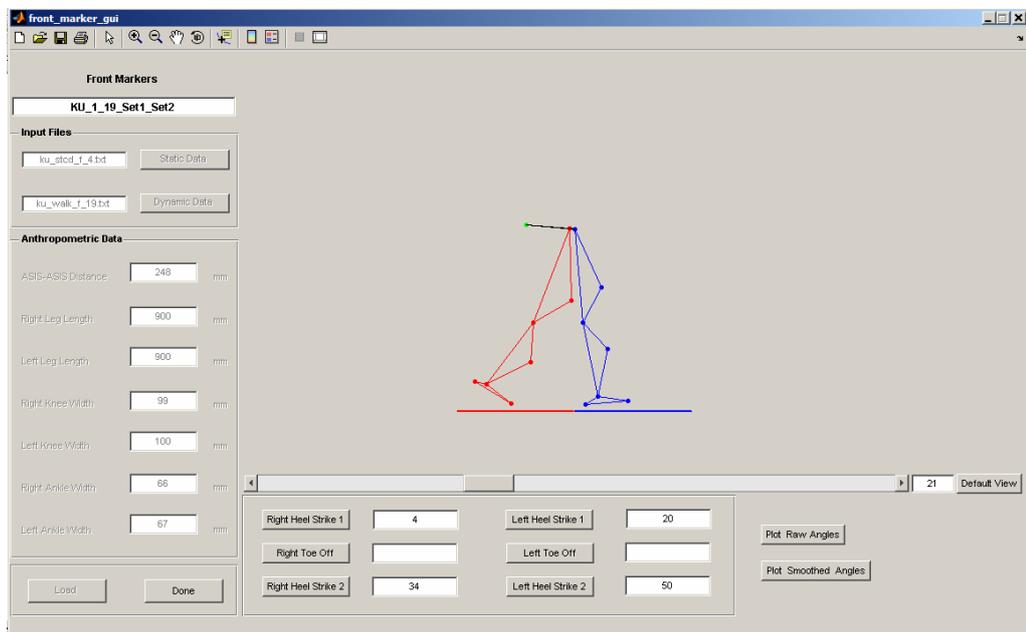
Figure 5.5 Analysis of Set-2 with Matlab® Code

Set-1 and Set-2 results were then plotted on the same graph for each raw joint angle over one gait cycle, which started and ended with the first and second heel strikes of the relevant foot. Important gait events of the analyzed dynamic trial are presented in Table 5.2:

Table 5.2 Gait Events

Event	Frame	
	Left Segment	Right Segment
Heel Strike 1 (HS1)	20	4
Toe Off (TO)	38	23
Heel Strike 2 (HS2)	50	34

Figure 5.6 presents computed pelvis angles. Examination of graphs reveals that plots obtained from both data sets overlapped completely. This was an expected result since these angles were calculated using pelvis segment marker coordinates, which were common to both data sets.
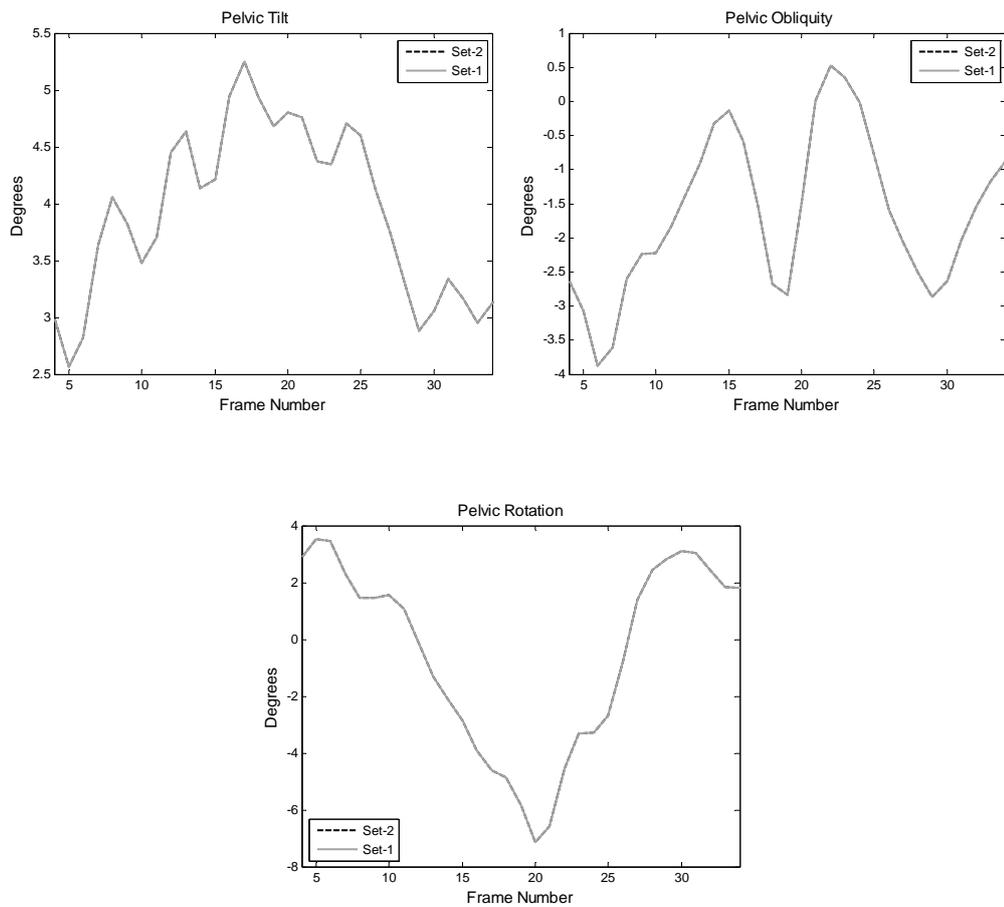
Figure 5.6 Raw Pelvis Angles

Raw hip angle graphs (Figure 5.7) illustrate that hip flexion/extension and abduction/adduction plots obtained from both sets were in quite good agreement. Very slight shifts were present in plots in some regions; however these differences can safely be considered negligible when compared to nominal angle values. Hip rotation angles computed from both sets, on the other hand, showed large amount of variability, as observed from Figure 5.7.
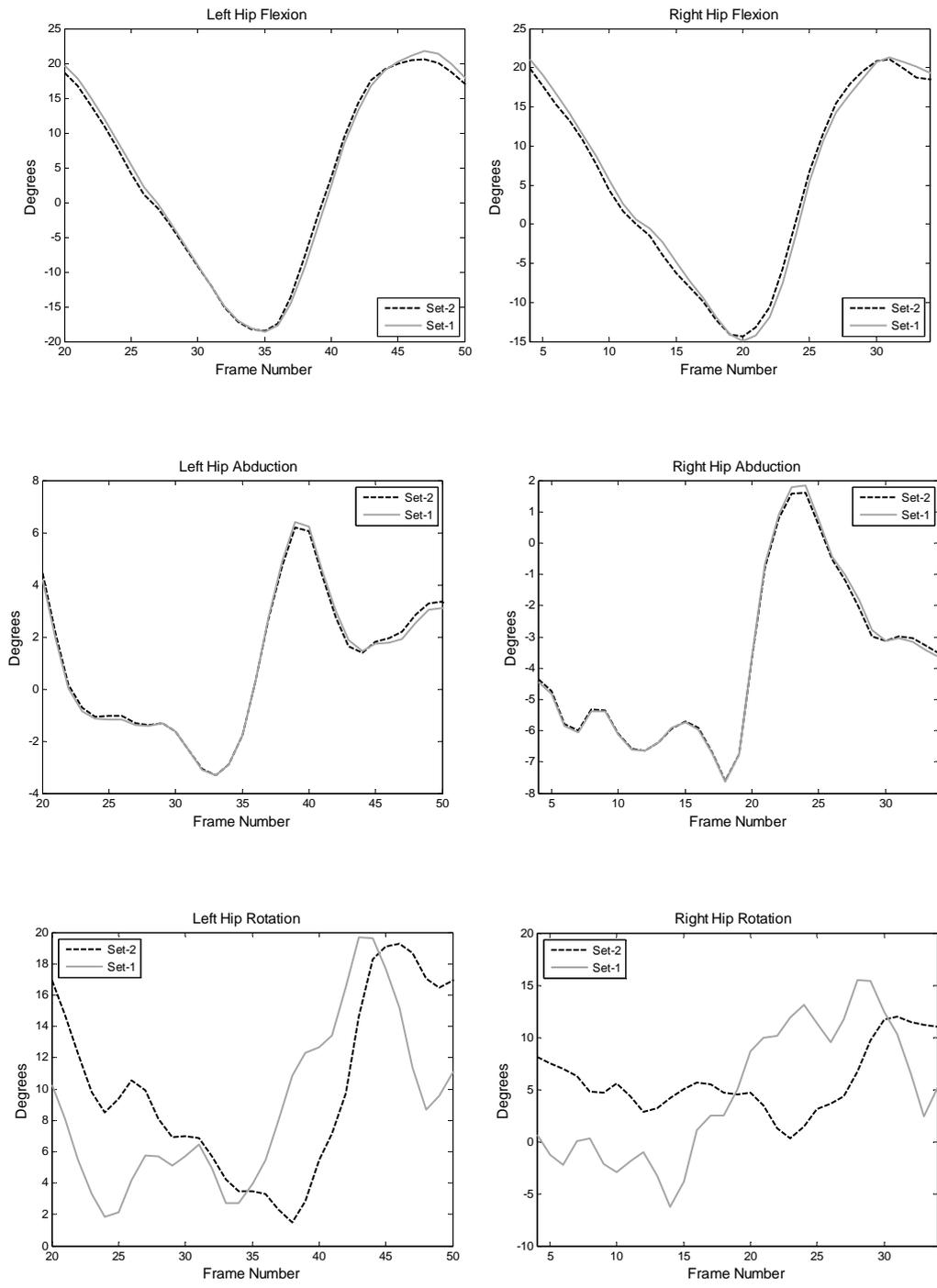
Figure 5.7 Raw Hip Angles

Raw knee joint angle plots are presented in Figure 5.8. In overall, knee flexion/extension angles were observed to be in good agreement, with small shifts in several regions. Internal/external rotation angles again exhibited considerable variations from each other. Examination of knee valgus/varus angle plots revealed another unexpected phenomenon. Set-1 and Set-2 valgus/varus plots deviated from each other in an interval that also corresponds to increasing knee flexion/extension angles. Within this interval, magnitudes of Set-1 (i.e. side marker) valgus/varus angles were much larger than that of Set-2 (i.e. front marker) angles.
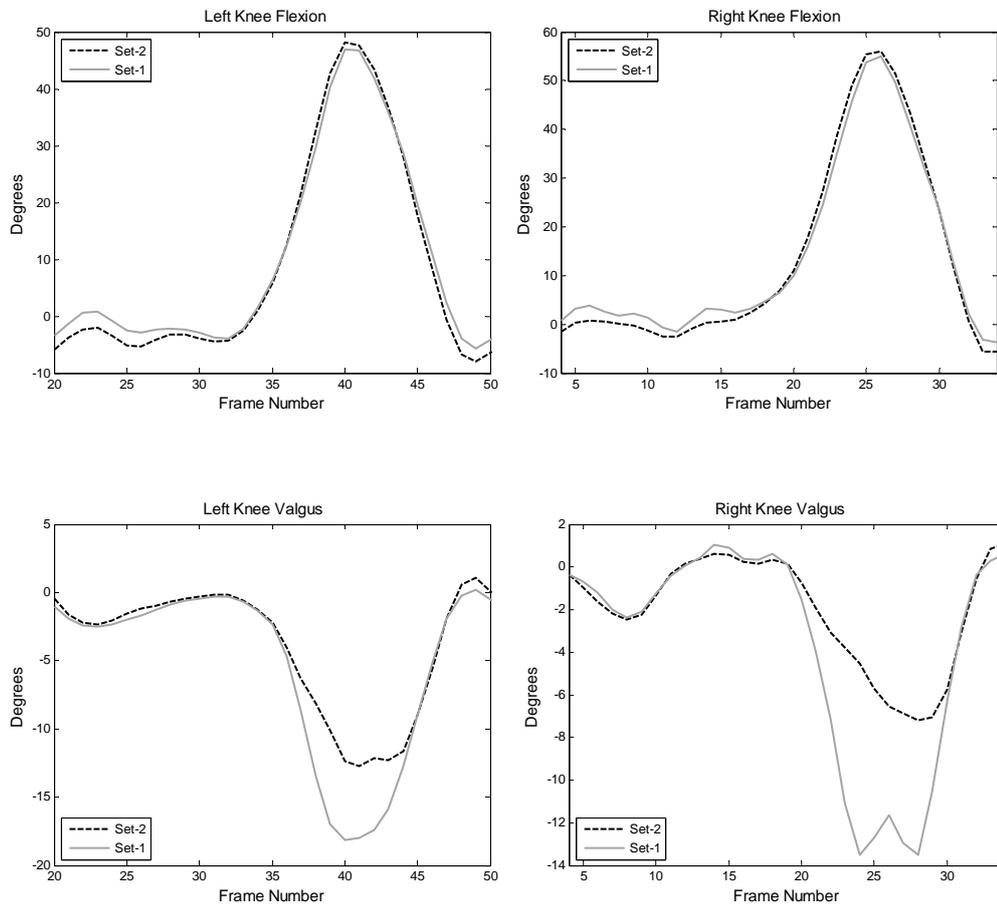
Figure 5.8 Raw Knee Angles
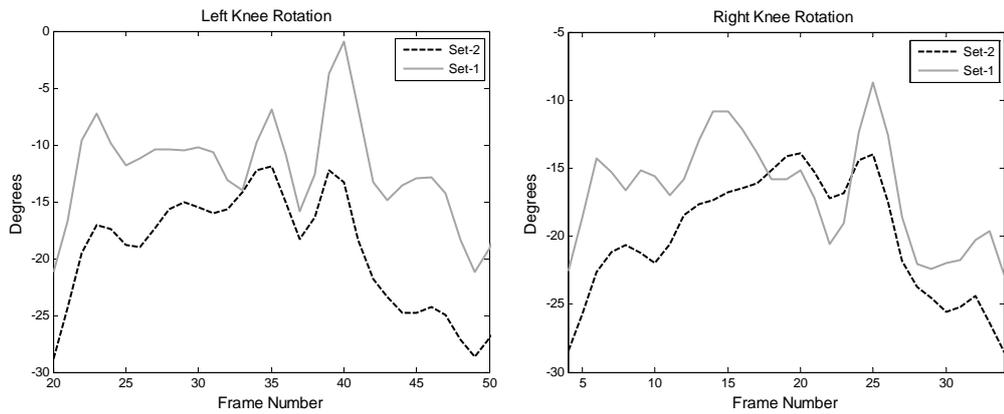
Figure 5.8 (Continued) Raw Knee Angles

Examination of Figure 5.9 reveals the differences between foot angles calculated from both data sets. Ankle dorsi/plantar flexion angle graphs of Set-1 and Set-2 exhibited similar trends; however some shifts were present between graphs. Similar to the results obtained for other joints, foot internal/external rotation angles also turned out to be dissimilar for front and side data sets. Finally, foot alignment angle plots revealed that computed angles agreed to a large extend, again with some slight shifts in several regions.
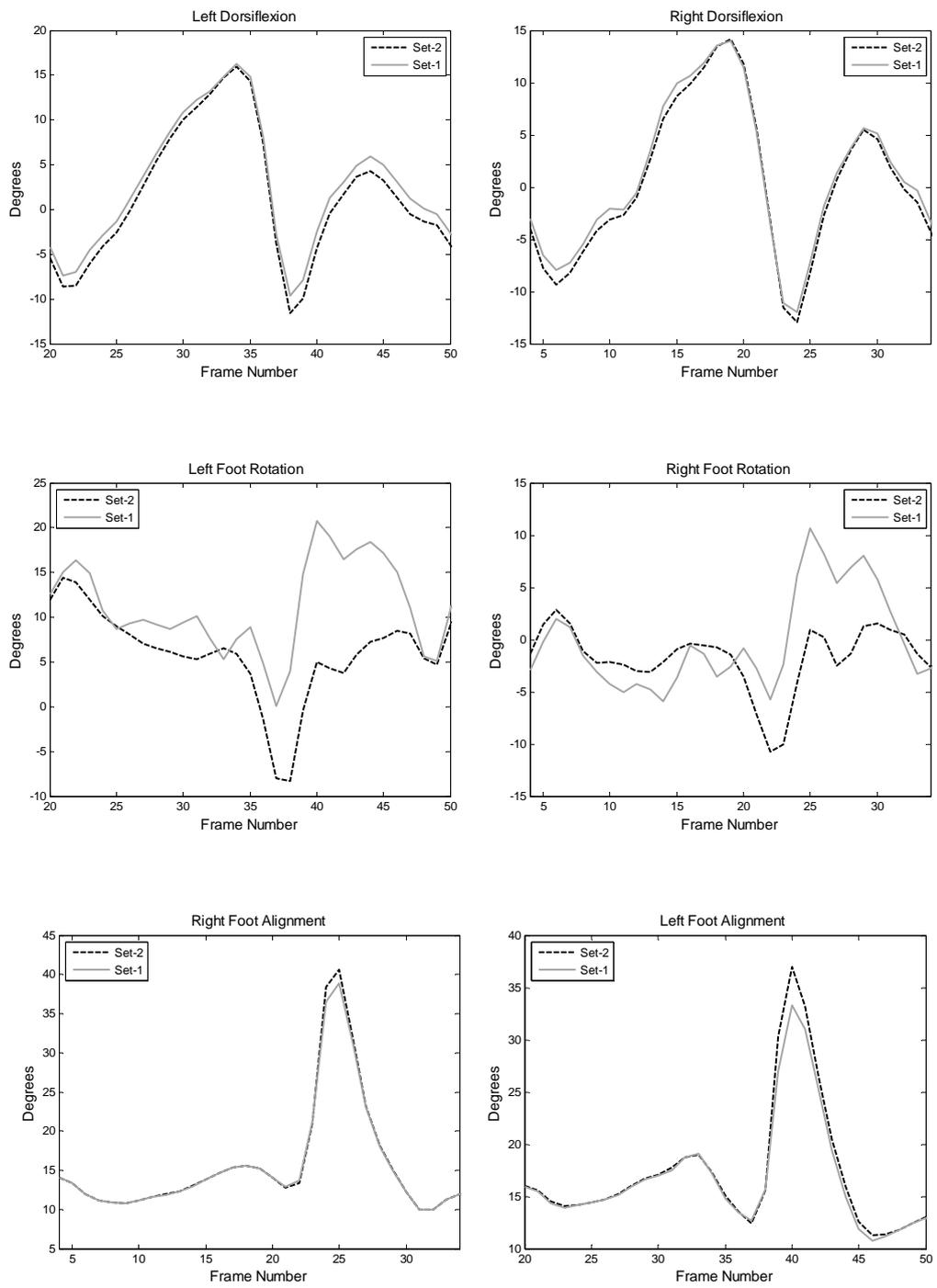
Figure 5.9 Raw Foot Angles

78

Results of Set-1 and Set-2 comparisons for all dynamic trials of each subject are presented in *Appendix C*. Examination of these graphs leads to following general remarks:

- It was observed that differences in thigh and shank marker locations resulted in variations between angles calculated for the two cases. This is an expected result since errors are present in the system. Two most prominent error sources are instrumental errors and errors introduced due to movement of soft tissue under the markers.

- Joint angles computed for each subject's different trials exhibited quite similar trends; which imply the system is successful in representing repeatability of successive trials for each subject. On the other hand, investigation of results from different trials of the same subject revealed that intra-subject variability was reflected on the joint angle plots; slight differences were observed between graphs of each trial of the same subject.

- Effects of different positioning of thigh and shank markers yielded similar results in right and left extremities.

- Due to nature of the kinematics calculation procedure, error propagates from proximal to distal segments. This effect was also observed in the examined graphs; differences between Set-1 and Set-2 plots increased when traveling from pelvis to foot.

- General observation revealed that flexion/extension and abduction/adduction angles (except knee valgus/varus) are not sensitive to changes in thigh and shank marker locations.

- The angles that are most affected from thigh and shank marker relocation were internal/external rotation angles. In rotation plots of each joint, angles computed from Set-1 and Set-2 were found to be almost irrelevant, which suggests the protocol is ineffective in identifying internal/external rotations of the segments.

- Knee valgus/varus plots of Set-1 and Set-2 exhibited significant differences within an interval corresponding to increase in knee flexion/extension angles. Set-1 (i.e. side marker) angles appeared to be significantly larger in magnitude when compared to Set-2 (i.e. front marker) angles in all examined knee varus/valgus graphs, independent of the subject.

In conclusion, Kiss protocol yielded satisfactory results in terms of sensitivity to locations of "free" thigh and shank markers, except for internal/external rotation and knee valgus/varus angles. The large amount of variability observed in internal/external rotation angles can be attributed to the low signal-to-noise ratio as discussed by Güler (1998). In fact, this is a common problem of gait analysis systems and is predictable since tracking segment rotations in the transverse plane is difficult due to the spatial arrangement of the cameras. On the other hand, unexpected differences were observed between knee valgus/varus angles of front and side data sets. Occurrence of this phenomenon in all examined trials suggested that there is a common underlying cause of such behavior, clarification for which was needed and was sought through further investigations.

5.4.2 Individual Effects of Thigh and Shank Marker Positions

As discussed in the previous section, comparison of the joint kinematics calculated from data sets 1 and 2 revealed that joint angles were affected from changes in thigh and shank marker locations. The differences observed within

plots resulted from the combination of changes in both thigh and shank marker locations. Therefore, in order to be able to determine the causes of variations observed in knee valgus/varus angles, individual contributions of thigh and shank marker location changes on resulting kinematics were assessed.

Valgus/varus angles calculated from Set-2, Set-3 and Set-4 data were plotted together with Set-1 angles in three separate graphs in order to facilitate visualization of separate contributions of thigh and shank marker locations on the observed differences. Right segment valgus/varus angle graphs for 18th trial of subject KU are provided below as an illustration (Figure 5.10). First graph, containing Set-1 and Set-3 plots, presents comparison of two cases where the only difference is in shank marker positions. Similarly, joint angle plots of Set-1 and Set-4 presented in the second graph visualizes the effects of thigh marker position change on valgus/varus angles. Finally, combined effect of both thigh and shank marker relocation is presented in the third graph with data sets 1 and 2.

(a)

(b)

(c)
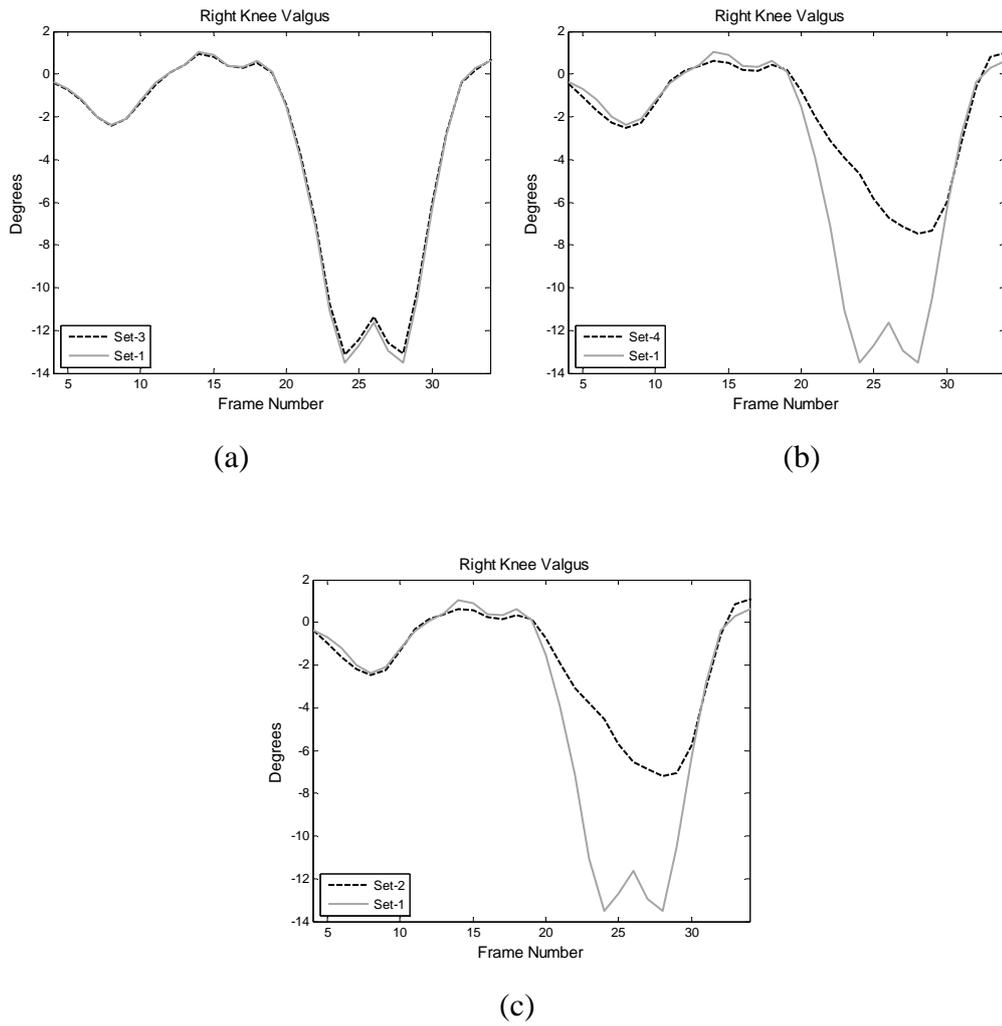
Figure 5.10 Valgus/Varus Angle Comparisons with Different Data Sets

(Solid lines denote Set-1 angles, dashed lines denote
(a) Set-3, (b) Set-4 and (c) Set-2 angles)

Individual effects of thigh and shank marker location changes on valgus/varus angles are clearly reflected in Figure 5.10. Comparison of the graphs reveals that relocating the shank marker did not have any notable effect on the calculated angles. On the contrary, moving thigh marker from side to front

resulted in a significant upward shift in the plot, as observed from Figure 5.10. The same phenomenon was encountered when knee valgus/varus plots of all trials were examined with different data sets; therefore it was concluded that thigh marker relocation from side to front position gives rise to significant changes in these angles. Knee valgus/varus graphs of one selected trial for each subject are provided in *Appendix D.*

5.4.3 Investigation on Set-1 and Set-4 Results

In all gait trials performed with different subjects, similar variations were observed between computed Set-1 and Set-4 knee valgus/varus angles. This common pattern suggested that there was a certain underlying physical cause of these differences. Several parameters were analyzed to identify this phenomenon. Since it was found out that thigh marker location change was responsible for the observed differences; analyses were performed with Set-1 and Set-4 data, where the only difference between two data sets was locations of thigh markers.

Joint angles were calculated from transformation matrices between anatomical reference frames of segments proximal and distal to each joint. For the case of knee joint, proximal and distal segments became thigh and shank, respectively. Transformation matrix between segment anatomical reference frames were, therefore:

$$\hat{C}^{(t,s)} = \hat{C}^{(G,t)T}\hat{C}^{(G,s)} \tag{5.1}$$

Evidently, if differences were present between Set-1 and Set-4 angles, then above discussed proximal to distal transformation matrices of two sets had to be different from each other. Each transformation matrix contained contributions from both thigh and shank anatomical frames; therefore, a direct

correlation was expected between deviation of anatomical frames from each other and differences observed between calculated angles.

In order to quantify deviation of anatomical reference frames from each other at every time instant, root mean squared errors (RMSE) associated with the reference frames were calculated. At each instant, transformation between Set-1 and Set-4 anatomical frames could be obtained as 3x3 orthogonal matrices; which provided information about relative orientation of the frames. Ideally, anatomical frames obtained from two data sets had to be identical, their transformation matrix reducing to an identity matrix. Thus, calculated RMSE provided information about amount of deviation of Set-1 and Set-4 anatomical frames from each other; or, stating differently, amount of deviation of the transformation matrix between anatomical frames from identity matrix, at each time instant.

Transformation matrices between Set-1 and Set-4 anatomical reference frames were computed as

$$\hat{C}^{(t_1, t_4)} = \hat{C}^{(G, t_1)T} \hat{C}^{(G, t_4)} \tag{5.2}$$

$$\hat{C}^{(s_1, s_4)} = \hat{C}^{(G, s_1)T} \hat{C}^{(G, s_4)} \tag{5.3}$$

where t and s denote thigh and shank segments, and 1 and 4 denote Set-1 and Set-4, respectively.

Root mean squared errors of thigh and shank anatomical frames were calculated from the following relation:

$$RMSE = \left(\frac{\displaystyle\sum_{i=1}^{3} \sum_{j=1}^{3} (c_{ij}^{\,2} - I_{ij}^{\,2})}{9} \right)^{1/2} \tag{5.4}$$

where c_{ij} and I_{ij} denote i^{th} row and j^{th} column element of $\hat{C}^{(t_1,t_4)}$ (or $\hat{C}^{(s_1,s_4)}$) and $\hat{I}$ (identity matrix), respectively.

Root mean squared errors associated with thigh and shank anatomical frames were plotted for right and left segments (Figures 5.11 and 5.12), together with knee valgus/varus angles for 18th trial of Subject KU. It was observed that RMSE of thigh and shank frames represent the same trend; however, errors in shank segment were smaller in magnitude when compared to thigh. Furthermore, largest anatomical frame RMSE within the gait cycle corresponded to the time instant where deviation between Set-1 and Set-4 angles were maximum for both segments; which supported the hypothesis that anatomical frame errors and valgus/varus angle differences are directly related.
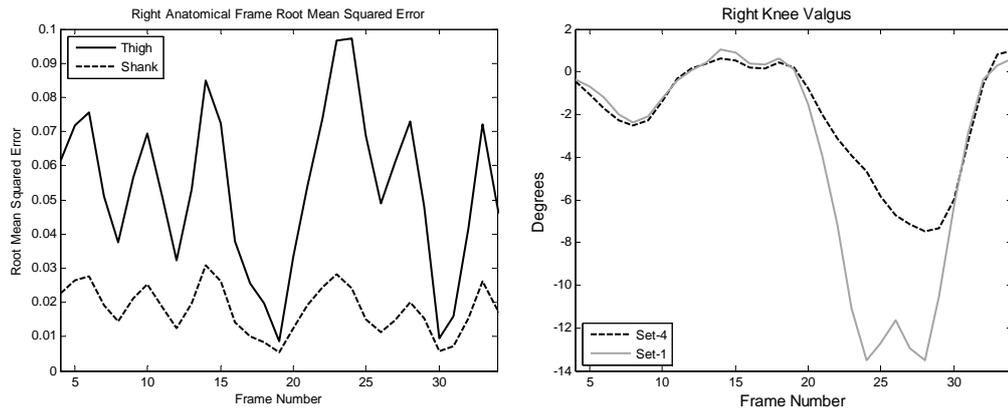
Figure 5.11 Right Segment Anatomical Frame Root Mean Squared Error
and Knee Valgus/Varus Angles

85
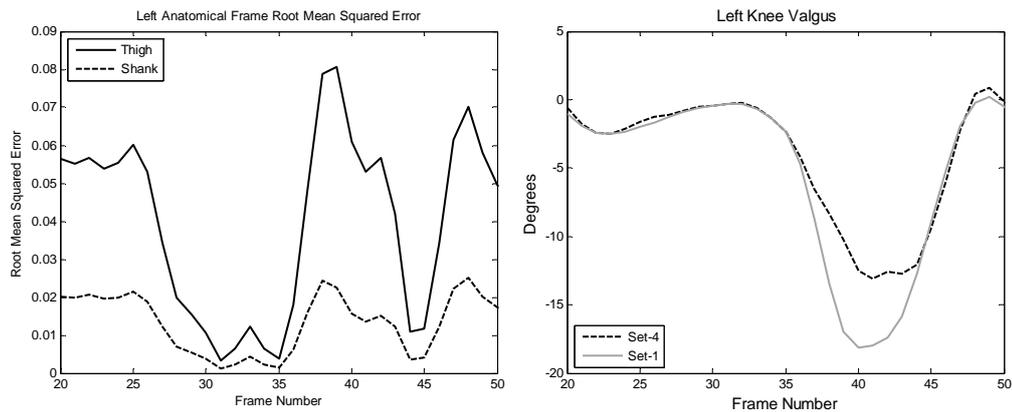
Figure 5.12 Left Segment Anatomical Frame Root Mean Squared Error
and Knee Valgus/Varus Angles

Variations between Set-1 and Set-4 anatomical frames might arise due to two reasons: Numerical errors in reconstructing anatomical frames in dynamic trial, and violation of rigidity assumption. Through a preliminary investigation, numerical errors present in kinematic calculations were found to be rather small, and therefore, negligible. On the other hand, validity of rigidity assumption in calculations was an important parameter that needed to be checked.

If Set-1 and Set-4 technical frames constructed from surface markers were not fixed with respect to each other, anatomical frames obtained through employment of "constant" transformations would also turn out to be different from each other. Due to the nature of the data collection procedure, body segments were defined by the use of markers but the actual relationship between these segments and markers attached on the skin could not be accessed. Therefore, it was not possible to track changes in technical frame position and orientation with respect to the body throughout the gait cycle. However, transformations between side and front technical frames during gait

provided information about the validity of rigidity assumption employed in calculations.

Ideally, Set-1 and Set-4 technical frame transformations had to be constant through gait, and furthermore, also had to be equal to the transformation between technical frames in static shot. Similar to anatomical frames, root mean squared error related to technical frames were then calculated; providing a measure of the deviation of transformation between technical frames in gait from transformation in static shot. Expression for the RMSE then became:

$$RMSE = \left(\frac{\sum\limits_{i=1}^{3}\sum\limits_{j=1}^{3}(c_{ij}{}^2 - c_{s,ij}{}^2)}{9} \right)^{1/2}$$

(5.5)

where c_{ij} and $c_{s,ij}$ denote i^{th} row and j^{th} column element of $\hat{C}^{(t_1{}^*,t_4{}^*)}$ (or $\hat{C}^{(s_1{}^*,s_4{}^*)}$) and $\hat{C}_s{}^{(t_1{}^*,t_4{}^*)}$ (or $\hat{C}_s{}^{(s_1{}^*,s_4{}^*)}$) respectively; with $\hat{C}$ being the transformation matrix in dynamic trial and $\hat{C}_s$ being the transformation matrix in static shot.

Figure 5.13 shows calculated root mean squared errors of thigh technical frames. RMSE patterns of both technical and anatomical reference frames were found to be identical, with the error reaching its maximum value at the instant where Set-1 and Set-4 valgus/varus angles show largest deviations from each other. This outcome stated that presence of differences in anatomical reference frames constructed from the two data sets was directly related to relative orientation changes between Set-1 and Set-2 thigh technical frames.
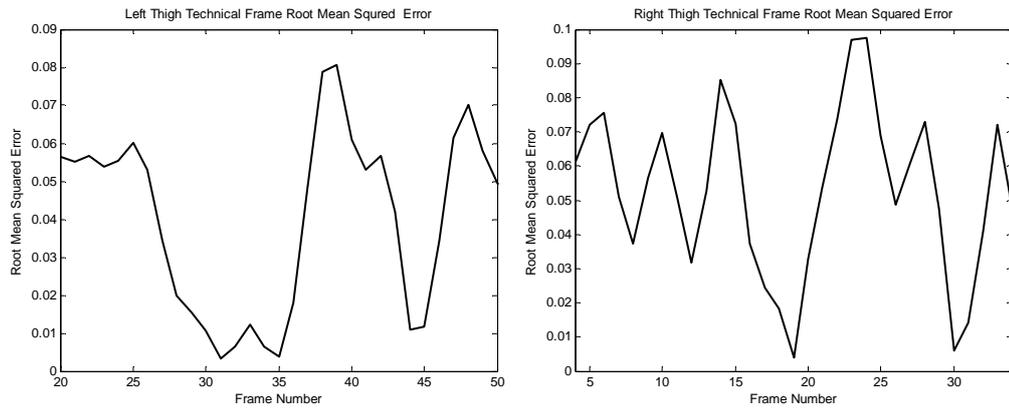
Figure 5.13 Thigh Technical Frame Root Mean Squared Errors

Causes of variations in thigh technical frame orientations with respect to each other were assessed through examination of thigh segment marker coordinates. Thigh marker, knee marker and hip joint center (HJC) were employed in constructing thigh technical reference frame. Therefore, variations in distances between these markers, as well as the angle between knee-HJC and knee-thigh vectors during gait were worth investigating regarding rigidity of marker-based segment definitions.

Thigh-knee marker distances for Set-1 and Set-4 are presented for right and left segments in Figure 5.14. Mean and standard deviations of thigh-knee marker distances for right and left segments are also provided in Table 5.3.
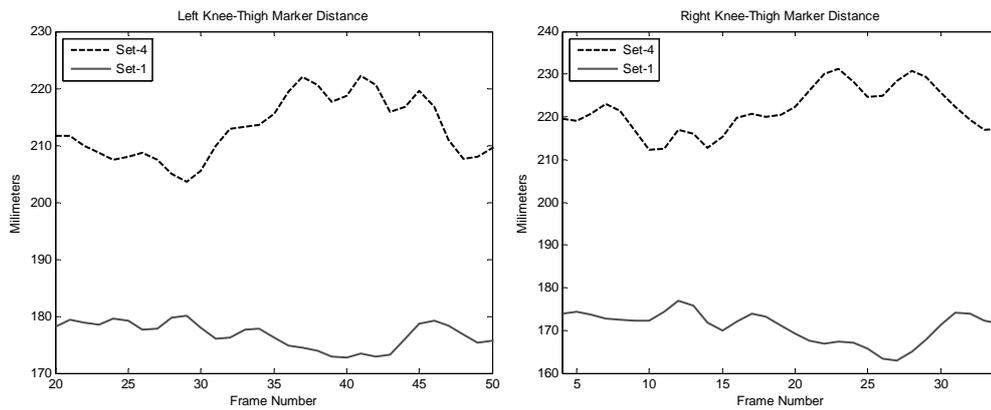
Figure 5.14 Knee-Thigh Marker Distances

Table 5.3 Mean Values and Standard Deviations of

Knee-Thigh Marker Distances

Knee-Thigh Marker Distance	Mean (Millimeters)	Standard Deviation (Millimeters)
Right Segment, Set 1	170,35	4,03
Right Segment, Set 4	221,43	6,12
Left Segment, Set 1	177,03	2,45
Left Segment, Set 4	212,86	6,07

Thigh-knee marker distance data revealed no information that could directly be linked to the movement of thigh segment technical frames relative to each other, which should be arising from changes in marker locations. However, an investigation on the plots reveals that knee-thigh marker distances increased and decreased, respectively, for front and side thigh marker locations within the interval where valgus/varus angles deviated from each other. Furthermore,

89

Set-4 distances showed larger standard deviations compared to Set-1 values for both right and left segments.

The angle between vectors knee-HJC and knee-thigh, defined as α, is shown in Figure 5.15. Variation of this angle in time is presented below for side and front data sets (Figure 5.16). Mean values and standard deviations of α are also presented in Table 5.4.

Figure 5.15 Definition of Angle α
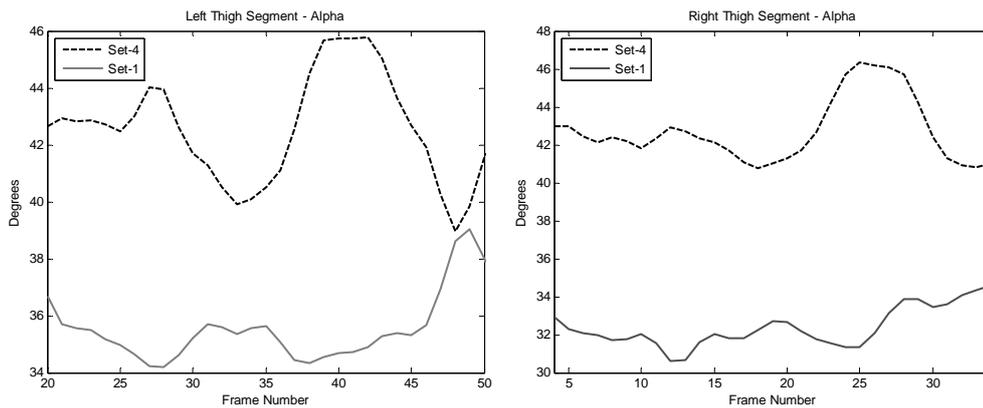
Figure 5.16 Angle between Knee-Thigh and Knee-Hip Joint Center Vectors (α)

Table 5.4 Mean Values and Standard Deviations of the Angle between
Knee-Thigh and Knee-Hip Joint Center Vectors (α)

Angle between knee-thigh and knee-HJC vectors , α	Mean (Degrees)	Standard Deviation (Degrees)
Right Segment, Set 1	32,42	1,04
Right Segment, Set 4	42,69	1,75
Left Segment, Set 1	35,54	1,18
Left Segment, Set 4	42,65	1,72

Figure 5.16 reveals that α values also showed variations throughout the gait cycle. Similar to the case with knee-thigh marker distances, α values obtained for front thigh marker set were greater in magnitude as compared to mean value within the interval where valgus/varus angle differences were observed for Set-1 and Set-4. Again, Set-4 angles had larger standard deviations for both right and left segments as compared to Set-1 values.

Analyses of Set-1 and Set-4 data were performed for all trials, following the methodology presented in this section. Results are presented for one selected trial of each subject in *Appendix E.*

In summary, analyses performed with two different shank and thigh marker locations showed that variations in these marker locations imposed changes on resulting joint kinematics. Most unexpected outcome of these analyses was the changes observed in knee valgus/varus angles. This phenomenon was found to be a consequence of relocating thigh marker from lateral to anterior aspect of the segment. With the hypothesis that differences in calculated angles resulted from violation of rigidity assumption, further assessments were performed to

identify causes of the problem. It was observed that, within the interval where valgus/varus angles of both data sets deviated from each other, errors associated with constructed technical and anatomical frames were largest. Assessments on knee-thigh marker distances, as well as the angle between knee-thigh and knee-hip joint center vectors revealed that these parameters varied within the gait cycle. This is true for both sets; however, differences observed in knee valgus/varus angles were results of the differences between parameters of the two sets. This effect is reflected in graphs of α, where front set thigh segment angle showed a considerable trend difference as compared to side marker set within the related interval of knee valgus/varus difference. Since information about marker movement relative to body segments during gait trials were not available, definite cause of this situation could not be identified. However, presence of the same phenomenon in all trials of different subjects suggested that there was a common reason to this problem. Front thigh marker set plots of α revealed that its increase during swing phase of the foot also corresponded to interval of difference in valgus/varus angles. This trend of α within the swing phase demonstrated that a substantive change took place in thigh marker coordinates in this interval; the most probable reason being movement of markers relative to the bone, due muscle activations in the frontal segments where thigh markers were attached.

CHAPTER 6

AN INVESTIGATION ON PERFORMANCES OF
VARIOUS JOINT CENTER ESTIMATION METHODS
IN METU GAIT ANALYSIS SYSTEM

6.1 Background

Estimation of joint center coordinates is a fundamental, yet challenging task in gait analysis studies. Being sited "inside" the body, these anatomical landmarks cannot directly be tracked by the cameras; therefore their locations have to be determined from surface marker coordinates via utilization of mathematical models.

Presence of errors in locating joint centers directly influence position and orientation of constructed segmental anatomical frames, which in turn affect estimation of joint kinematics and kinetics. In other words, accurate and precise determination of joint centers is crucial to obtain reliable results in gait analysis studies. In this sense, performance of a joint center estimation method becomes an important parameter that directly affects gait analysis system performance.

As for all motion analysis systems that employ stereophotogrammetric techniques, joint kinematics and kinetics calculations performed in METU Gait Analysis System are also directly affected from errors in determination of joint centers. Söylemez (2002) investigated results of hip joint center dislocation as well as effects of varying centering device placement on joint kinematics outputs of Kiss; concluding that resulting kinematics were significantly affected from variations in joint center coordinates. Söylemez also stated that a

new method must be implemented for estimating joint angles without utilization of centering devices to locate ankle and knee centers.

Several approaches have hitherto been adopted in literature for estimation of joint centers from stereophotogrammetric data, as discussed in Section 2. Both predictive and functional approaches are widely employed in gait analysis studies to locate hip joint centers. Although being a straightforward approach, utilization of predictive methods in clinical studies is considered unsafe since they are based on small population data (Della Croce et al., 2005). Furthermore, these methods may fail in accurately determining hip joint center in certain cases such as pelvic deformities. Functional methods, on the other hand, may provide better estimation of subject-specific hip joint center locations since movement information of thigh segment relative to pelvis is utilized in the calculations. Main limitation of functional methods is that they require special hip motion trials with adequate sagittal and frontal plane movement range for accurate estimation of hip joint center, which may be inapplicable for patients with limited range of motion.

Various knee axis and center estimation methods are also presented in literature. Determination of knee joint center from medial and lateral femoral epicondyle locations through anatomical landmark calibration procedures is a commonly employed method. Performance of this method is highly dependent on skill of the performer since accurate and repeatable identification of femoral epicondyles is difficult. Helical axis method is another approach utilized for identification of knee axis; however, it is widely affected by measurement errors and may provide results that are not clinically interpretable. One other commonly employed knee joint center location method is used in conjunction with Helen Hayes marker set; locating knee joint center by assuming it lays in thigh frontal plane defined by thigh segment markers. Vicon Motion Systems (Vicon Motion Systems Ltd., Oxford, UK), a commercial gait analysis system

widely employed in clinical gait analysis laboratories throughout the world, uses this method for knee joint center estimation. Main drawback of this method is that its performance is highly dependent on correct positioning of the thigh marker.

In this part of the study, several hip and knee joint center estimation methods were adapted to Kiss protocol, with the purpose of investigating their performances through experiments performed at METU Gait Analysis Laboratory. These selected methods are presented in this chapter, and results provided by the methods are evaluated based on calculated joint center coordinates and their effects on joint kinematics.

6.2 Hip Joint Center Estimation Methods

In this study, three different hip joint center estimation methods available in literature were employed. First method utilizes the predictive approach as presented by Davis et al. (1991). Other two methods use functional approach for determining hip joint center. First functional method utilizes an iterative sphere fitting algorithm, which computes hip joint center from trajectory of the knee joint center. Second functional method employs constructed pelvis and thigh reference frames to identify hip joint center location using linear least squares approach.

6.2.1 Davis' Method

The method proposed by Davis et al. (1991) employs a predictive approach developed from radiographic hip studies. The method locates hip joint center in pelvis reference frame via a regression equation that uses anthropometric measurements from the subject, marker radius and generalized constants.

In current protocol of METU Gait Analysis Laboratory, Davis' method is utilized for hip joint center estimation. Formulation of this method is presented by Söylemez (2002) as follows:

$$X_H = [-x_{dis} - r_{marker}]\cos(\beta) + C\cos(\theta)\sin(\beta) \qquad (6.1)$$

$$Y_H = [-x_{dis} - r_{marker}]\sin(\beta) - C\cos(\theta)\cos(\beta) \qquad (6.2)$$

$$Y_H = -\sigma\left[C\sin(\theta) - \frac{d_{ASIS}}{2}\right] \qquad (6.3)$$

where

$$C = 0.115 L_{leg} - 15.3 \qquad (6.4)$$

$$x_{dis} = 0.1288 \cdot L_{leg} - 48,56 \qquad (6.5)$$

$$\beta = 18°, \quad \theta = 28.4°$$

r_{marker} = 12.7 mm (Marker radius)

$\sigma = +1$ for the right extremity and $\sigma = -1$ for the left extremity

L_{leg} : Leg length, in mm

d_{ASIS} : Distance between right and left Anterior Superior Iliac Spines

As presented by Equations (6.1)–(6.5), Davis' method determines hip joint center as a fixed point in pelvis reference frame. Then, hip joint center coordinates in fixed laboratory reference frame at each time instant are computed using the following equation:

$$\overline{r}_{HJC}{}^{(G)} = \overline{r}_{PLVC}{}^{(G)} + \hat{C}^{(G,p)}\overline{r}_{HJC,P}^{(p)} \tag{6.6}$$

where $\overline{r}_{PLVC}{}^{(G)}$ denotes pelvis center coordinates expressed in fixed laboratory reference frame, $\hat{C}^{(G,p)}$ is the transformation matrix between pelvis and fixed laboratory frames, and $\overline{r}_{HJC,P}^{(p)}$ is the hip joint center localized to pelvis frame with its expression given as

$$\overline{r}_{HJC,P}^{(p)} = \begin{bmatrix} X_H \\ Y_H \\ Z_H \end{bmatrix} \tag{6.7}$$

6.2.2 Iterative Sphere Fitting Algorithm

First functional hip joint center estimation method adapted to Kiss protocol was an iterative sphere fitting algorithm presented by Hicks and Richards (2005). In their study, Hicks and Richards compared performances of three sphere fitting algorithms using computer generated data and employed the method that yielded the most satisfactory results for clinical assessment. This method, which is an iterative sphere fitting algorithm utilizing Newton's method, was adapted to Kiss protocol for assessment of its performance in METU Gait Analysis System.

Main objective of the employed sphere fitting algorithm is to minimize the following expression:

$$\varepsilon_i = \sqrt{(x_i - x_c)^2 + (y_i - y_c)^2 + (z_i - z_c)^2} - r \tag{6.8}$$

In the above equation (x_i, y_i, z_i) are coordinates of any point in the given data set, (x_c, y_c, z_c) are coordinates of the sphere center, r is sphere radius and ε_i is the error function.

The algorithm computes sphere radius and sphere center coordinates by assuming the error associated with each data point is zero. Then, for a set containing n data points, the system of equations becomes:

$$\varepsilon_1 = \sqrt{(x_1 - x_k)^2 + (y_1 - y_k)^2 + (z_1 - z_k)^2} - r_k = 0$$

$$\varepsilon_2 = \sqrt{(x_2 - x_k)^2 + (y_2 - y_k)^2 + (z_2 - z_k)^2} - r_k = 0 \tag{6.9}$$

$$\vdots$$

$$\varepsilon_n = \sqrt{(x_n - x_k)^2 + (y_n - y_k)^2 + (z_n - z_k)^2} - r_k = 0$$

where k represents number of iterations.

The calculation procedure starts at $k = 0$ with initial guesses for (x_k, y_k, z_k) and r_k. In each iteration, improvement vector δ_k is calculated to obtain new estimates of sphere center and radius as follows:

$$\begin{bmatrix} x_{k+1} \\ y_{k+1} \\ z_{k+1} \\ r_{k+1} \end{bmatrix} = \begin{bmatrix} x_k \\ y_k \\ z_k \\ r_k \end{bmatrix} + \delta_k \tag{6.10}$$

The improvement vector δ_k is calculated from the equation

$$J_k \delta_k = -F_k \qquad (6.11)$$

where F_k is the error function and J_k is the Jacobian of this function, with expressions given as

$$F_k = \begin{bmatrix} \varepsilon_1 \\ \varepsilon_2 \\ \vdots \\ \varepsilon_n \end{bmatrix} = \begin{bmatrix} \sqrt{(x_1 - x_k)^2 + (y_1 - y_k)^2 + (z_1 - z_k)^2} - r_k \\ \sqrt{(x_2 - x_k)^2 + (y_2 - y_k)^2 + (z_2 - z_k)^2} - r_k \\ \vdots \\ \sqrt{(x_n - x_k)^2 + (y_n - y_k)^2 + (z_n - z_k)^2} - r_k \end{bmatrix} \qquad (6.12)$$

$$J_k = \begin{bmatrix} \dfrac{\partial \varepsilon_1}{\partial x_k} & \dfrac{\partial \varepsilon_1}{\partial y_k} & \dfrac{\partial \varepsilon_1}{\partial z_k} & \dfrac{\partial \varepsilon_1}{\partial r_k} \\[2mm] \dfrac{\partial \varepsilon_2}{\partial x_k} & \dfrac{\partial \varepsilon_2}{\partial y_k} & \dfrac{\partial \varepsilon_2}{\partial z_k} & \dfrac{\partial \varepsilon_2}{\partial r_k} \\[2mm] \vdots & \vdots & \vdots & \vdots \\[2mm] \dfrac{\partial \varepsilon_n}{\partial x_k} & \dfrac{\partial \varepsilon_n}{\partial y_k} & \dfrac{\partial \varepsilon_n}{\partial z_k} & \dfrac{\partial \varepsilon_n}{\partial r_k} \end{bmatrix} = \begin{bmatrix} -\dfrac{(x_1 - x_k)}{r_k} & -\dfrac{(y_1 - y_k)}{r_k} & -\dfrac{(z_1 - z_k)}{r_k} & -1 \\[2mm] -\dfrac{(x_2 - x_k)}{r_k} & -\dfrac{(y_2 - y_k)}{r_k} & -\dfrac{(z_2 - z_k)}{r_k} & -1 \\[2mm] \vdots & \vdots & \vdots & -1 \\[2mm] -\dfrac{(x_n - x_k)}{r_k} & -\dfrac{(y_n - y_k)}{r_k} & -\dfrac{(z_n - z_k)}{r_k} & -1 \end{bmatrix}$$

$$(6.13)$$

Hicks and Richards (2005) utilized knee joint center coordinates expressed in pelvis reference frame as the input data to the algorithm. Initial guess for hip joint center coordinates were obtained from the least squares algorithm presented in their study.

In adaptation of this method to Kiss system, reconstructed knee joint center coordinates were used to compute the hip joint center. As an initial guess, hip joint center coordinates computed from the predictive method (Davis et al., 1991) were used and iterations were performed until difference between two successive iterations was less than 10^{-3} mm, as presented by Hicks and Richards (2005).

The algorithm calculates hip joint center coordinates localized to pelvis frame, from knee and hip joint center (as initial guess for algorithm) coordinates which are also expressed in pelvis frame. Therefore, global coordinates of these points were first converted into pelvis frame coordinates by use of the following relations:

$$\overline{r}_{HJC,p}{}^{(p)} = \hat{C}^{(G,p)T} \left(\overline{r}_{HJC}{}^{(G)} - \overline{r}_{PLVC}{}^{(G)} \right) \tag{6.14}$$

$$\overline{r}_{KJC,p}{}^{(p)} = \hat{C}^{(G,p)T} \left(\overline{r}_{KJC}{}^{(G)} - \overline{r}_{PLVC}{}^{(G)} \right) \tag{6.15}$$

In the above equations, $\overline{r}_{KJC,p}{}^{(p)}$ and $\overline{r}_{HJC,p}{}^{(p)}$ are knee and hip joint center coordinate vectors, expressed in pelvis reference frame.

Hip joint center coordinates obtained from the sphere fitting algorithm were then converted into global coordinates as:

$$\overline{r}_{HJC}{}^{(G)} = \overline{r}_{PLVC}{}^{(G)} + \hat{C}^{(G,p)} \overline{r}_{HJC,p}{}^{(p)} \tag{6.16}$$

where $\overline{r}_{HJC,p}{}^{(p)}$ is the new hip joint center coordinate vector localized to pelvis frame, calculated using the sphere fitting algorithm.

6.2.3 Linear Least Squares Algorithm

Second functional hip joint center estimation method adapted to Kiss protocol is an algorithm proposed by Piazza et al. (2004). The method is based on minimization of the distance between estimated pelvis and thigh frame localized hip joint center coordinates, using a linear least squares approach.

Defining hip joint center coordinates in pelvis and thigh anatomical frames as (x, y, z) and (u, v, w); and the 4x4 homogeneous transformation matrix between thigh and pelvis frames as

$$T_{P/T} = \begin{bmatrix} 1 & 0 & 0 & 0 \\ t_x & r_{xx} & r_{xy} & r_{xz} \\ t_y & r_{yx} & r_{yy} & r_{yz} \\ t_z & r_{zx} & r_{zy} & r_{zz} \end{bmatrix}$$ (6.17)

the following function representing squared error can be written for hip:

$$\varepsilon_i^{\,2} = (t_x + r_{xx}u + r_{xy}v + r_{xz}w - x)^2 + (t_y + r_{yx}u + r_{yy}v + r_{yz}w - y)^2 + (t_z + r_{zx}u + r_{zy}v + r_{zz}w - z)^2$$ (6.18)

The above relation expresses hip joint center localized to thigh frame, in pelvis frame to define the square of the distance between pelvis-fixed and thigh-fixed joint centers for i^{th} data in the given set.

For a set consisting of n points, the total squared error is then:

$$SE = \sum_{i=1}^{n} \varepsilon_i^{\,2}$$ (6.19)

Total squared error is minimized by differentiating the above equation with respect to the unknown variables $x, y, z, u, v,$ and w, and setting them equal to zero. The obtained set of linear equations is in the form

$$AX - b = 0$$

where $X^T = [x\ y\ z\ u\ v\ w]$ and A is the symmetric matrix:

$$A = \begin{bmatrix} n & 0 & 0 & -\sum r_{xx} & -\sum r_{xy} & -\sum r_{xz} \\ 0 & n & 0 & -\sum r_{yx} & -\sum r_{yy} & -\sum r_{yz} \\ 0 & 0 & n & -\sum r_{zx} & -\sum r_{zy} & -\sum r_{zz} \\ -\sum r_{xx} & -\sum r_{yx} & -\sum r_{zx} & a_{44} & a_{45} & a_{46} \\ -\sum r_{xy} & -\sum r_{yy} & -\sum r_{zy} & a_{54} & a_{55} & a_{56} \\ -\sum r_{xz} & -\sum r_{yz} & -\sum r_{zz} & a_{64} & a_{65} & a_{66} \end{bmatrix}$$

(6.20)

with

$$a_{44} = \sum r_{xx}^2 + r_{yx}^2 + r_{zx}^2 \tag{6.21}$$

$$a_{45} = a_{54} = \sum r_{xy} r_{xx} + \sum r_{yy} r_{yx} + \sum r_{zy} r_{zx} \tag{6.22}$$

$$a_{46} = a_{64} = \sum r_{xz} r_{xx} + \sum r_{yz} r_{yx} + \sum r_{zz} r_{zx} \tag{6.23}$$

$$a_{55} = \sum r_{xy}^2 + \sum r_{yy}^2 + \sum r_{zy}^2 \tag{6.24}$$

$$a_{56} = a_{65} = \sum r_{xz} r_{xy} + \sum r_{yz} r_{yy} + \sum r_{zz} r_{zy} \tag{6.25}$$

$$a_{66} = \sum r_{xz}^2 + \sum r_{yz}^2 + \sum r_{zz}^2 \tag{6.26}$$

$$b = \begin{bmatrix} \sum t_x \\ \sum t_y \\ \sum t_z \\ -\left(\sum t_x r_{xx} + \sum t_y r_{yx} + \sum t_z r_{zx} \right) \\ -\left(\sum t_x r_{xy} + \sum t_y r_{yy} + \sum t_z r_{zy} \right) \\ -\left(\sum t_x r_{xz} + \sum t_y r_{yz} + \sum t_z r_{zz} \right) \end{bmatrix}$$

(6.27)

Hip joint center coordinates are then calculated by solving for *X*, where the first three elements are hip joint center coordinates localized to pelvis reference frame, and the remaining elements are the coordinates of hip joint center localized to thigh reference frame.

In adaptation of this method to Kiss protocol, homogeneous transformation matrix between pelvis and thigh anatomical frames were employed in the algorithm. As previously, global coordinates of computed hip joint center were determined via the equation

$$\bar{r}_{HJC}{}^{(G)} = \bar{r}_{PLVC}{}^{(G)} + \hat{C}^{(G,p)}\bar{r}_{HJC,p}{}^{(p)} \tag{6.16}$$

where $\bar{r}_{HJC,p}{}^{(p)}$ is the coordinate vector of hip joint center in pelvis frame, calculated from the linear least squares algorithm.

6.3 Knee Joint Center Estimation Methods

Three different methods for knee joint center estimation were adapted to Kiss protocol. First two of these methods are based on anatomical landmark calibration techniques; whereas last method calculates knee joint center solely from dynamic trial data without the need of a static trial. First method utilizes centering devices to locate the knee joint center in static trial, and it is currently employed in Kiss protocol. Second method is the direct attachment of Type 3 markers on medial and lateral femoral epicondyles to locate the knee axis and knee joint center. Finally, knee joint center estimation method employed by Vicon Clinical Manager (VCM) software of Vicon Motion Analysis System (Vicon Motion Systems Ltd., Oxford, UK) was selected to be the third method adapted to Kiss.

6.3.1 Knee Joint Center Estimation Using Centering Devices

The biomechanical model employed by Kiss protocol assumes that knee joint flexion/extension axis passes through lateral and medial femoral epicondyles. As discussed in Chapter 3, knee centering device employed in a regular gait experiment is positioned on the epicondyles so that knee axis is identified by the markers on the centering device. From coordinates of these two markers (IKCD and OKCD), knee axis unit vector is defined as:

$$\vec{u}_k = \frac{\vec{r}_{IKCD} - \vec{r}_{OKCD}}{\left| \vec{r}_{IKCD} - \vec{r}_{OKCD} \right|} \tag{6.28}$$

Knee joint center is then located from knee marker coordinates and knee axis in static trial as:

$$\overline{r}_{KJC}{}^{(G)} = \overline{r}_{KNEE}{}^{(G)} + \left(\frac{KW}{2} + r_{marker} \right) \overline{u}_k{}^{(G)} \tag{6.29}$$

where KW is knee width and r_{marker} is marker radius.

Knee axis can be reconstructed in dynamic trial, by expressing it in static thigh technical reference frame and then employing this information to locate the axis relative to thigh technical frame of dynamic trial.

Knee axis localized to technical reference frame in static shot is calculated using the following relation:

$$\overline{u}_k{}^{(t^*)} = \hat{C}^{(G,t^*)^T} \overline{u}_k{}^{(G)} \tag{6.30}$$

Then, similar to static trial calculations, global knee joint center coordinates in dynamic trial can be obtained from the following formula for each time instant:

$$\bar{r}_{KJC}{}^{(G)} = \bar{r}_{KNEE}{}^{(G)} + \left(\frac{KW}{2} + r_{marker} \right) \hat{C}^{(G,t^*)} \bar{u}_k{}^{(t^*)} \qquad (6.31)$$

6.3.2 Knee Joint Center Estimation from Direct Marker Attachment on Knee

As an alternative to employing centering devices, knee axis may be located in static shot by placing markers directly on lateral and medial femoral epicondyles.

Representing lateral and medial marker position vectors as $\vec{r}_{KN,L}$ and $\vec{r}_{KN,M}$, knee axis is located similar as in the case of centering device method as follows:

$$\vec{u}_k = \frac{\vec{r}_{KN,L} - \vec{r}_{KN,M}}{\left| \vec{r}_{KN,L} - \vec{r}_{KN,M} \right|} \qquad (6.32)$$

Once knee axis is determined, knee joint center coordinates in static and dynamic trials can be obtained by the use of Equations (5.29) – (5.31).

6.3.3 VCM Method

The method employed by Vicon Clinical Manager (VCM) software locates the knee joint center in dynamic trial, without use of centering devices (as presented by Davis et al., 1991). This method requires attachment of markers on thigh segment such that the hip joint center, knee marker (on lateral femoral epicondyle) and thigh marker construct the frontal plane of the segment. Knee

joint center is then located by aid of a "chord" function, which places the knee joint center at a distance of half knee width from knee marker in frontal plane (Figure 6.1), along knee axis (Civek, 2006).
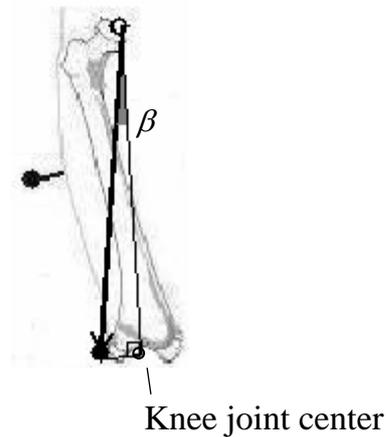
Figure 6.1 Locating Knee Joint Center with Chord Function

When knee width and the distance between knee-hip joint center markers are known, knee joint center can easily be located from the geometry of the problem.

Knee joint center coordinates localized to thigh technical reference frame are calculated as:

$$r_{KJC,V}{}^{(t^*)} = \begin{bmatrix} 0 \\ \left(\dfrac{KW + r_{mar\ker}}{2} \right) \cdot \sin(\beta) \\ \left(\dfrac{KW + r_{mar\ker}}{2} \right) \cdot \cos(\beta) \end{bmatrix} \qquad (6.33)$$

where

$$\beta = \operatorname{atan2}\left(\left(\frac{KW + r_{marker}}{2}\right), \sqrt{d_{KN,HJC}^{\,2} - \left(\frac{KW + r_{marker}}{2}\right)^2}\right) \qquad (6.34)$$

Global knee joint center coordinates are then calculated via the coordinate transformation

$$\overline{r}_{KJC}{}^{(G)} = \overline{r}_{KNEE}{}^{(G)} + \hat{C}^{(G,t^*)} \overline{r}_{KJC,V}{}^{(t^*)} \qquad (6.35)$$

Finally, knee axis is located as:

$$\vec{u}_k = \frac{\vec{r}_{KJC} - \vec{r}_{KNEE}}{\left|\vec{r}_{KJC} - \vec{r}_{KNEE}\right|} \qquad (6.36)$$

6.4 Experiments

Performances of joint center estimation methods adapted to Kiss were investigated through gait experiments. Each new method adapted to the system required modifications to standard experimental procedure; therefore conducted experiments were planned such that requirements of each method were met. Experiments were carried out with three subjects (ED, GK, and KU). having no previous history of musculoskeletal injury or illness. One trial session was performed for each subject, involving acquisition of experimental data for both front/side marker comparison and implementation of new joint center estimation methods, as discussed in Chapter 5. In the first part of the experiment a standard static trial was carried out, in which centering devices were employed for identification of knee and ankle axes (Figure 6.2).
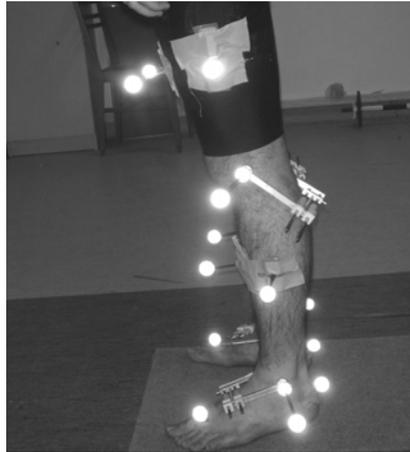
Figure 6.2 Static Shot with Centering Devices

Special care was taken in placing thigh markers since VCM method performance is directly dependent on correct positioning of the thigh marker. Marker placement should be performed so that hip joint center, thigh and knee markers define thigh frontal plane. Knee marker location is the lateral femoral epicondyle as well in VCM protocol, therefore knee marker position was determined by the use of centering devices. As a reference in locating thigh marker, greater trochanter was identified by palpation. Then thigh marker was placed with the aid of a mirror, being in line with greater trochanter and knee marker. After positioning the markers, one static shot with 1 second duration was taken while subject stood in natural upright posture. At the end of the first static trial, centering devices were removed and Type 3 markers were attached directly on lateral and medial femoral epicondyles and malleoli for the second static trial (Figure 6.3). Again, one static shot was recorded for 1 second.

Figure 6.3 Static Shot with Type 3 Markers

Functional hip joint center estimation methods require special hip motion trials to accurately determine the joint center. Subjects carried out a Varied Hip Motion (VHM) trial as suggested by Piazza et al. (2004) in the experiments for this purpose. After completion of the second static shot, medial markers were removed from the subject and VHM trials were performed. Each trial consisted of two circumductions, flexion/extension, abduction/adduction and two further circumductions of the hip and was carried out for left and right legs separately (Figure 6.4). VHM trials were recorded for 14-15 seconds.
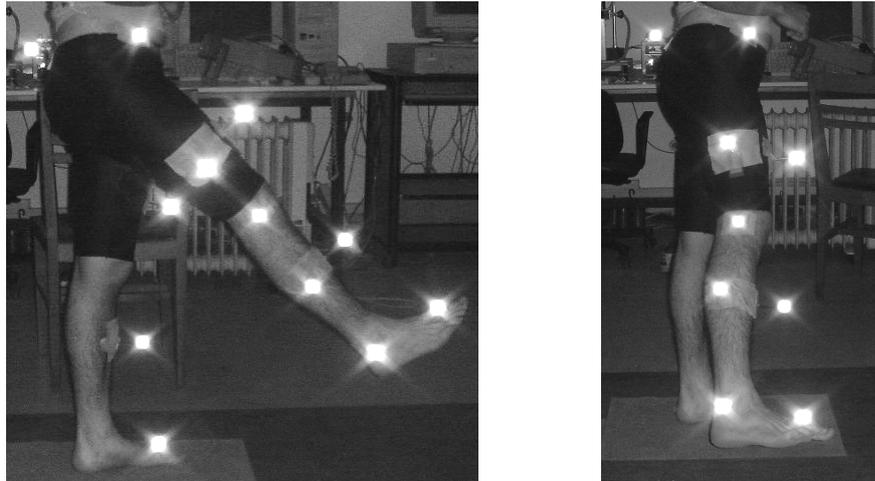
Figure 6.4 Varied Hip Motion (VHM) Trial

Gait trials were performed in the final part of the experiments. Records of 5 seconds duration were taken while the subjects walked along the walkway at a self selected pace. Anthropometric measurements of the subjects were also recorded after the gait trials.

6.5 Analysis

For each trial, recorded camera data were first processed by Motion Tracking program to reconstruct three dimensional marker trajectories. This information was then input in text format to the newly developed, graphical user interfaced Matlab® code together with anthropometric measurements taken from the subject. Gait events were identified interactively for the analyzed gait trial (Figure 6.5). After determination of the gait events, a new window for determination of joint centers using the adapted methods were opened with the "Joint Center Trajectories" button (Figure 6.6).
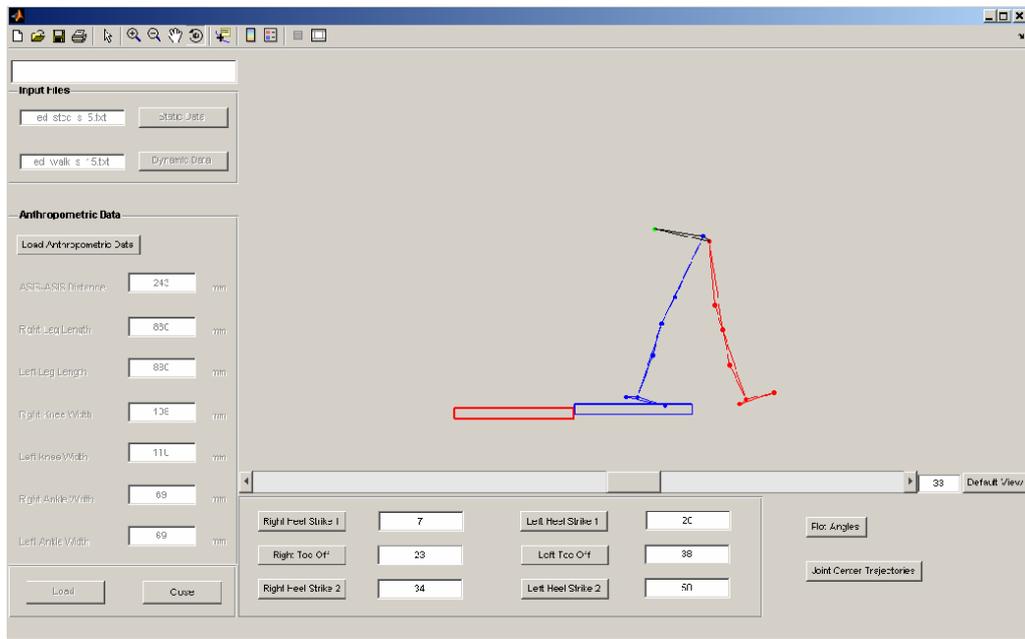
Figure 6.5 Main Window of Program
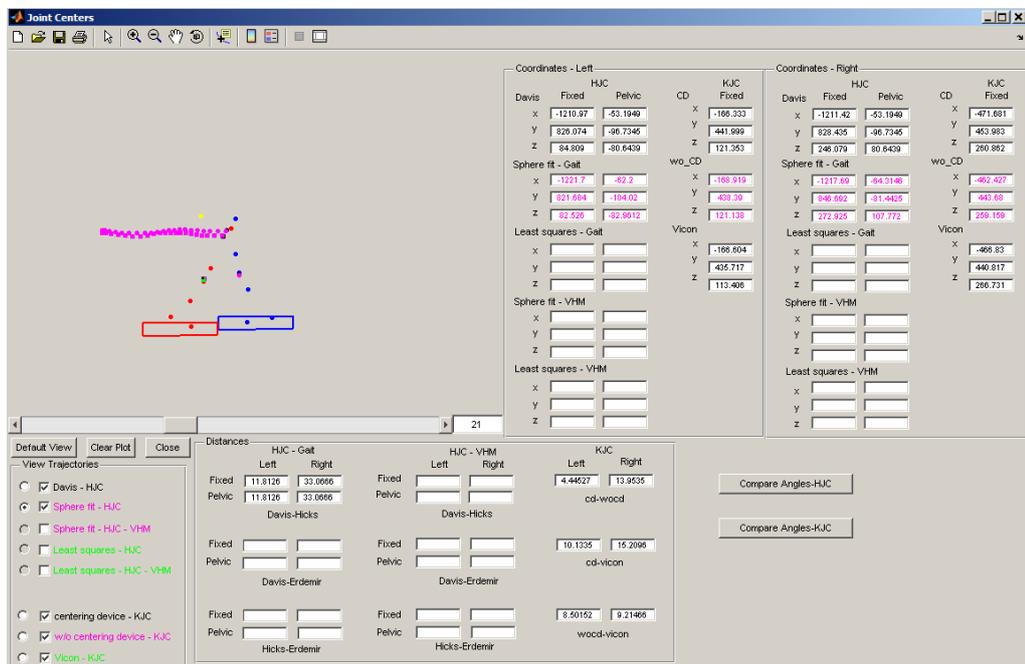
Figure 6.6 Joint Centers Window

"Joint Centers" window enables interactive selection of hip and knee joint center estimation methods to calculate joint center coordinates. If desired, joint center trajectories computed by selected methods can also be viewed. Coordinates of each selected joint center, as well as distances between centers are also displayed as presented in Figure 6.6.

Joint center coordinates estimated from different methods were reconstructed in the gait trial to enable comparison of the results. For functional methods, hip joint centers were separately determined from VHM and gait trial data; then calculated VHM results were transferred into gait trial by use of coordinate transformation. Using Davis' method, hip joint centers were determined from gait trial data. Knee joint centers estimated from static shots with centering device and direct marker attachment were again reconstructed in dynamic trial. Finally, knee joint center was calculated in gait trial for each instant with VCM method.

After determination of hip and knee joint centers, joint angles were calculated. Five different sets of joint angles were constructed, employing results from one hip joint center estimation method in each. Similarly, three separate sets of joint angles were constructed with the three different knee joint center estimation methods.

6.6 Results and Discussion

6.6.1 Estimation of Joint Centers

Performances of new joint center estimation methods adapted to Kiss were firstly assessed in terms of locations of the calculated joint centers. Since the actual positions of hip and knee joint centers were not available, results of each

method were compared with results of hip and knee joint center estimation methods currently employed by Kiss protocol.

Distances between hip joint centers obtained from Davis' method and new methods were computed for right and left segments in each trial, as presented in Table 6.1.

Table 6.1 Hip Joint Center Distances Calculated by Functional Methods
Relative to Davis' Method for All Trials

	Sphere Fit Gait (mm)	Sphere Fit VHM (mm)	Least Squares Gait (mm)	Least Squares VHM (mm)
ED Trial 15, Right	33,07	24,93	11,24	19,33
ED Trial 18, Right	49,86	24,93	10,94	19,33
ED Trial 21, Right	26,39	24,93	12,05	19,33
GK Trial 17, Right	84,09	36,45	7,95	24,19
GK Trial 21, Right	81,26	36,45	6,23	24,19
GK Trial 22, Right	49,65	36,45	11,07	24,19
KU Trial 15, Right	58,92	33,48	1,24	17,45
KU Trial 18, Right	92,23	33,48	2,97	17,45
KU Trial 19, Right	56,29	33,48	0,53	17,45
ED Trial 15, Left	11,81	46,75	8,33	23,76
ED Trial 18, Left	40,03	46,75	3,55	23,76
ED Trial 21, Left	14,00	46,75	6,76	23,76
GK Trial 17, Left	56,39	33,29	1,17	26,77
GK Trial 21, Left	16,35	33,29	3,12	26,77
GK Trial 22, Left	98,60	33,29	4,70	26,77
KU Trial 15, Left	35,26	30,53	12,47	23,05
KU Trial 18, Left	49,65	30,53	14,21	23,05
KU Trial 19, Left	48,63	30,53	15,09	23,05

Similarly, distances of knee joint centers obtained from new methods relative
to centering device results are tabulated in Table 6.2.

Table 6.2 Knee Joint Center Distances Calculated by New Methods Relative to Centering Device Results for All Trials

	Direct Marker Attachment (mm)	VCM Method (mm)
ED Trial 15, Right	13,96	15,27
ED Trial 18, Right	13,96	15,24
ED Trial 21, Right	13,96	15,26
GK Trial 17, Right	3,16	9,06
GK Trial 21, Right	3,16	9,05
GK Trial 22, Right	3,16	9,07
KU Trial 15, Right	15,06	13,51
KU Trial 18, Right	15,06	13,48
KU Trial 19, Right	15,06	13,49
ED Trial 15, Left	4,45	10,17
ED Trial 18, Left	4,45	10,09
ED Trial 21, Left	4,45	10,17
GK Trial 17, Left	12,57	14,05
GK Trial 21, Left	12,57	14,05
GK Trial 22, Left	12,57	14,05
KU Trial 15, Left	12,32	16,73
KU Trial 18, Left	12,32	16,72
KU Trial 19, Left	12,32	16,69

Following remarks can be made regarding the results obtained from evaluated methods:

- All employed hip joint center estimation methods locate hip joint center as a fixed point in pelvis reference frame. Therefore, distances between hip joint centers obtained using different techniques remained constant throughout gait cycle. Similarly, distances between knee joint centers obtained from centering device and direct marker attachment static trials were found to be time invariant since they are located once in the relevant static trial with respect to thigh technical frame.

- Due to the nature of the calculation procedure, hip joint centers estimated from Davis' method and VHM trial results of functional methods, as well as knee joint center locations computed from static trials with centering devices and direct marker attachment, were common to all trials of the same subject.

- VCM method locates knee joint center with respect to thigh technical frame at each time instant. Thus, calculated distances were different throughout the gait cycle and largest distance values with respect to standard method were tabulated in Table 6.2.

- No common pattern could be observed in distance results of employed hip joint center estimation methods, for right and left segments of the same trial, and for different trials of the same subject. Distance of joint centers relative to Davis' method were obtained differently for each method in each trial, largest observed distance being 98,6 millimeters, obtained for 22nd trial of subject GK with sphere fitting method from gait trial data.

- Distances obtained with knee joint center estimation method from direct marker attachment relative to centering devices did not provide consistent results for right and left segments within the same trial, and among trials.

- Consistent distance values were obtained within different trials of each subject with VCM method.

Further assessment regarding performances of the adapted joint center estimation methods in Kiss protocol were performed by computing joint angles with each method and comparing the results. Söylemez (2002) presented a sensitivity analysis where hip joint center coordinates were perturbed ± 30 mm in three principal directions of pelvis reference frame; concluding that these perturbations do not have significant effects on joint kinematics. However, distance values obtained in this study exceeded 30 mm for most of the trials, therefore a new investigation on joint angles were needed. A similar assessment was also necessary to determine effects of knee joint center locations on joints kinematics results of the protocol.

6.6.2 Joint Kinematics Results of Adapted Joint Center Estimation Methods

Hip Joint Center Estimation Methods:

For each performed trial, five different hip joint center values were obtained through adaptation of the new methods to the system. Joint kinematics calculations were then performed separately with each computed hip center and resulting joint angles were plotted.

Changing hip joint center coordinates directly influences hip and knee joint angles. Kinematic results obtained for one selected trial of one subject (Subject KU, Trial 18) are presented below.
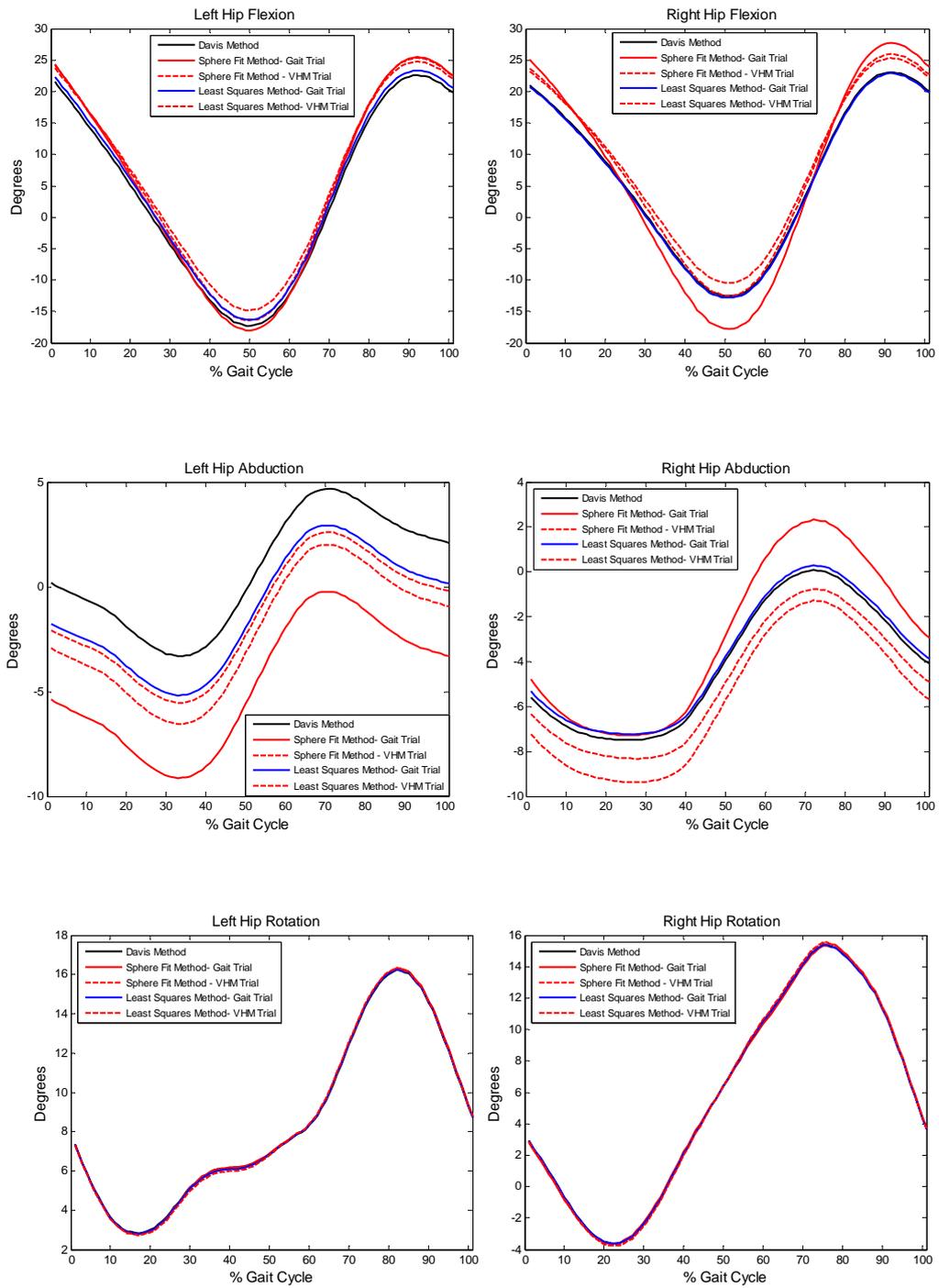
Figure 6.7 Hip Angle Results of Hip Joint Center Estimation Methods

118
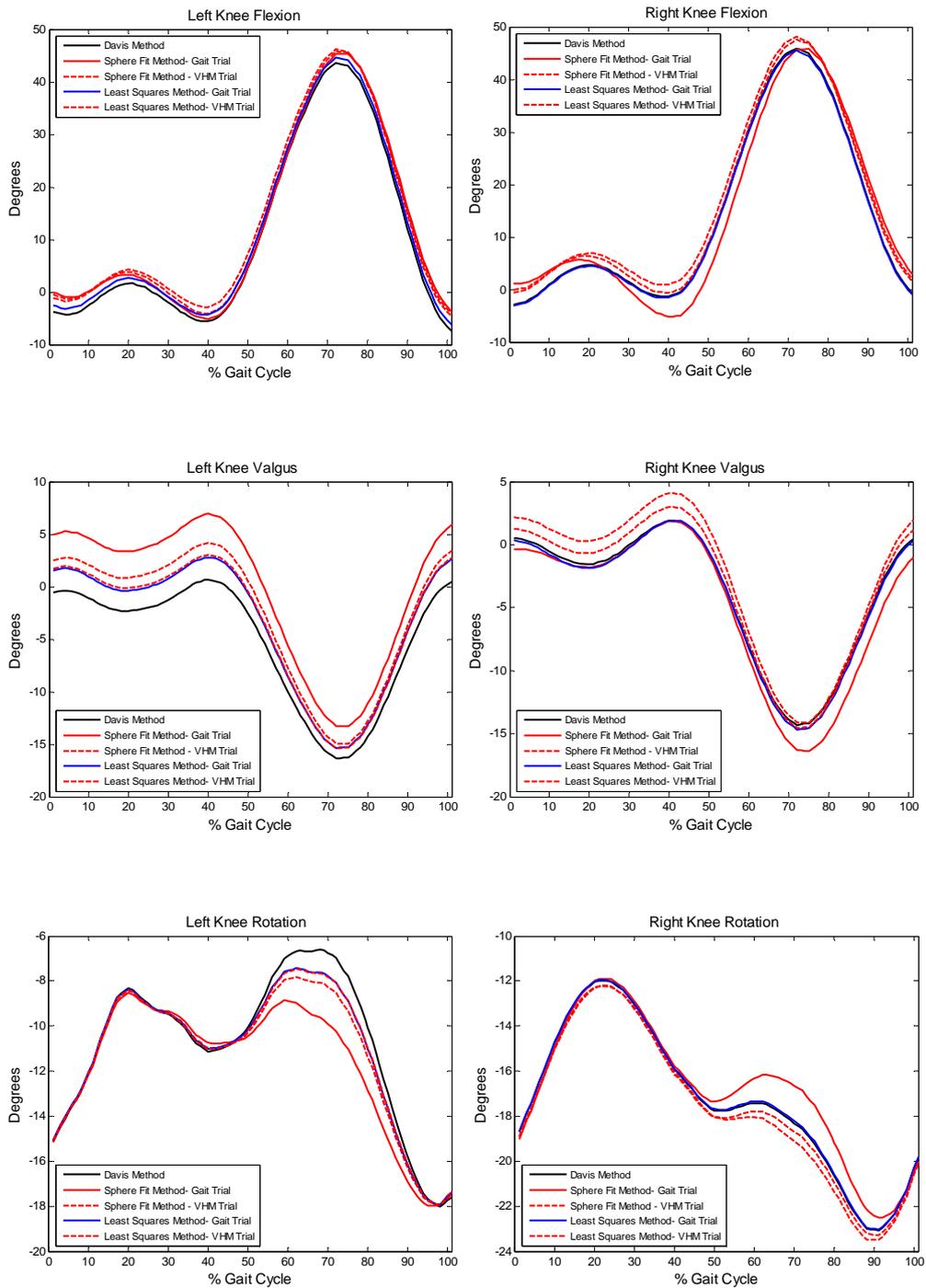
Figure 6.8 Knee Angle Results of Hip Joint Center Estimation Methods

119

Figures 6.7 and 6.8 present joint kinematics with adapted hip joint center estimation methods. Only hip rotation angles were unaffected from differences in hip joint center locations. All remaining joint angles exhibited variations, which were in the form of upward/downward shifts without significant difference in trends. Largest angle variations were observed in left hip abduction/adduction and valgus/varus angles, where the curves were shifted within a range of 5 degrees.

<u>Knee Joint Center Estimation Methods:</u>

Three sets of joint angles were calculated with three different knee joint centers obtained from the adapted methods for each trial. Hip, knee and ankle joint angles, which are affected from changes in knee joint center location, are presented for 18th trial of subject KU in Figures 6.9, 6.10 and 6.11.
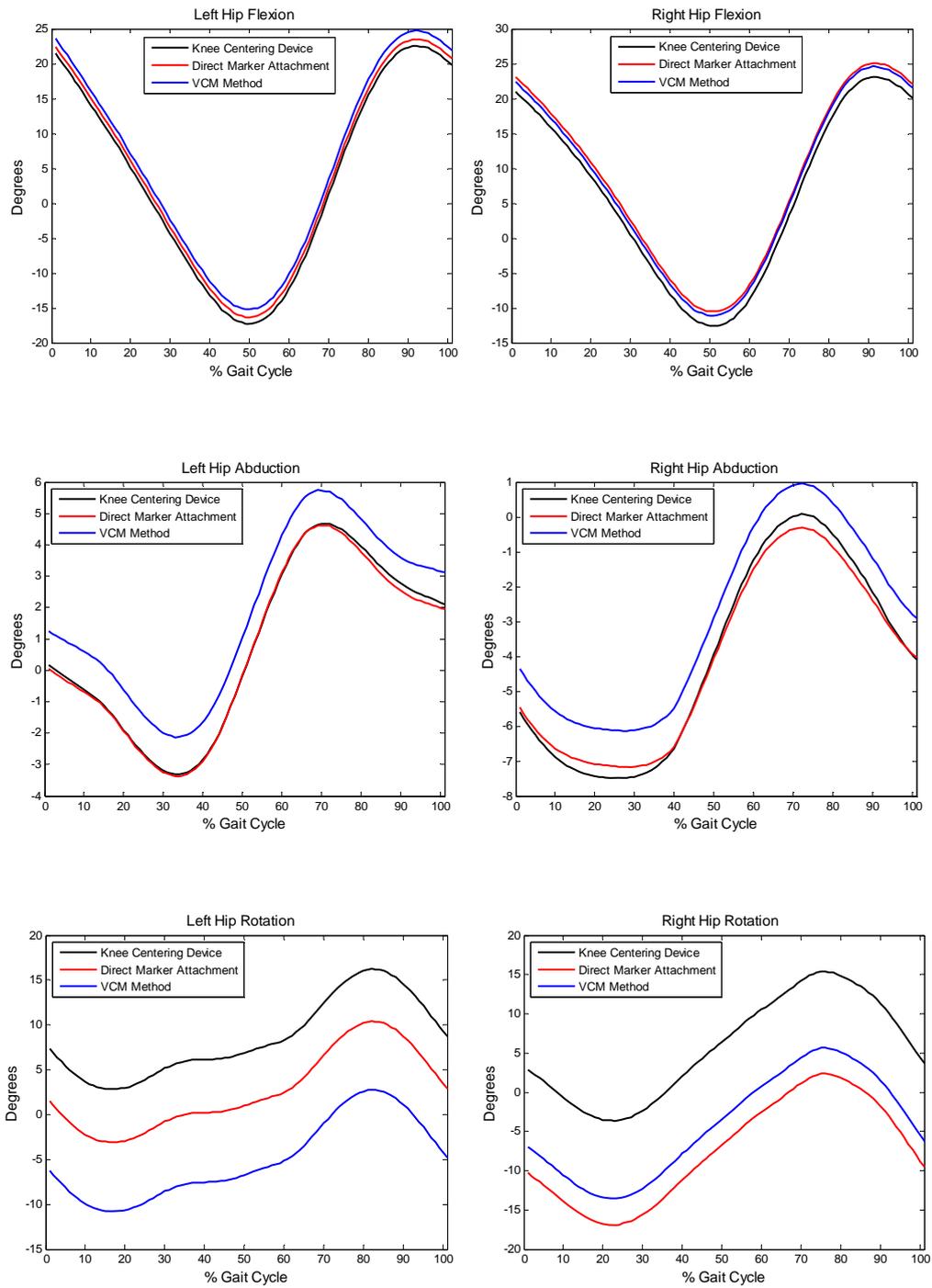
Figure 6.9 Hip Angle Results of Knee Joint Center Estimation Methods
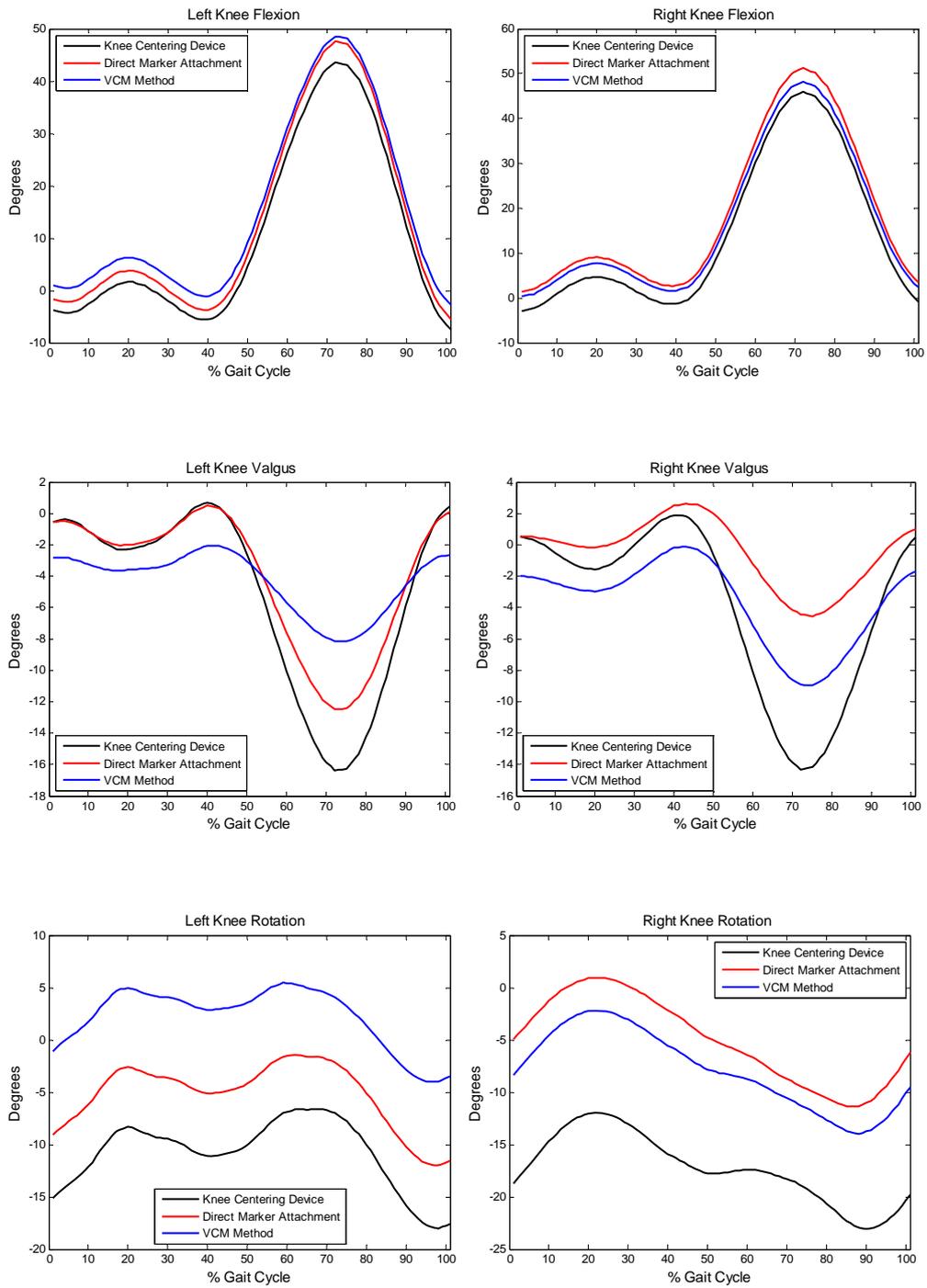
Figure 6.10 Knee Angle Results of Knee Joint Center Estimation Methods
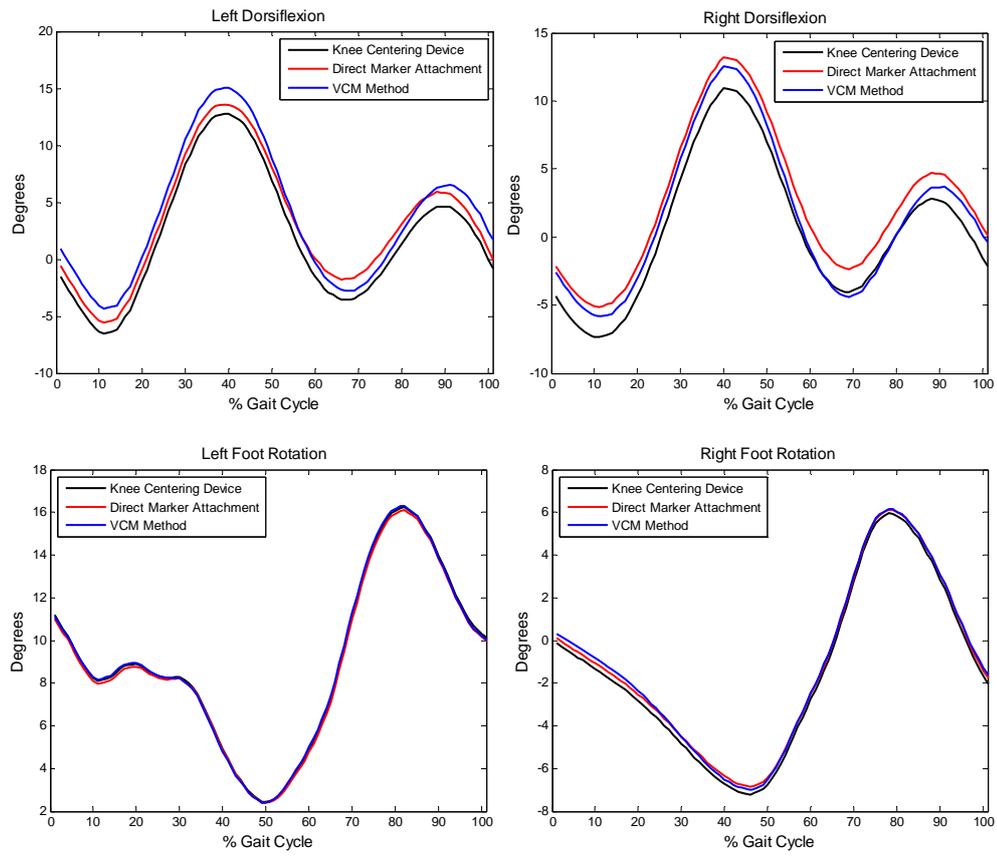
Figure 6.11 Foot Angle Results of Knee Joint Center Estimation Methods

As observed from the graphs, knee joint centers calculated by the three methods affected the resulting joint angles considerably. These effects were in the form of constant downward and upward shifts in hip and knee rotation angles, respectively. On the other hand, knee valgus/varus angles exhibited large variability between methods, both in trend and magnitude. In hip abduction plots, VCM method differed from the remaining two methods with a constant upward shift. Slight upward shifts were also present in sagittal plane angles (i.e. hip flexion, knee flexion, dorsiflexion). Foot rotation angles were least affected from changes in knee joint center locations.

123

6.6.3 Statistical Evaluation

One-way analysis of variance (ANOVA) were performed on joint angles obtained from all trials to investigate whether significant differences existed in joint kinematics results obtained from adapted joint center estimation methods. Significant effects found in variance analyses were followed by Tukey pairwise mean comparisons, with a statistical significance level of $\alpha = 0.05$. Analyses were performed separately for knee joint center and hip joint center estimation methods.

Tables 6.5 and 6.6 present results of these statistical analyses. For each calculated joint angle, methods that yielded significantly different results were tabulated. Method abbreviations are presented in Tables 6.3 and 6.4.

Table 6.3 Abbreviations for Hip Joint Center Estimation Methods

Hip Joint Center Estimation Methods	
M1	Davis' Method
M2	Sphere Fitting Method – Gait Trial
M3	Sphere Fitting Method – VHM Trial
M4	Least Squares Method – Gait Trial
M5	Least Squares Method – VHM Trial

Table 6.4 Abbreviations for Knee Joint Center Estimation Methods

Knee Joint Center Estimation Methods	
M1	Centering Device
M2	Direct Marker Attachment
M3	VCM Method

Table 6.5

Statistical Analysis Results for Hip Joint Center Estimation Methods

	Angles	M1	M2	M3	M4	M5
Significantly Different With	Right Hip Flexion	None	None	None	None	None
	Left Hip Flexion	None	None	None	None	None
	Right Hip Abduction	M3	M3	All	M3	M3
	Left Hip Abduction	M2, M3	All	All	M2, M3	M2, M3
	Right Hip Rotation	None	None	None	None	None
	Left Hip Rotation	None	None	None	None	None
	Right Knee Flexion	None	None	None	None	None
	Left Knee Flexion	None	None	None	None	None
	Right Knee Valgus	None	None	None	None	None
	Left Knee Valgus	M5	M5	M5	M5	All
	Right Knee Rotation	M3	M3	M1, M2, M4	M3	None
	Left Knee Rotation	M3	None	M1, M4	M3	None

Table 6.6

Statistical Analysis Results for Knee Joint Center Estimation Methods

	Angles	M1	M2	M3
Significantly Different With	Right Hip Flexion	None	None	None
	Left Hip Flexion	None	None	None
	Right Hip Abduction	None	None	None
	Left Hip Abduction	M3	M3	All
	Right Hip Rotation	All	M1	M1
	Left Hip Rotation	All	M1	M1
	Right Knee Flexion	M2	M1	None
	Left Knee Flexion	None	None	None
	Right Knee Rotation	All	All	All
	Left Knee Rotation	All	All	All
	Right Knee Valgus	All	All	All
	Left Knee Valgus	All	All	All
	Right Dorsiflexion	None	None	None
	Left Dorsiflexion	None	None	None
	Right Foot Rotation	None	None	None
	Left Foot Rotation	None	None	None

Above results reveal that employed hip and knee joint center estimation methods yielded different results for different joint angles. Examination of Table 6.5 reveals that hip flexion/extension, hip internal/external rotation, knee flexion/extension and knee valgus/varus (right) angles presented no significant method-related differences. Remaining joint angles, on the other hand, were affected significantly from differences in estimated hip joint centers. For these angles right and left segment results were observed to be inconsistent.

Furthermore, methods that yielded significantly different results were found to be dissimilar for different joint angles.

Table 6.6 also presents results similar to those obtained from hip joint center estimation methods. Hip flexion/extension, hip abduction/adduction (right), knee flexion/extension (left), foot dorsi/plantar flexion and foot internal/external rotation angles yielded no significantly different results. For knee internal/external rotation and valgus/varus angles, all three method results were significantly different from each other. For hip abduction/adduction and knee flexion/extension, right and left segment angles presented different results. Again, significant differences that were observed between methods were not consistent for different joint angles, as observed from the tabulated data.

CHAPTER 7

SUMMARY AND CONCLUSIONS

7.1 General Conclusions

This thesis deals with sensitivity evaluation of joint kinematics calculations of Kiss gait analysis system, to implementation of methodological and protocol related modifications. The study is composed of two main parts: First part involves assessment of effects of thigh and shank marker relocation on joint kinematic results of the system. In the second part of the thesis, several hip and knee joint center estimation methods were adapted to the system and their performances in Kiss protocol were investigated.

As the primary step of thesis work, current joint kinematics calculations of Kiss protocol were re-generated in Matlab® environment and obtained results were validated against Kiss-GAIT outputs. Comparison of raw joint angles yielded satisfactory results. On the other hand, dissimilarities were examined between smoothed angle outputs of re-generated code and Kiss-GAIT; which were attributed to different joint angle smoothing procedures employed by the programs. Therefore, it was concluded that re-generation of joint kinematics calculations were accomplished successfully.

To investigate effects of "free" thigh and shank marker location changes on joint kinematics results, gait experiments were carried out with modifications introduced to marker placement methodology. In the experiments, front and side markers were attached on thigh and shank segments, which enabled simultaneous acquisition of their coordinates and thus direct comparison of resulting joint kinematics without intra-subject variability.

Results obtained from front and side marker sets revealed that internal/external rotation and knee valgus/varus angles were significantly affected from changes in shank and thigh marker locations. Differences observed in internal/external rotation angles were not found to be surprising since estimation of transverse plane angles is difficult due to low signal-to-noise ratios (Güler 1998).

On the other hand, variations in knee valgus/varus angles resulting from shank and thigh marker relocation were quite unexpected. Further investigation revealed that these differences resulted from positioning of the thigh marker. It was hypothesized that this phenomenon was due to violation of the rigidity assumption, which was supported by root mean squared error values calculated for technical and anatomical reference frames. Root mean squared error values exhibited largest magnitudes within the interval where angles deviated from each other. It was also observed that relative positions of thigh segment markers showed variations throughout gait cycle.

Within the interval where deviations between knee valgus/varus angles were present, front thigh marker movement with respect to the underlying bony segment was larger as compared to movement of side thigh marker. This effect is believed to be resulting from activation of muscles underneath thigh front marker during walking.

One important point to note is that, although front thigh marker moved, with respect to remaining thigh segment markers, relatively more as compared to side marker, valgus/varus angles computed from front markers were found to be more realistic than side marker angle results. Examination of valgus/varus angle plots revealed that maximum absolute values of front marker valgus/varus angles were around 0-10 degrees, whereas maximum absolute side marker angle values were found to be up to 20 degrees. Such large valgus/varus angles are not realistic for normal individuals; therefore obtained

results suggest that utilization of side thigh markers may be resulting in systematic calculation errors and consequently knee valgus/varus angle artefacts. Examinations on joint angle graphs revealed that knee valgus/varus angles computed using side thigh markers were directly affected from knee flexion/extension angles within the interval where flexion/extension angles increased. This result further strengthens the possibility that employment of side thigh markers resulted in "cross-talk" between knee valgus/varus and flexion/extension, which are supposedly two independent sets of angles.

In the second part of the thesis, several hip and knee joint center estimation methods were adapted to Kiss protocol. Main limitation of this part of the study was that actual hip and knee joint center locations were unknown. Thus, in the absence of a "gold standard" for these centers, direct evaluation and comparison of individual method performances was not possible. Therefore joint center coordinates obtained from new methods were compared with joint center estimation methods currently employed by the protocol.

No consistent and interpretable results were obtained in terms of joint center distances with different estimation methods, both within trials of same subjects, and for trials between subjects. Previous studies in literature state that functional hip joint center estimation methods produce better results when varied hip motion trials are performed, as compared to walking where the movement is limited mainly to the sagittal plane. Therefore, with the varied hip motion trial data, it could be expected that least squares and sphere fitting methods provided similar estimates for hip joint angles; which was not observed in computed hip joint center coordinates.

Similar to the case of hip joint center estimation, methods employed for knee joint center estimation also yielded inconsistent results in terms of calculated joint center locations. Knee centering device and direct marker attachment

methods were expected to yield similar results, since both methods employ the same methodology for estimation of knee axis and center. Differences observed between results of these methods may be due several reasons: Centering devices were placed on the subject so that their edges were located on medial and lateral femoral epicondyles. Type 3 markers were also placed on these locations after removal of the centering devices for the second method; however during this procedure slight misplacements of the markers might have been possible, which result in differences in knee axis and center estimation. Furthermore due to the geometry of the knee and soft tissue underneath attached markers, point markers might have moved relative to the underlying bone and thus failed to accurately locate the epicondyles, resulting in different knee axis and center definitions as compared to centering devices. Although not affected from the above considerations, VCM method is also prone to errors since it is highly dependent on correct positioning of the thigh marker. Therefore, even slight misplacements of the thigh markers might have affected resulting knee joint center estimates considerably.

The implemented methods were further evaluated through investigation of their effects on joint kinematics results of the system. Statistical analyses of all trials for hip and knee joint centers revealed significant differences between methods; however, no result that could be generalized for all angle outputs could be extracted from statistical analyses.

Discrepancies observed between results of the utilized joint center estimation methods might be affected from various parameters, some of which are directly associated with method characteristics whereas others are related to the gait analysis system. Obviously, individual performances of the methods play the most important role in estimating joint centers. For two functional methods utilizing same motion information but different algorithms, results may turn out to be irrelevant as seen in this study. However, there are also system-

related parameters that indirectly influence performances of the methods. Instrumentation and soft tissue movement errors affect both joint center locations and resulting kinematics. In addition, inaccuracies in locating palpable anatomical landmarks and incorrect marker placements might have been present in the conducted experiments, which are highly dependent on the performer's skills. Inconsistent results provided by statistical analyses may also be resulting from small data size, which covers information from a total of nine trials. Experiments should be conducted with more subjects to get more reliable results from the performed statistical analyses.

At this stage, joint center coordinate results of the implemented methods and the resulting joint kinematics do not provide adequate information to comment on individual performances of the methods, either in joint center location estimation or in applicability of the methods in the system. Information regarding true joint center locations is therefore compulsory to be able to assess individual performances of these methods in METU Gait Analysis System.

All programs built up and employed in this thesis work were developed in Matlab®. One important contribution of this study is thus the re-generation of joint kinematics calculations of Kiss protocol in a powerful and flexible programming environment such as Matlab®. It is believed that future research in this field will greatly benefit from the work presented in this study.

7.2 Future Work

Based on the results of this thesis work, following suggestions will be presented for future studies at METU Gait Analysis Laboratory:

- Performance of the data acquisition system directly affects resulting joint kinematics and kinetics. Camera sampling rate was 25 Hz when performing

the experiments of this thesis, due to problems in the laboratory hardware. Such low sampling rates are not sufficient for gait analysis applications, and necessary recoveries in the system should immediately be performed so that a sampling rate of at least 50 Hz is employed for kinematic data acquisition.

- Violation of rigidity assumption for marker-based segments is an important problem of the system that directly affects reliability of the calculated joint kinematics, as seen from investigations with front and side markers. Relative movement of constructed markers result from combination of soft tissue movement and errors in reconstruction of marker coordinates. Such instrumentation errors can be reduced by proper calibration and linearization of cameras. As stated by Civek (2006), immediate camera linearization is needed to enhance kinematic data acquisition performance in current system settings. As for soft tissue movement, the static double calibration technique presented by Afşar (2001) can be employed in the experiments for compensation of soft tissue movement artefacts. Furthermore, marker attachment methods that will reduce marker movement relative to skin can be developed, such as utilization of markers on special jigs or plates.

- In this study, only two (front and side) marker locations were selected and employed for investigation of thigh and shank marker relocation effects on the joint kinematics. Since these two thigh markers resulted in significantly different valgus/varus angles, a further detailed assessment needs to be performed to monitor changes in valgus/varus angles as a function of thigh marker locations.

- Results obtained from front/side marker comparison suggest that "cross-talk" is present between knee valgus/varus and flexion/extension angles

when side thigh markers are employed. Clarification of this phenomenon and investigation of its cause is essential to enhance system reliability. If applicable, a new position may be proposed for thigh marker. However, prior to making this proposal, both kinematic and kinetic analyses must be performed with the new marker location and obtained results must be validated against normative data from literature.

- Investigation of individual performances of the adapted joint center estimation methods was not possible in this study since true joint center locations were unknown. Work presented in this part of the thesis can be further enhanced by determining true joint center locations (e.g. via ultrasonography or X-ray imaging) and then evaluating joint center estimation method performances in the system. The methods that provide more satisfactory results than currently employed joint center estimation methods can then be employed in the gait analysis system. Again, both joint kinematics and kinetics must be investigated with the selected methods and results must be validated against normative data.

REFERENCES

Afşar, H., 2001. Evaluation and compensation of soft tissue movement artifacts for the KISS gait analysis system. MSc. Thesis, Middle East Technical University, Ankara, Turkey.

Andriacchi, T. P., Andresson, R.W. Stern D. and Galante, J.O., 1980. A study of lower-limb mechanics during stair climbing. Journal of Bone Joint Surgery 62, 749-757.

Andriacchi, T.P. and Alexander E.J., 2000. Studies of human locomotion: past, present and future. Journal of Biomechanics 33, 1217-1224.

Baker, R., 2006. Gait analysis methods in rehabilitation. Journal of NeuroEngineering and Rehabilitation, 3:4.

Banta, J., 1999. Gait analysis: past, present, and future. Developmental Medicine & Child Neurology 41, 363–363.

Bell, A.L., Brand, R.A. and Pedersen, D.R., 1989. Prediction of hip joint centre location from external landmarks. Human Movement Science 8, 3-16.

Bell, A. L., Pedersen, D. R. and Brand, R. A., 1990. A comparison of the accuracy of several hip center location prediction methods. Journal of Biomechanics 23, 617-621.

Besier, T.F., Sturnieks, D.L., Alderson, J.A. and Lloyd, D.G., 2003. Repeatability of gait data using a functional hip joint centre and a mean helical knee axis. Journal of Biomechanics 36, 1159–1168.

135

Best R. and Begg R., 2006. Overview of movement analysis and gait features. *In* Computational Intelligence for Movement Sciences: Neural Networks and Other Emerging Techniques, 1-69.

Cappozzo, A., 1984. Gait analysis methodology. Human Movement Science 3, 27-50.

Cappozzo, A., Catani F., Croce U. D. and Leardini A., 1995. Position and orientation in space of bones during movement: anatomical frame definition and determination. Clinical Biomechanics 10, 171-178.

Cappozzo, A., Della Croce, U., Leardini, A. and Chiari, L., 2005. Human movement analysis using stereophotogrammetry Part 1: theoretical background. Gait and Posture 21, 189-196.

Civek, E., 2006. Comparison of kinematic results between METU-KISS & Ankara University-Vicon gait analysis systems. MSc. Thesis, Middle East Technical University, Ankara, Turkey.

Davis III, R.B., 1988. Clinical gait analysis. Engineering in Medicine and Biology Magazine, IEEE 7, 35-40.

Davis III, R.B., Ounpuu, S., Tyburski, D. and Gage, J.R., 1991. A gait analysis data collection and reduction technique. Human Movement Science 10, 575-587.

Della Croce, U., Leardini, A., Chiari, L. and Cappozzo, A., 2005. Human movement analysis using stereophotogrammetry Part 4: assessment of anatomical landmark misplacement and its effects on joint kinematics. Gait and Posture 21, 226-237.

Gill, H., Morris, J., Biden, E., O'Connor, J., 1997. Optometric methods in biomechanical gait analysis, *In* Optical Measurement Methods in Biomechanics, Chapman and Hall, London, UK.

Grood, E. S. and Suntay, W. J., 1983. A joint coordinate system for the clinical description of three-dimensional motions: Application to the knee. Journal of Biomechanical Engineering 105, 136-144.

Güler H.C., 1998. Biomechanical modeling of lower extremity and simulation of foot during gait. PhD Thesis, Middle East Technical University, Ankara, Turkey.

Hicks, J.L. and Richards, J.G., 2005. Clinical applicability of using spherical fitting to find hip joint centers. Gait and Posture 22, 138-145.

Kadaba, M. P., Ramakrishnan, H. K. and Wootten, M. E., 1990. Measurement of lower extremity kinematics during level walking. Journal of Orthopaedic Research 8, 383-392.

Karpat, Y., 2000. Development and testing of kinematic data acquisition tools for a gait analysis system. MSc. Thesis, Middle East Technical University, Ankara, Turkey.

Leardini, A., Cappozzo, A., Catani, F., Toksvig-Larsen, S., Petitto, A., Sforza, V., Cassanelli, G. and Giannini, S., 1999. Validation of a functional method for the estimation of hip joint centre location. Journal of Biomechanics 32, 99-103.

Luttgens, K. and Wells, K.F., 1989. Kinesiology: scientific basis of human motion. Wm. C. Brown Publishers, Dubuque, IA, USA.

Pandy, M.G., 2001. Computer modeling and simulation of human movement. Annual Review of Biomedical Engineering 3, 245-273.

Perry J., 1992. Gait analysis: Normal and pathological function. Slack Incorporated, Thorofare, NJ, USA.

Piazza, S.J., Okita, N. and Cavanagh, P.R., 2001. Accuracy of the functional method of hip joint center location: effects of limited motion and varied implementation. Journal of Biomechanics 34, 967–973.

Piazza, S. J., Erdemir, A., Okita, N. and Cavanagh, P. R., 2004. Assessment of the functional method of hip joint center location subject to reduced range of hip motion. Journal of Biomechanics 37, 349-356.

Robertson, D.G.E. and Dowling, J.J., 2003. Design and responses of Butterworth and critically damped digital filters. Journal of Electromyography and Kinesiology 13, 569-573.

Seidel G.K., Marchinda D.M., Dijkers M., Soutas-Little, R.W. ,1995. Hip joint center location from palpable bony landmarks – a cadaver study. Journal of Biomechanics 28, 995-998.

Seikel, J.A., King, D.W. and Drumright, D.G., 1997. Anatomy and physiology for speech, language and hearing. Singular Publishing Group, San Diego, CA, USA.

Shafiq, M.S., 1998. Motion tracking in gait analysis. MSc. Thesis, Middle East Technical University, Ankara, Turkey.

Shiavi, R., Limbird, T., Frazer, M., Stivers, K., Strauss, A. and Abramovitz, J., 1987. Helical motion analysis of the knee – I. Methodology for studying kinematics during locomotion. Journal of Biomechanics 20, 459-469.

Simon, S.R., 2004. Quantification of human motion: gait analysis-benefits and limitations to its application to clinical problems. Journal of Biomechanics 37, 1869-1880.

Siston, R.A. and Delp, S.L., 2006. Evaluation of a new algorithm to determine the hip joint center. Journal of Biomechanics 39, 125–130.

Söylemez, B., 2002. An investigation on the gait analysis protocol of the "KISS" motion analysis system. MSc. Thesis, Middle East Technical University, Ankara, Turkey.

Stagni, R., Leardini, A., Cappozzo, A., Benedetti, M.G. and Capello, A., 2000. Effects of hip joint centre mislocation on gait analysis results. Journal of Biomechanics 33, 1479-1487.

Whittle, M. W., 2002. Gait analysis: An introduction. Butterworth-Heinemann, Oxford, UK.

Winter D.A., 1990. Biomechanics and motor control of human movement. John Wiley & Sons Inc., New York, USA.

Wu, G. and Cavanagh P.R., 1995. ISB recommendations for standardization in the reporting of kinematic data. Journal of Biomechanics 28, 1257-1261.

APPENDIX A

RAW JOINT ANGLES FROM
RE-GENERATED CODE AND KISS-GAIT
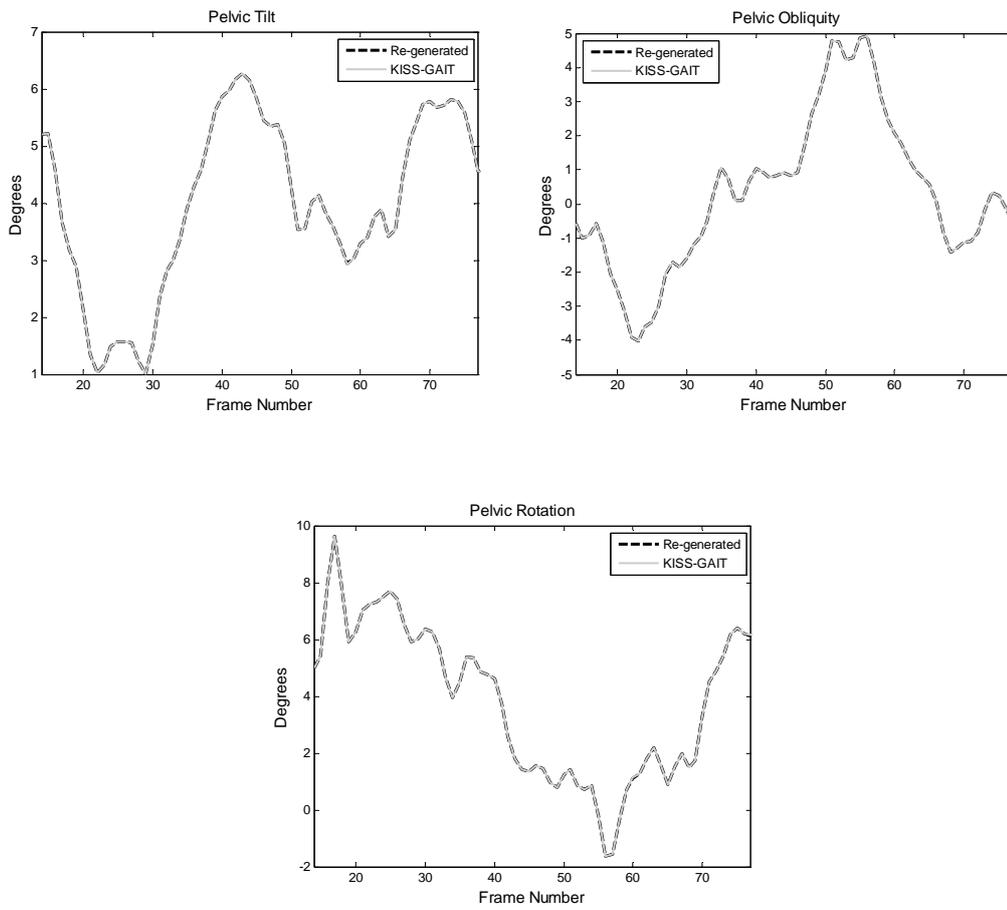
Figure A.1 Raw Pelvis Angles
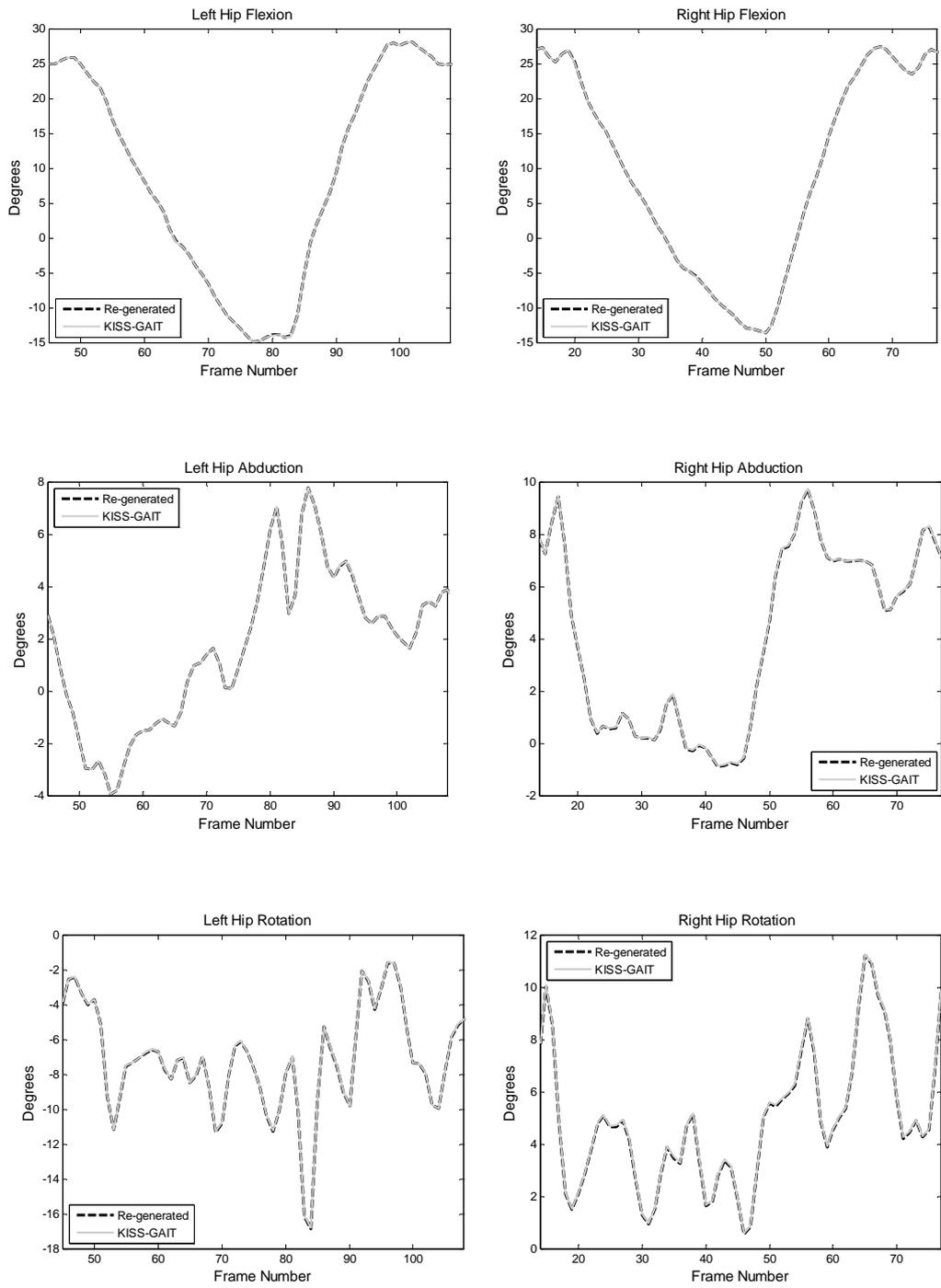
Figure A.2 Raw Hip Angles
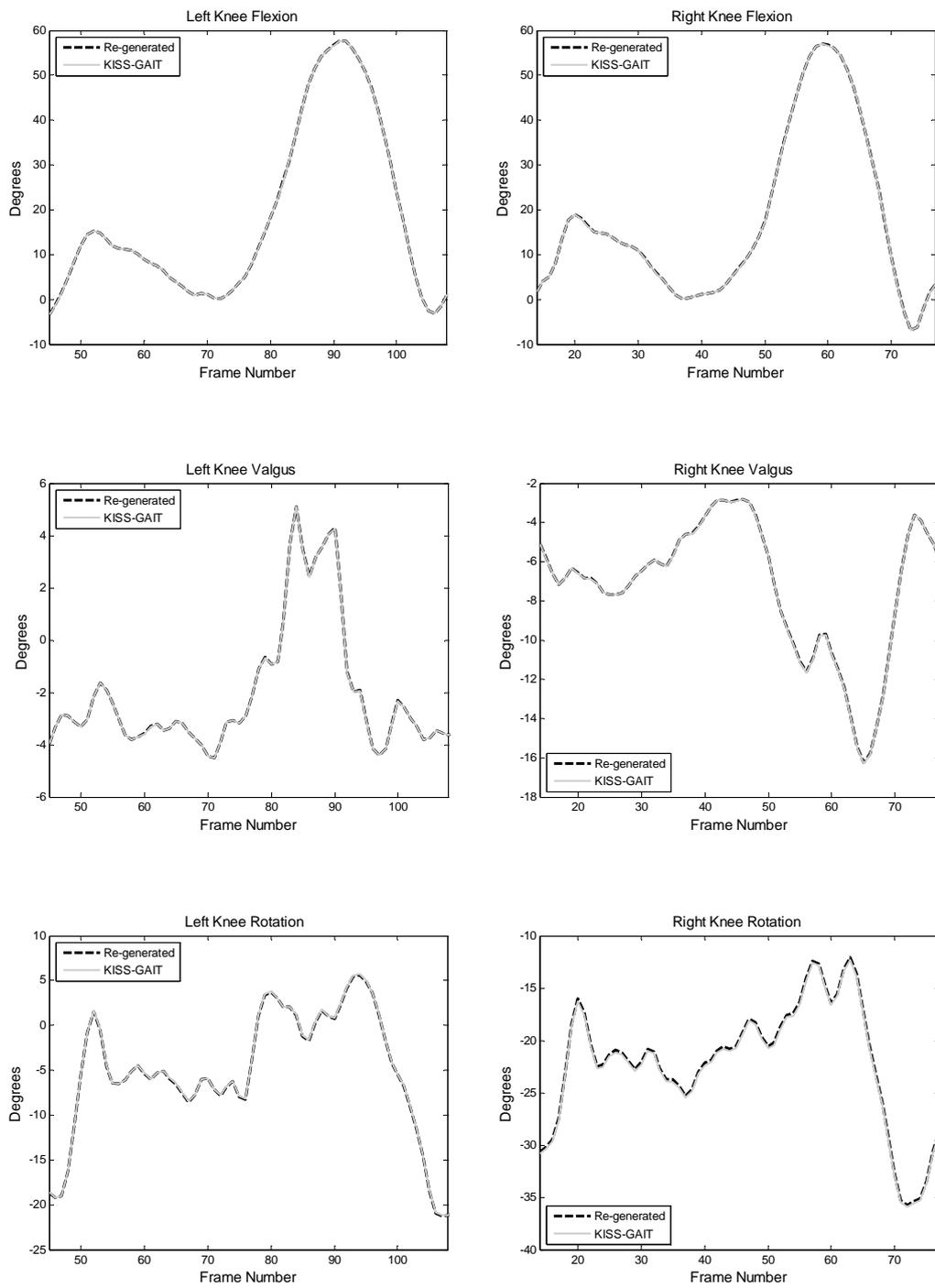
Figure A.3 Raw Knee Angles

142
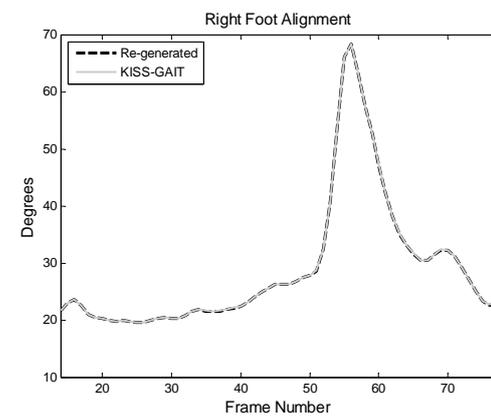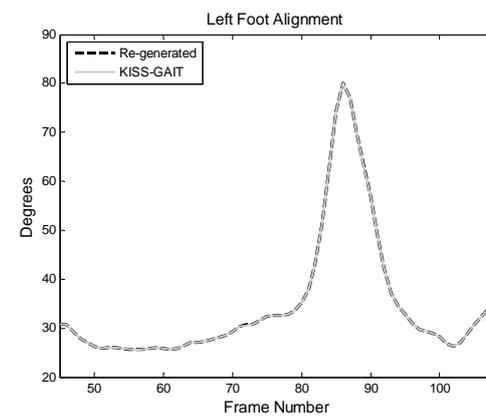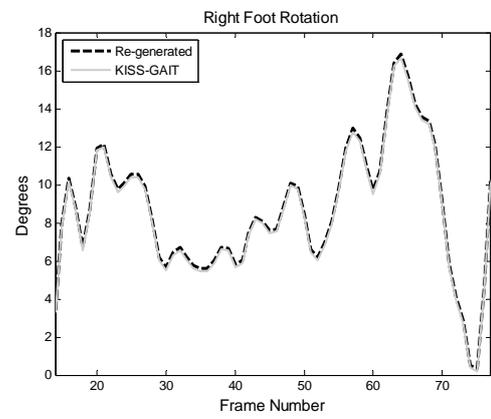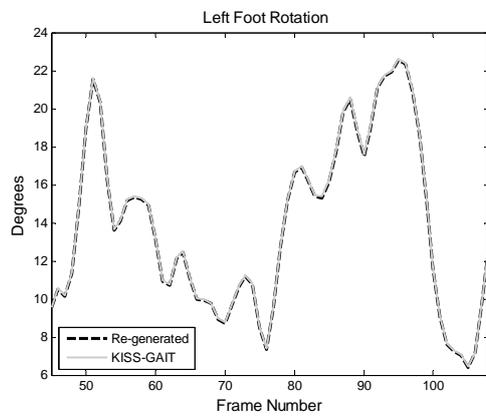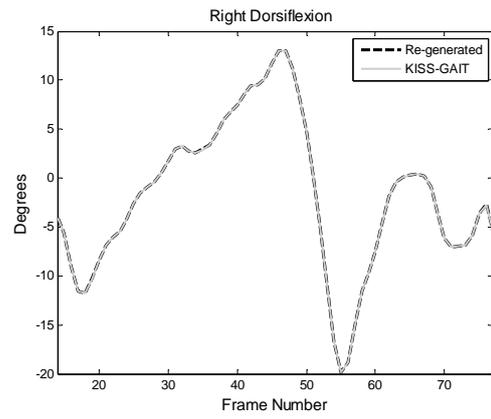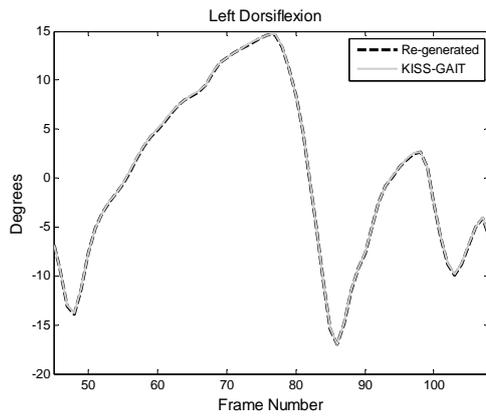
Figure A.4 Raw Foot Angles

SMOOTHED JOINT ANGLES FROM

RE-GENERATED CODE AND KISS-GAIT
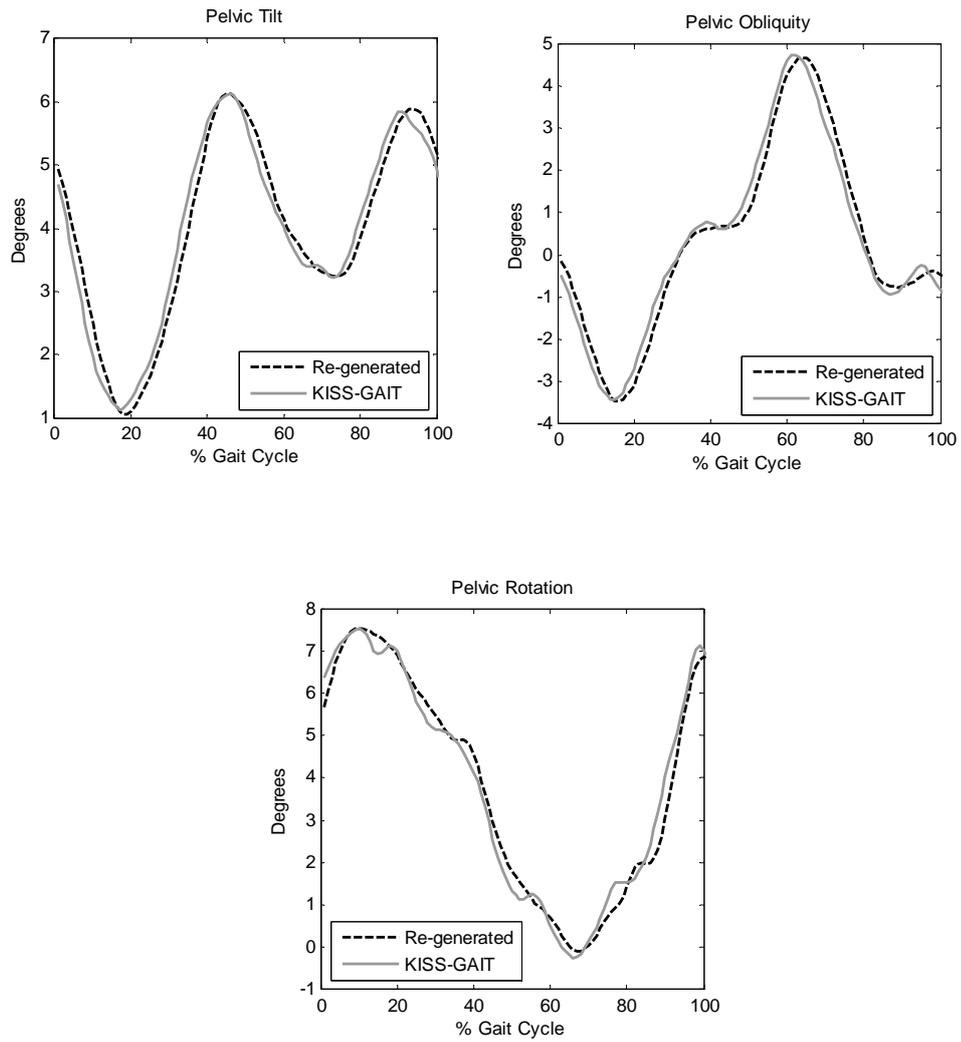
Figure B.1 Smoothed Pelvis Angles
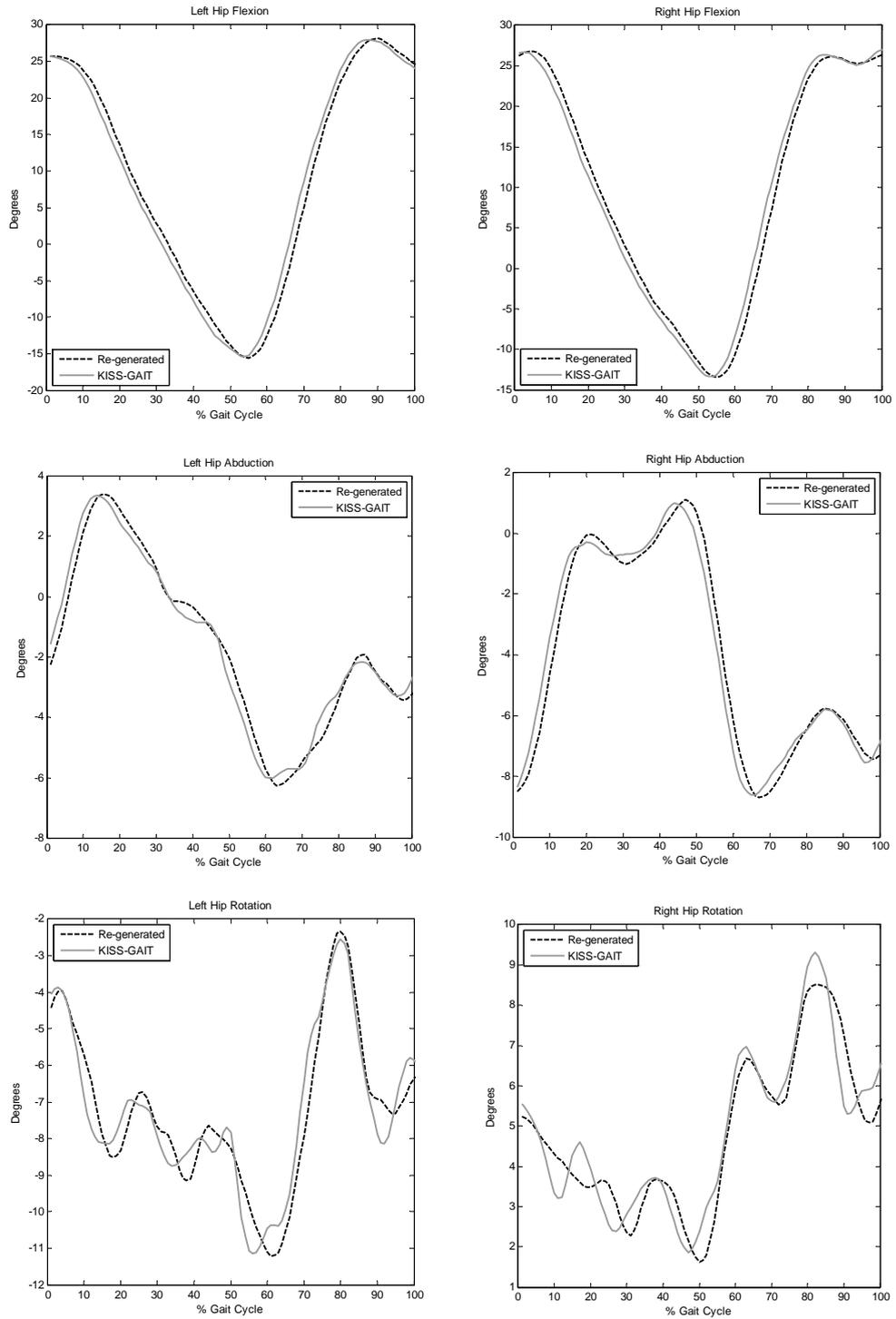
Figure B.2 Smoothed Hip Angles
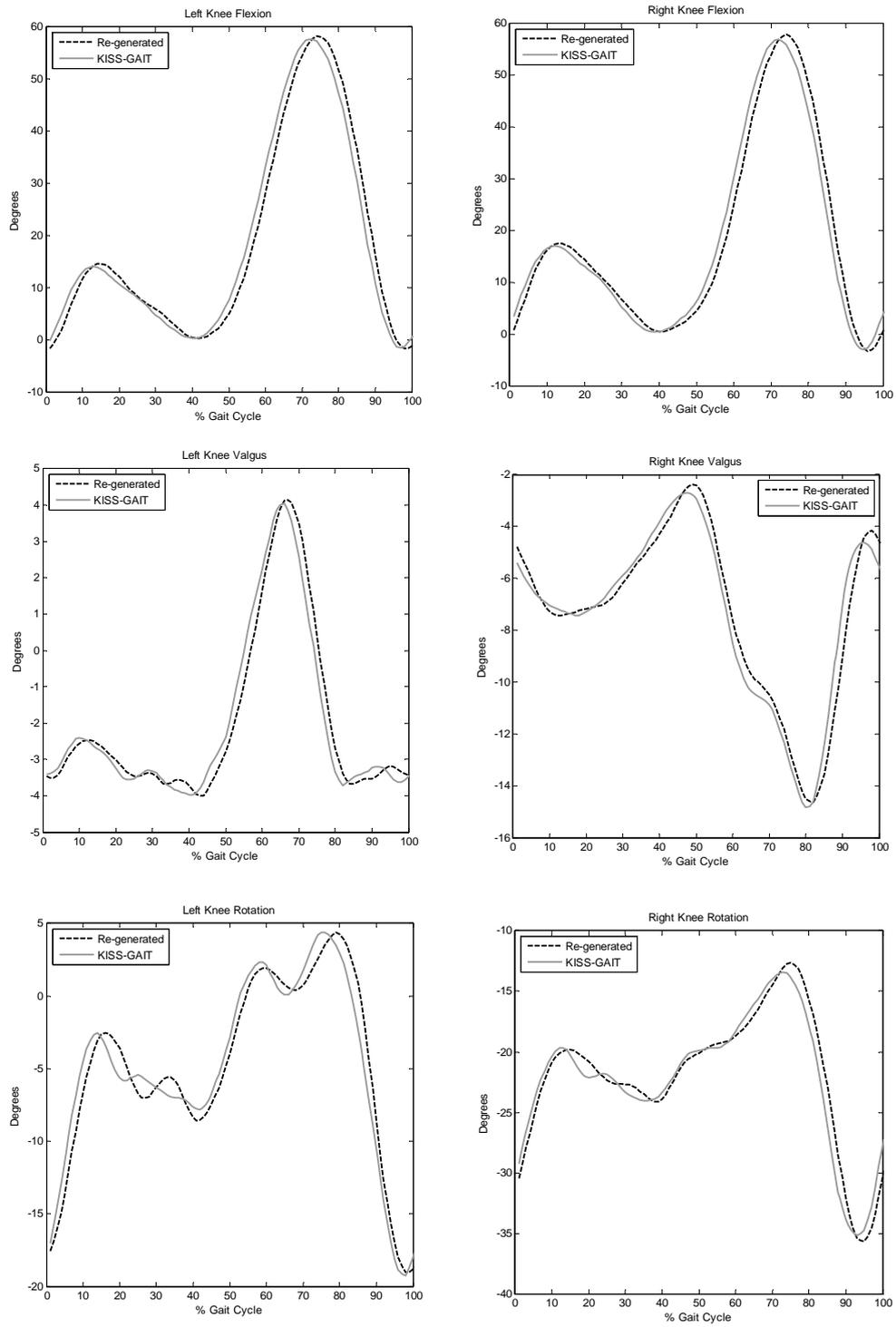
Figure B.3 Smoothed Knee Angles
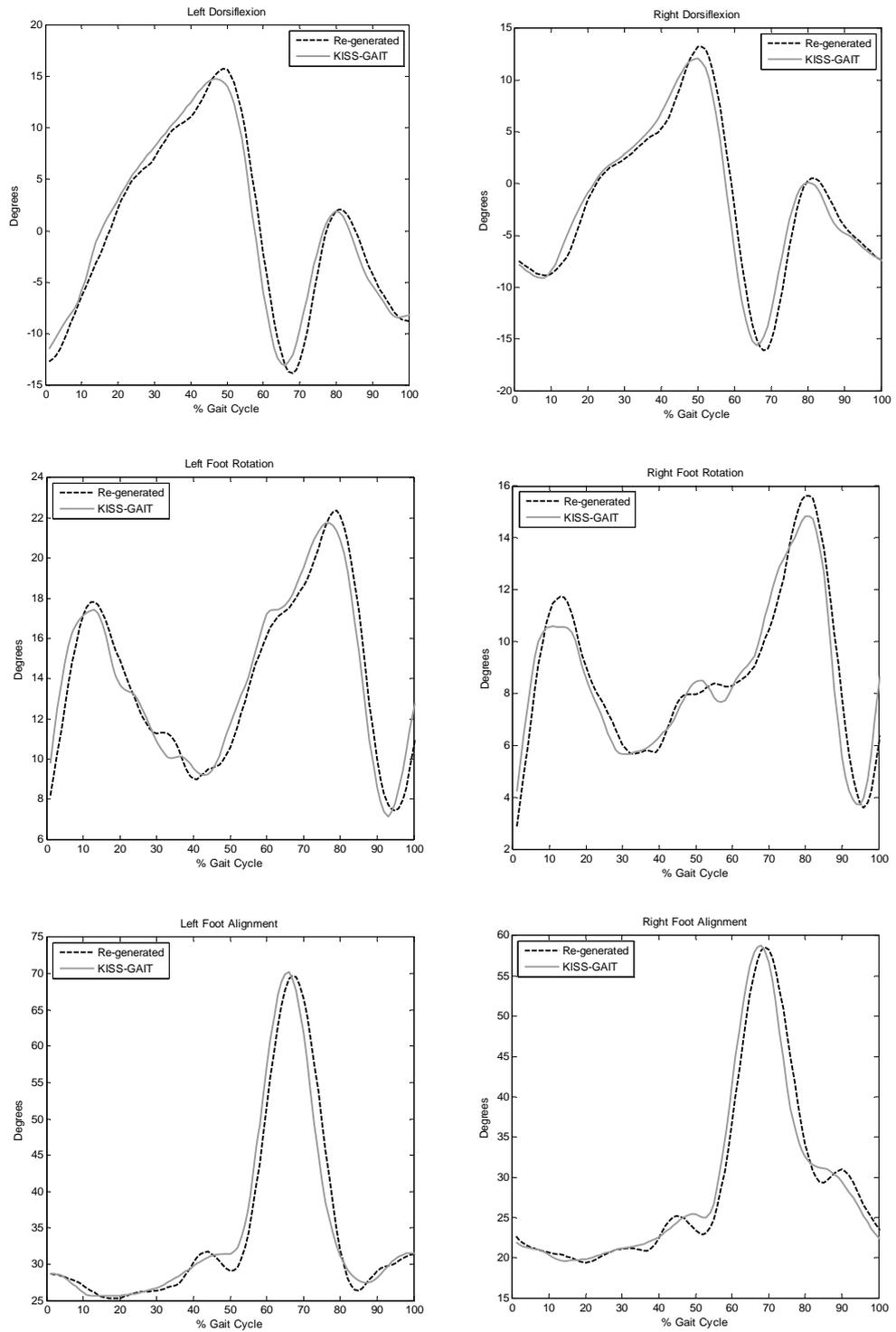
Figure B.4 Smoothed Foot Angles

147

APPENDIX C

COMPARISON OF RAW JOINT ANGLES
EMPLOYING SET-1 AND SET-2

C.1 Gait Events

Raw joint angles presented in this section are plotted within corresponding gait cycles of right and left segments. For easy reference, gait events of each trial are presented in the following tables.

C.1.1 Subject ED, Trial 15

Table C.1 Gait Events for 15th Trial of Subject ED

Frame	Left Segment	Right Segment
Heel Strike 1 (HS1)	21	7
Toe Off (TO)	38	23
Heel Strike 2 (HS2)	49	35

C.1.2 Subject ED, Trial 18

Table C.2 Gait Events for 18th Trial of Subject ED

Frame	Left Segment	Right Segment
Heel Strike 1 (HS1)	23	9
Toe Off (TO)	40	26
Heel Strike 2 (HS2)	51	37

C.1.3 Subject ED, Trial 21

Table C.3 Gait Events for 21st Trial of Subject ED

Frame	Left Segment	Right Segment
Heel Strike 1 (HS1)	18	4
Toe Off (TO)	34	21
Heel Strike 2 (HS2)	45	31

C.1.4 Subject GK, Trial 17

Table C.4 Gait Events for 17th Trial of Subject GK

Frame	Left Segment	Right Segment
Heel Strike 1 (HS1)	24	8
Toe Off (TO)	41	27
Heel Strike 2 (HS2)	55	40

C.1.5 Subject GK, Trial 21

Table C.5 Gait Events for 21st Trial of Subject GK

Frame	Left Segment	Right Segment
Heel Strike 1 (HS1)	26	10
Toe Off (TO)	47	30
Heel Strike 2 (HS2)	60	43

C.1.6 Subject GK, Trial 22

Table C.6 Gait Events for 22nd Trial of Subject GK

Frame	Left Segment	Right Segment
Heel Strike 1 (HS1)	24	9
Toe Off (TO)	43	28
Heel Strike 2 (HS2)	55	40

C.1.7 Subject KU, Trial 15

Table C.7 Gait Events for 15th Trial of Subject KU

Frame	Left Segment	Right Segment
Heel Strike 1 (HS1)	17	1
Toe Off (TO)	36	20
Heel Strike 2 (HS2)	48	32

C.1.8 Subject KU, Trial 18

Table C.8 Gait Events for 18th Trial of Subject KU

Frame	Left Segment	Right Segment
Heel Strike 1 (HS1)	25	9
Toe Off (TO)	44	28
Heel Strike 2 (HS2)	56	40

C.1.9 Subject KU, Trial 19

Table C.9 Gait Events for 19th Trial of Subject KU

Frame	Left Segment	Right Segment
Heel Strike 1 (HS1)	20	4
Toe Off (TO)	38	23
Heel Strike 2 (HS2)	50	34

C.2 Raw Joint Angles

Raw hip, knee and ankle joint angle plots obtained from data sets 1 and 2 are presented below, for all performed trials.

C.2.1 Subject ED, Trial 15

Hip Angles
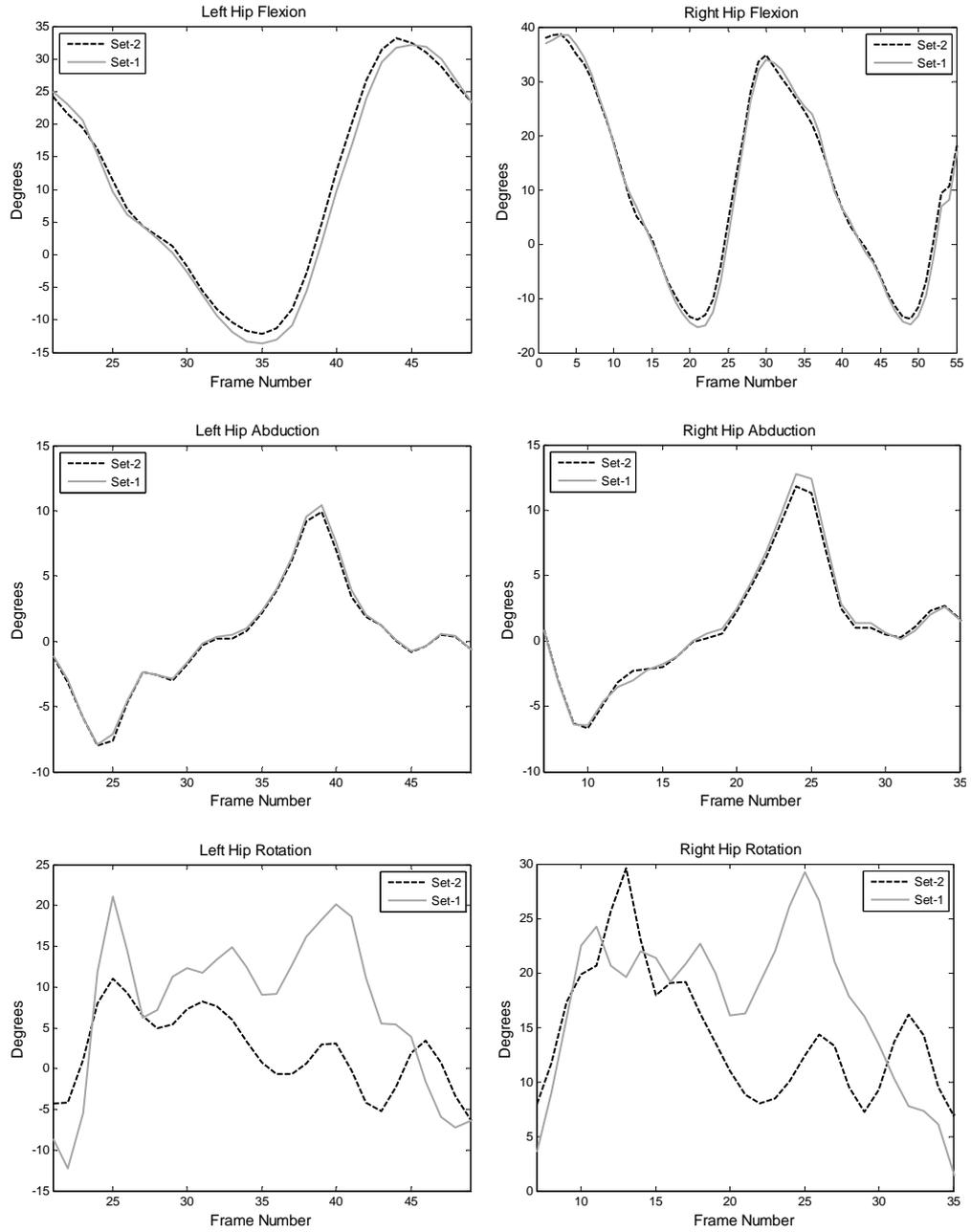
Figure C.1 Hip Angles for 15th Trial of Subject ED
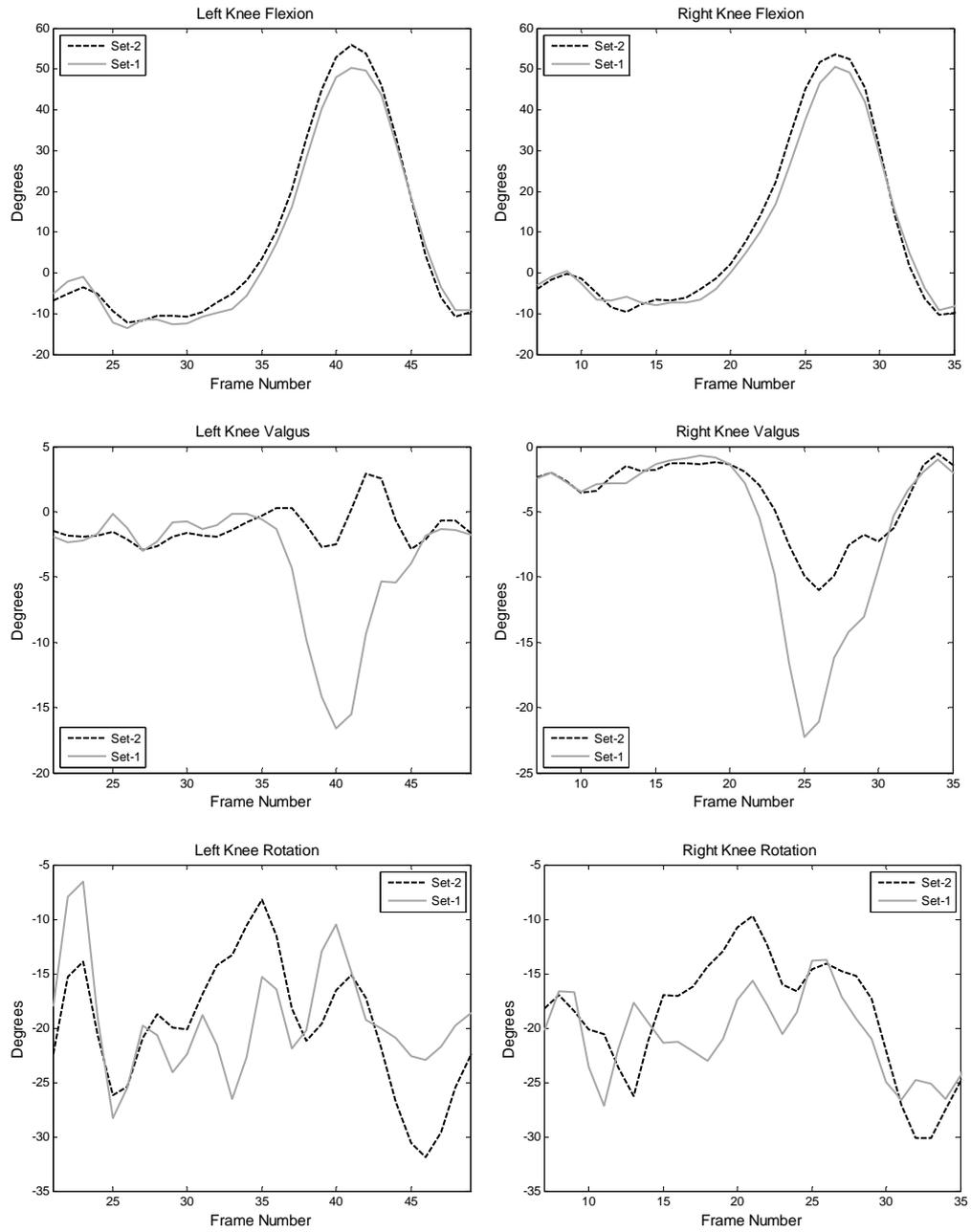
Knee Angles

Figure C.2 Knee Angles for 15th Trial of Subject ED

153
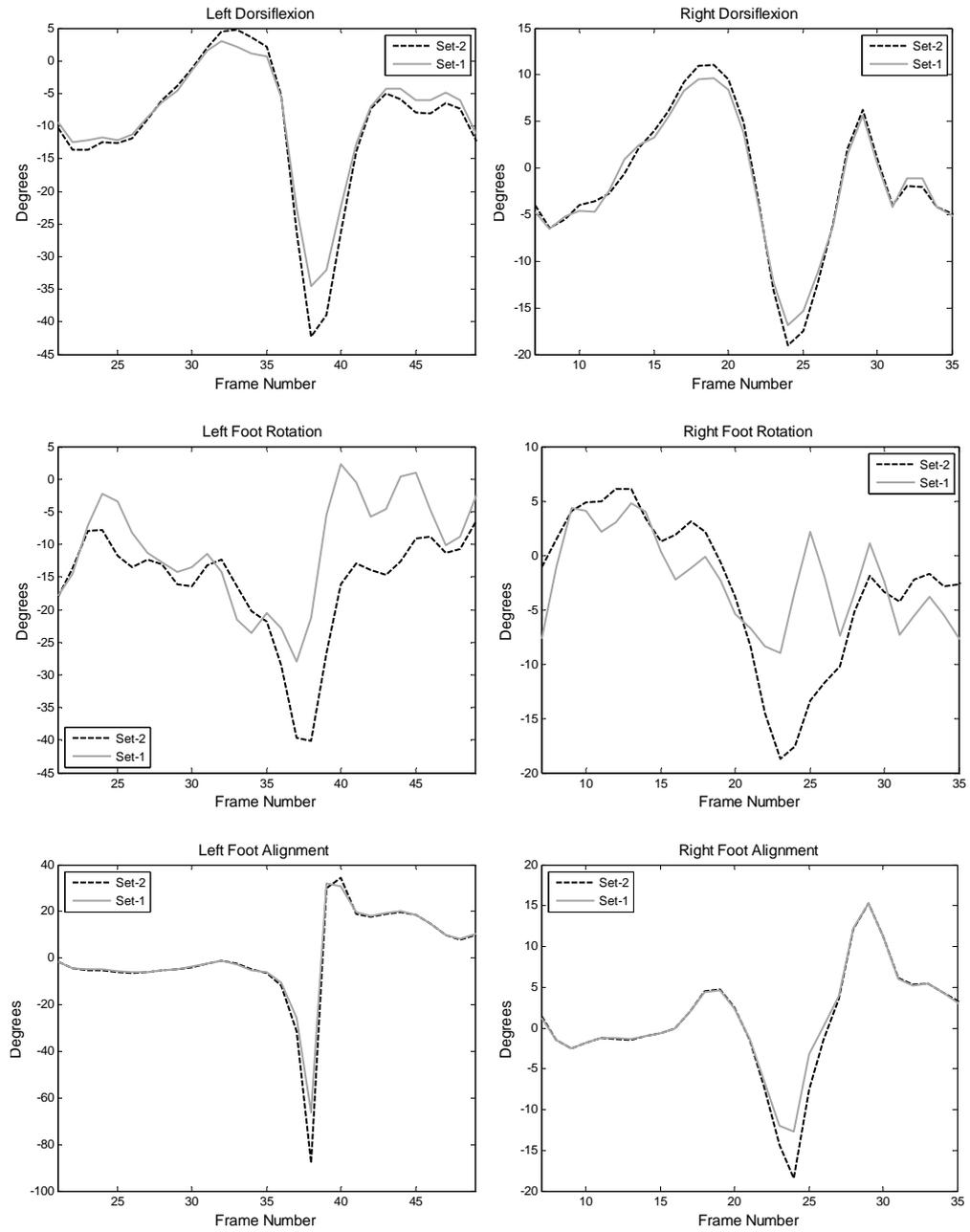
Foot Angles

Figure C.3 Foot Angles for 15th Trial of Subject ED

C.2.2 Subject ED, Trial 18

Hip Angles
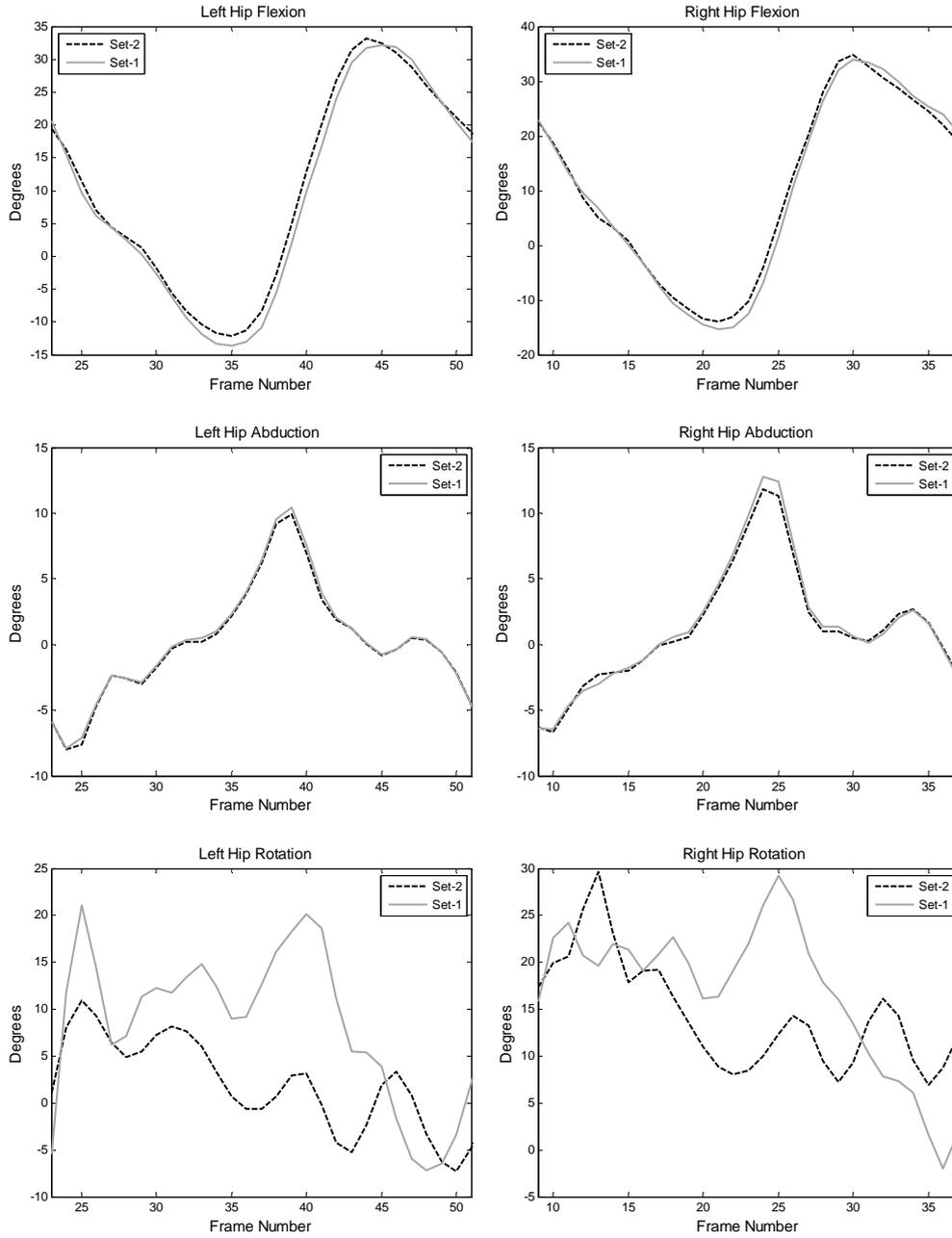
Figure C.4 Hip Angles for 18th Trial of Subject ED
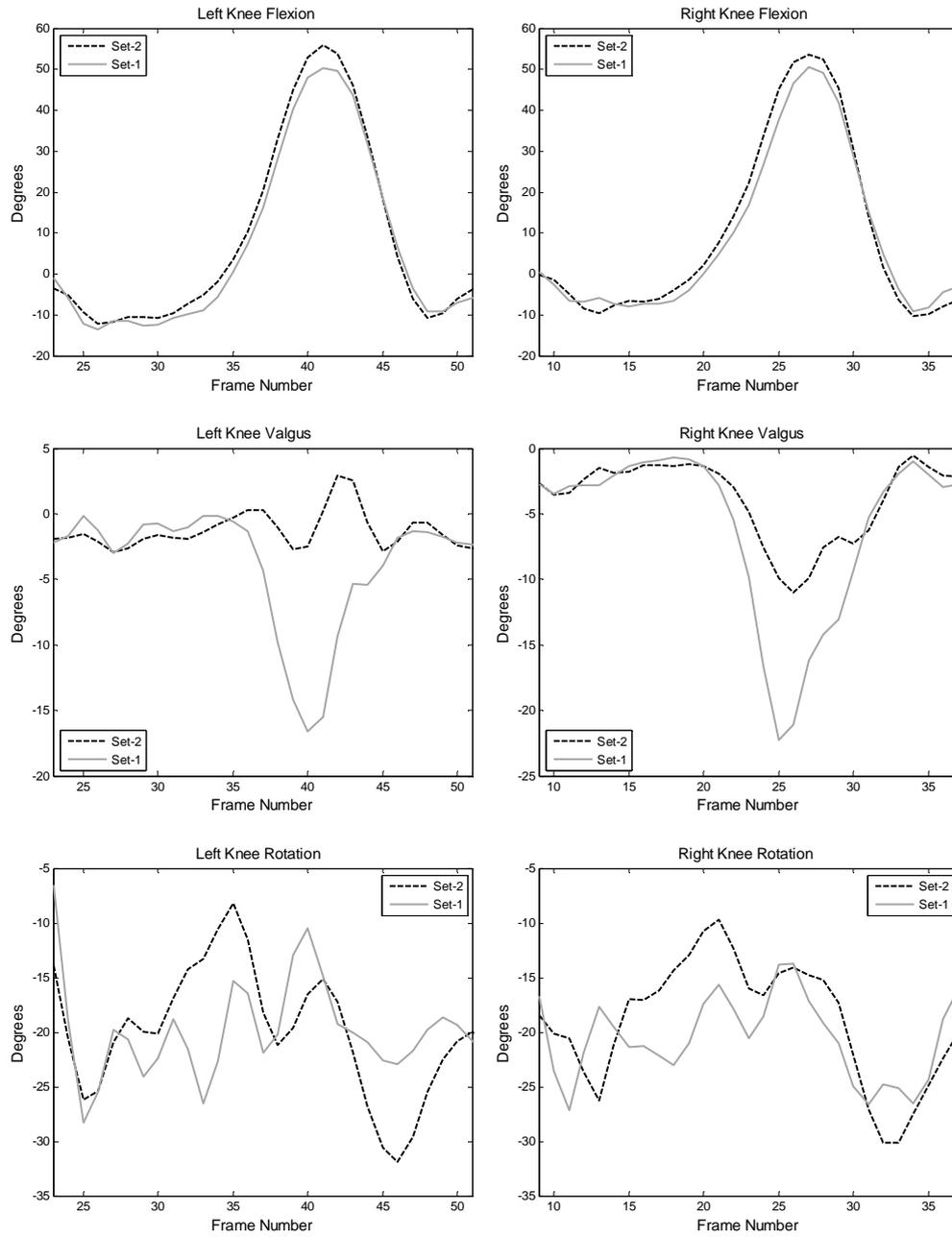
Knee Angles

Figure C.5 Knee Angles for 18th Trial of Subject ED

156
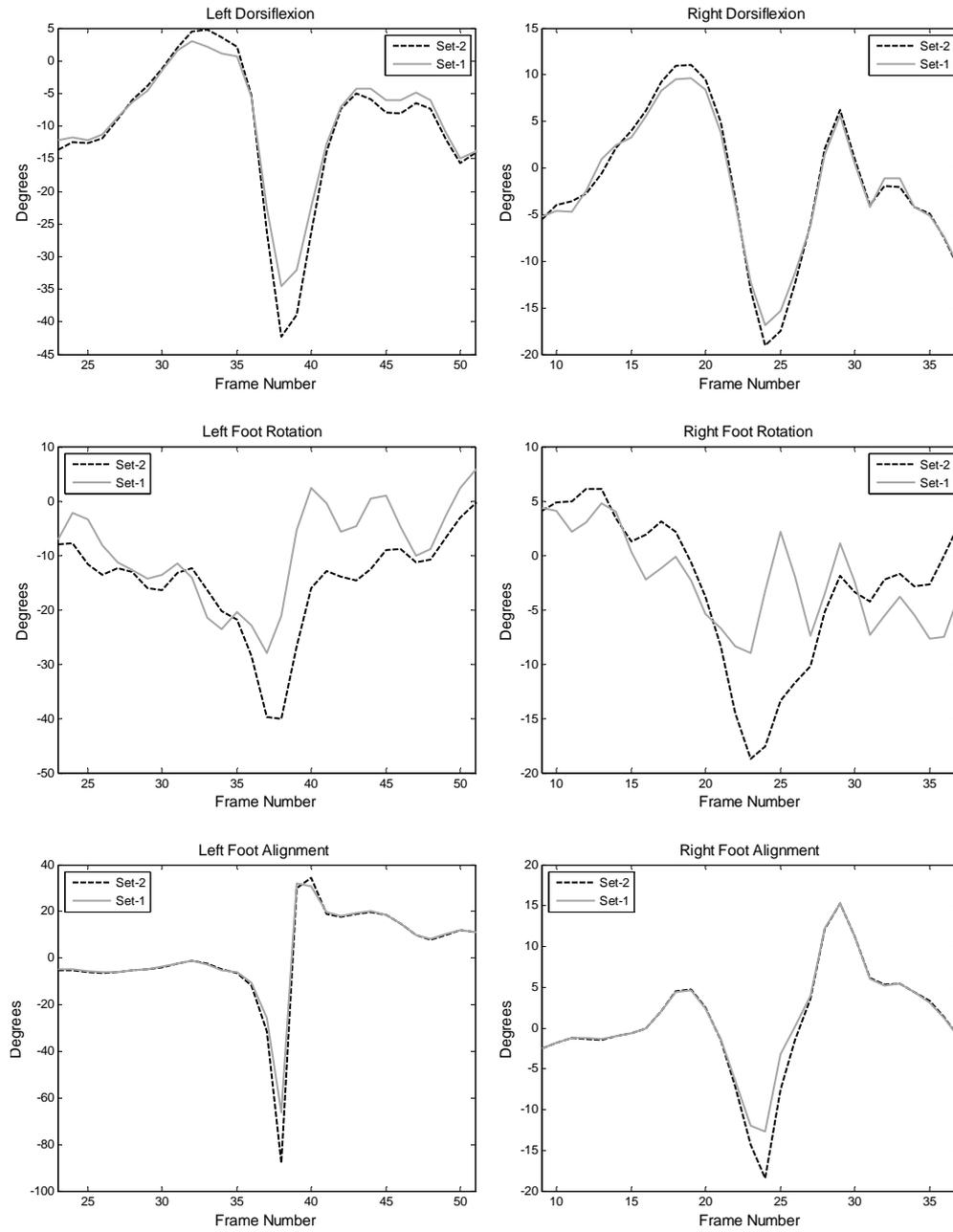
Foot Angles

Figure C.6 Foot Angles for 18th Trial of Subject ED

C.2.3 Subject ED, Trial 21

Hip Angles
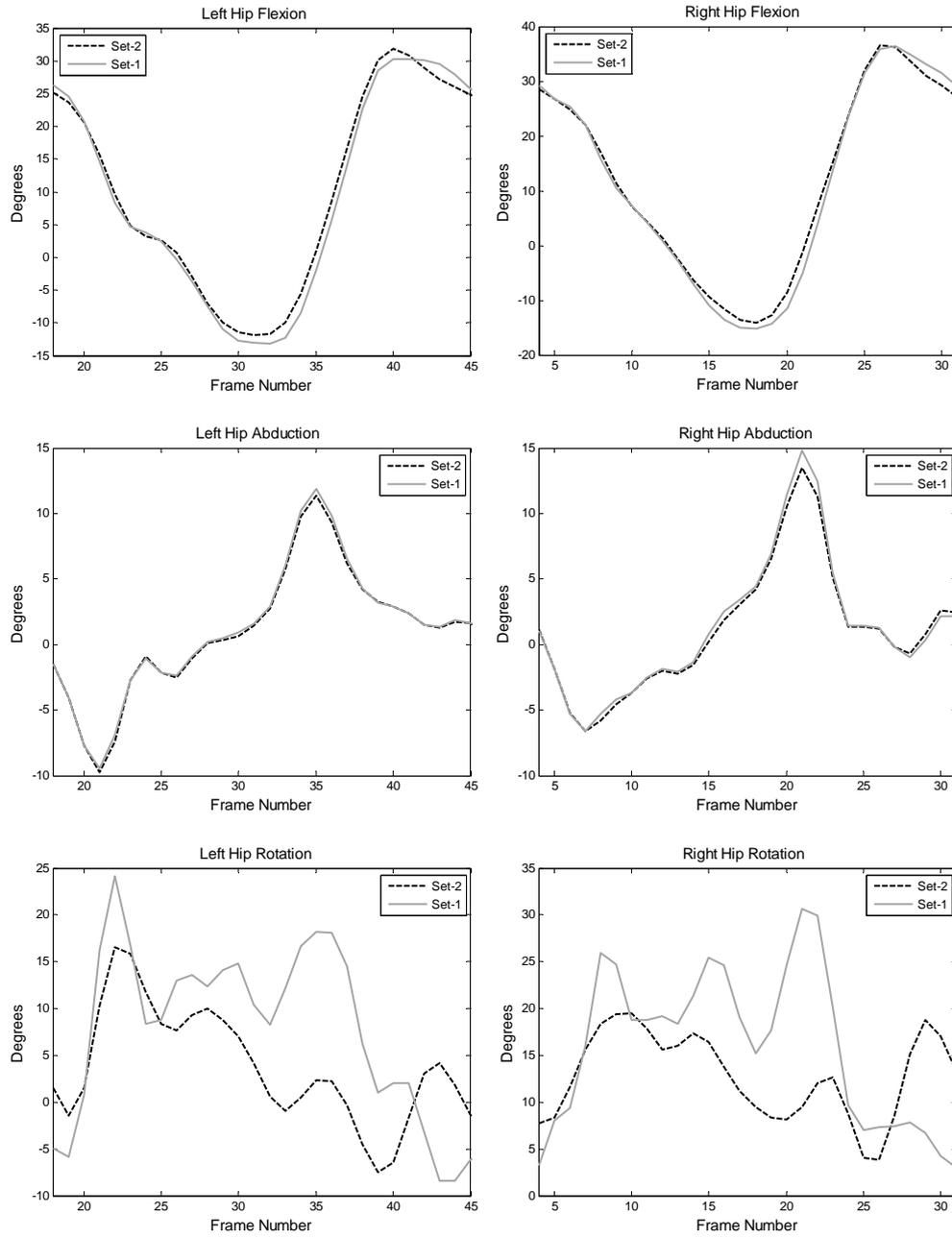
Figure C.7 Hip Angles for 21st Trial of Subject ED
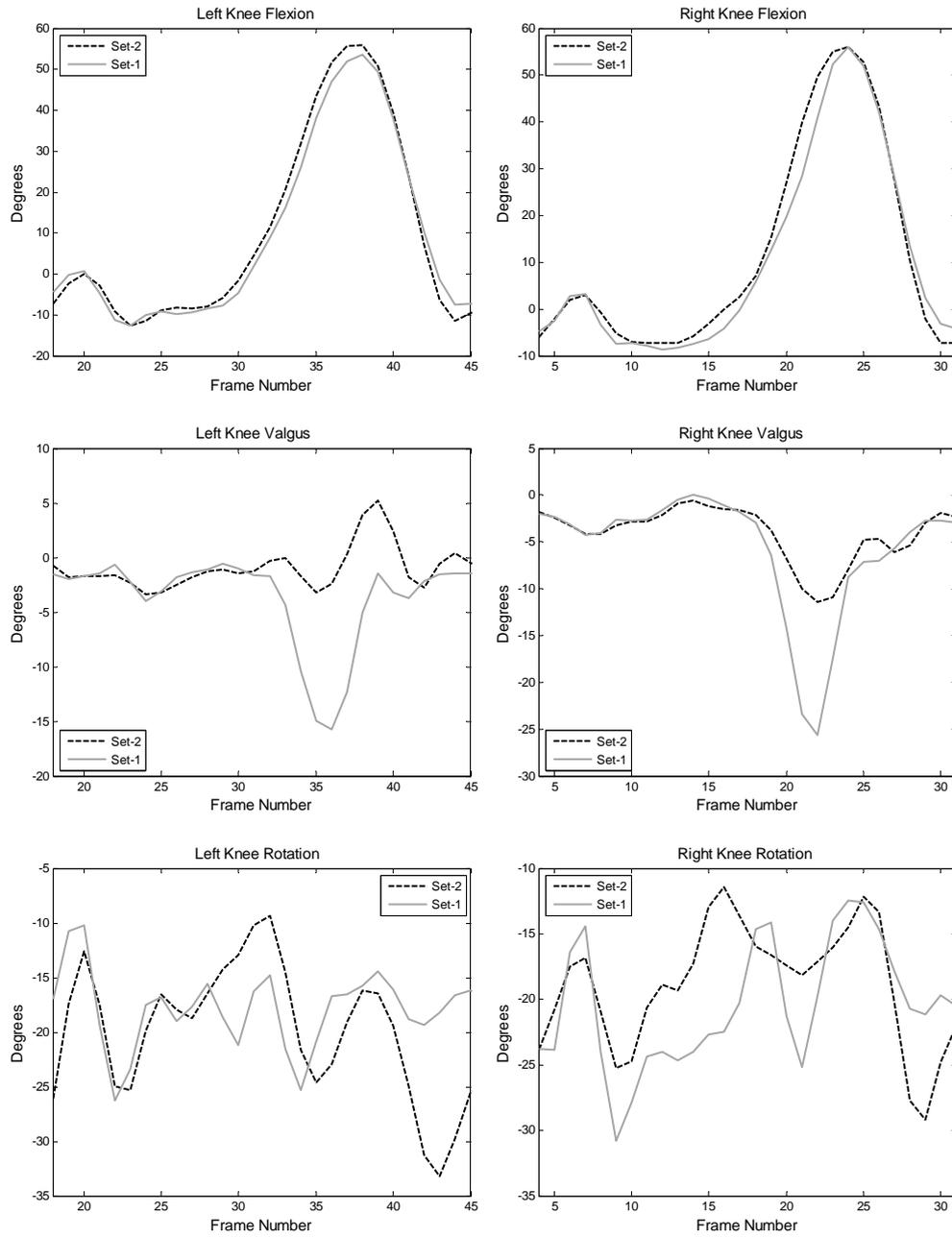
Knee Angles

Figure C.8 Knee Angles for 21st Trial of Subject ED

159
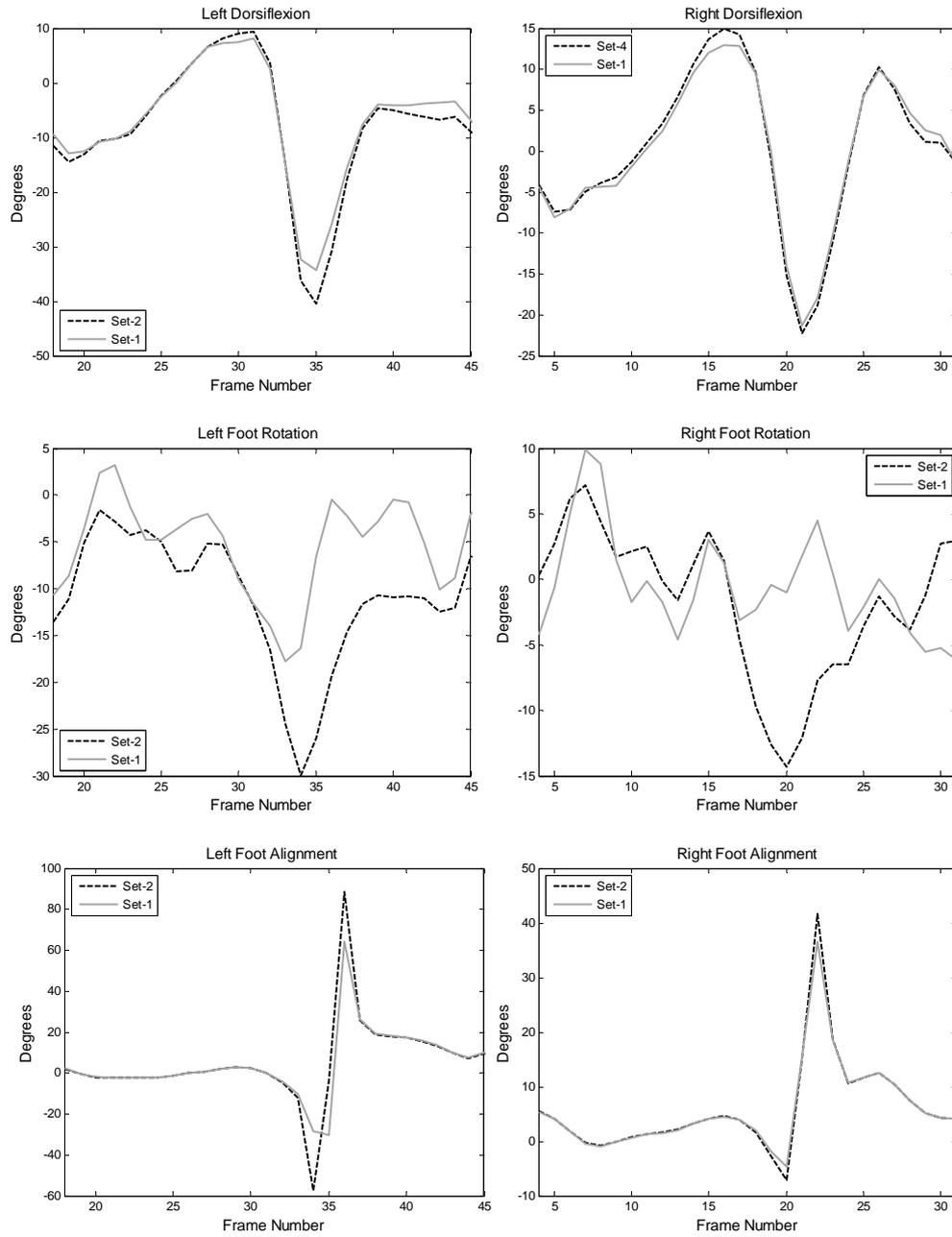
Foot Angles

Figure C.9 Foot Angles for 21st Trial of Subject ED

C.2.4 Subject GK, Trial 17

<u>Hip Angles</u>
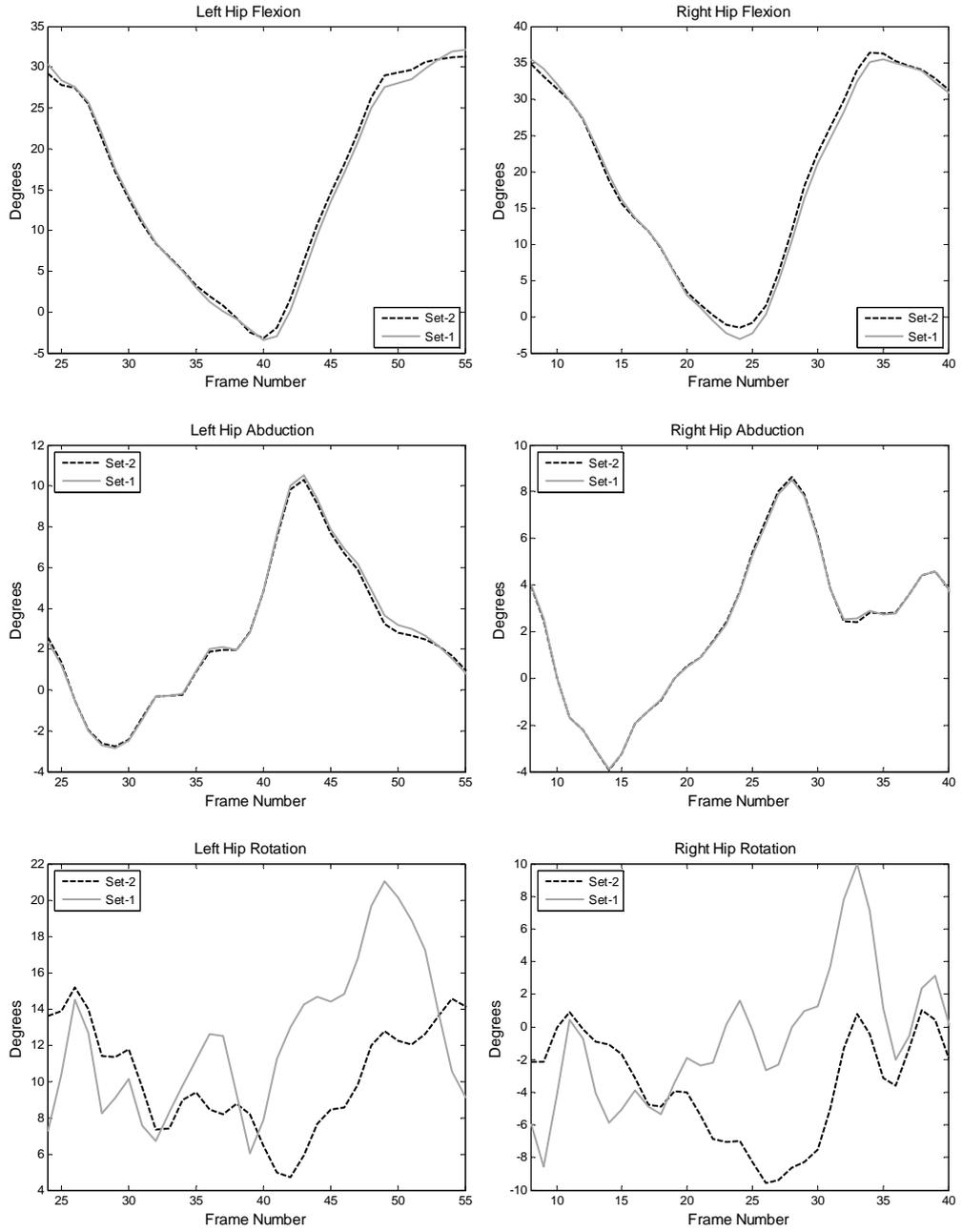
Figure C.10 Hip Angles for 17th Trial of Subject GK
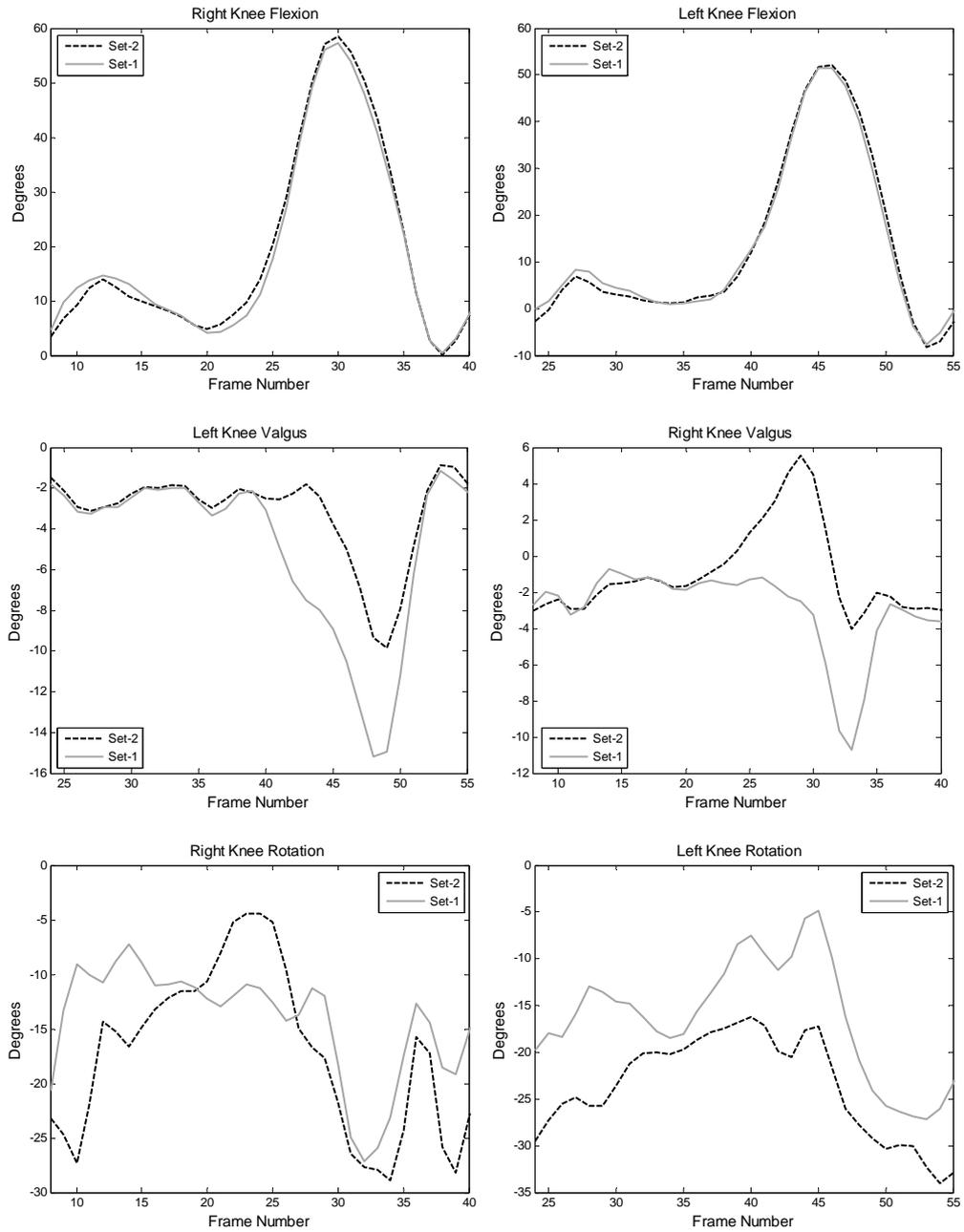
Knee Angles

Figure C.11 Knee Angles for 17th Trial of Subject GK

162

Foot Angles

Figure C.12 Foot Angles for 17th Trial of Subject GK

163

C.2.5 Subject GK, Trial 21

<u>Hip Angles</u>
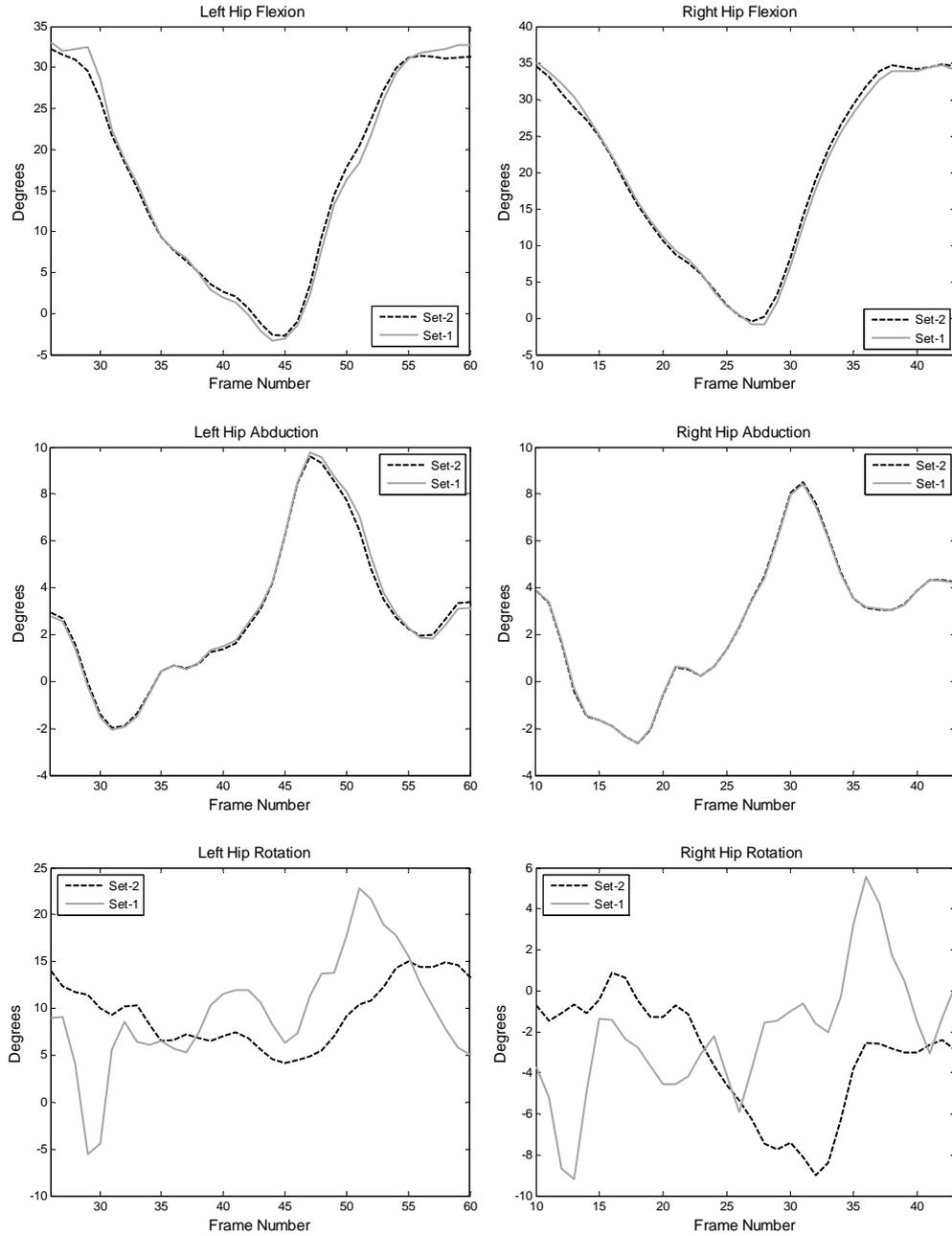
Figure C.13 Hip Angles for 21st Trial of Subject GK
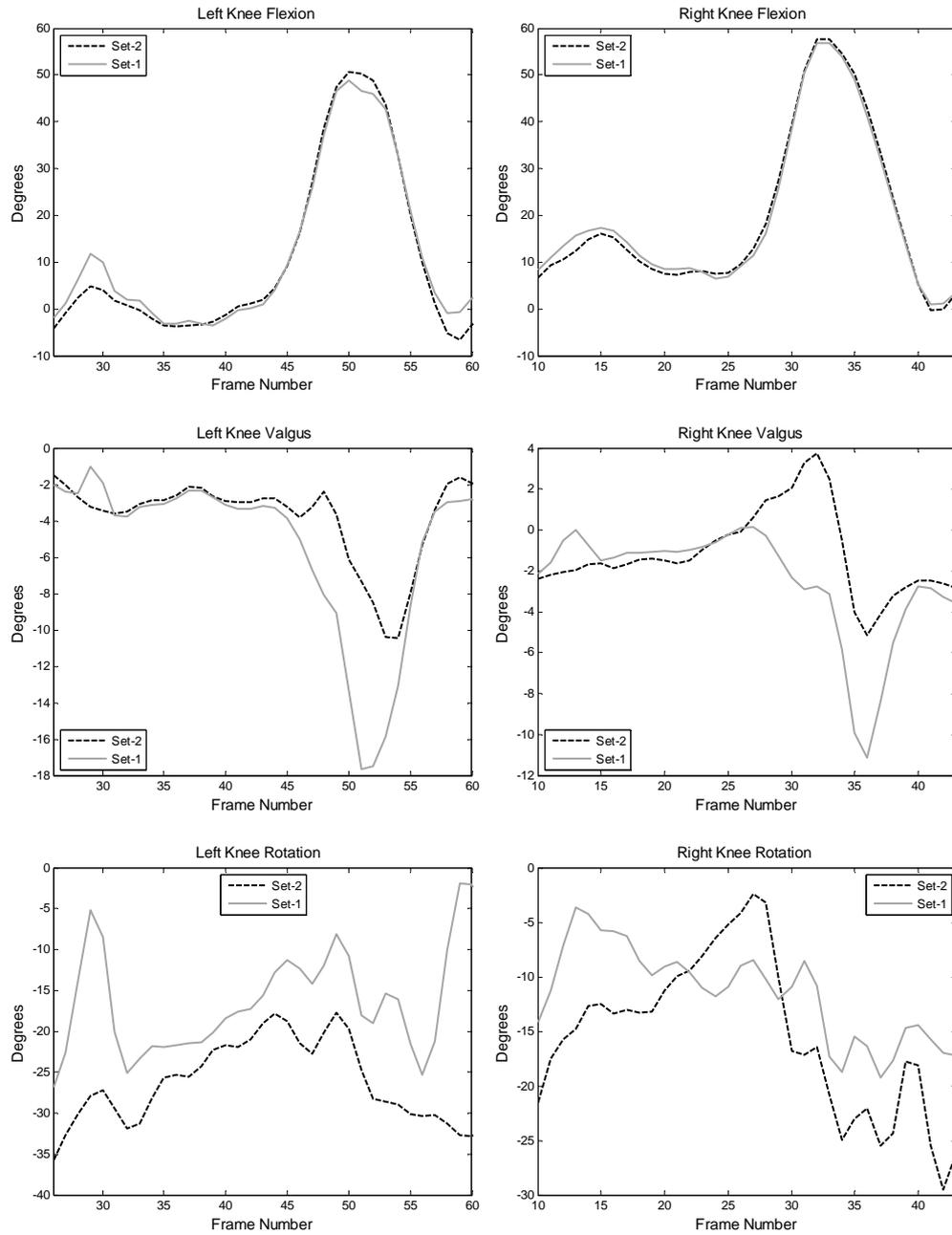
Knee Angles

Figure C.14 Knee Angles for 21st Trial of Subject GK

165

Foot Angles

Figure C.15 Foot Angles for 21st Trial of Subject GK

C.2.6 Subject GK, Trial 22

__Hip Angles__
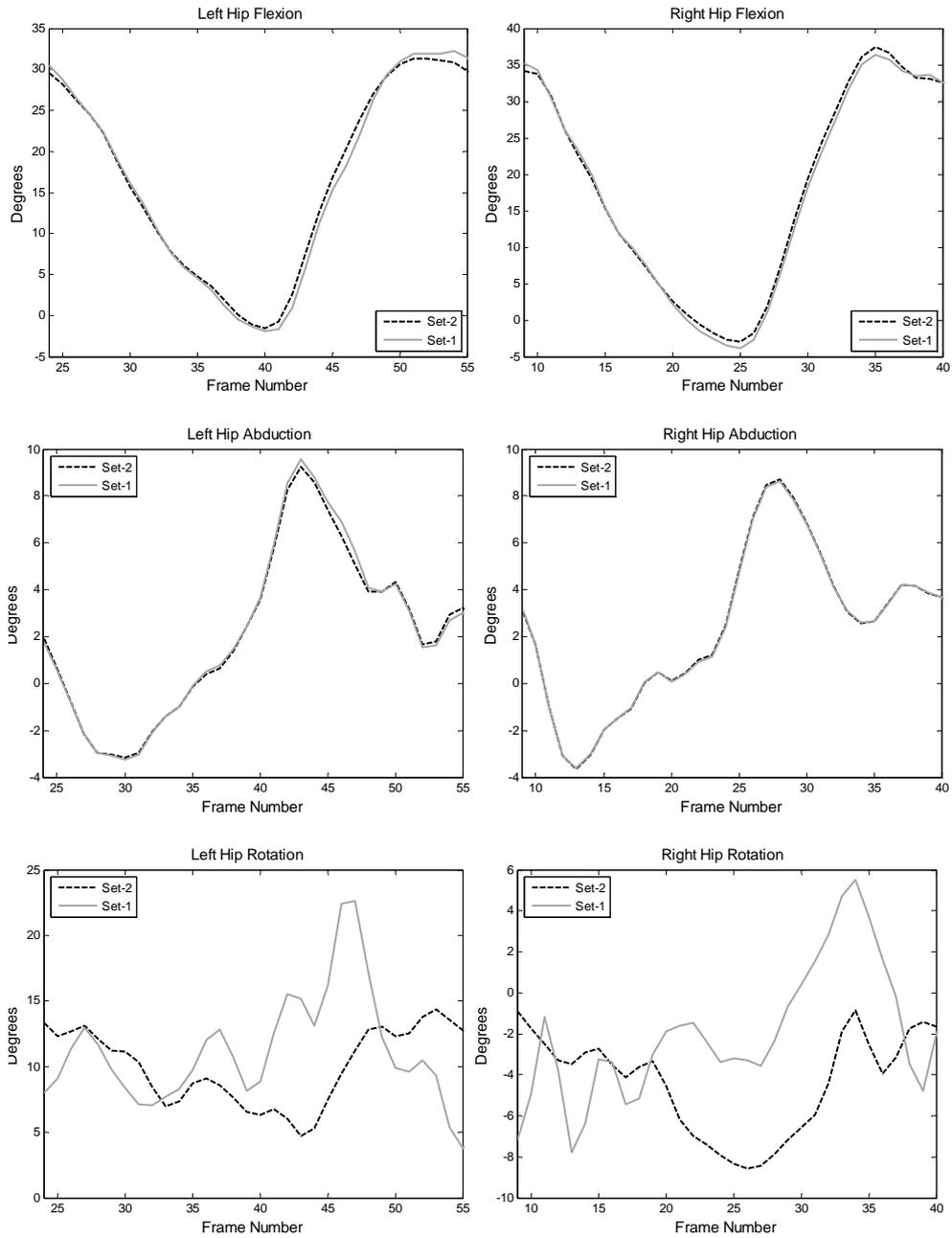
Figure C.16 Hip Angles for 22nd Trial of Subject GK
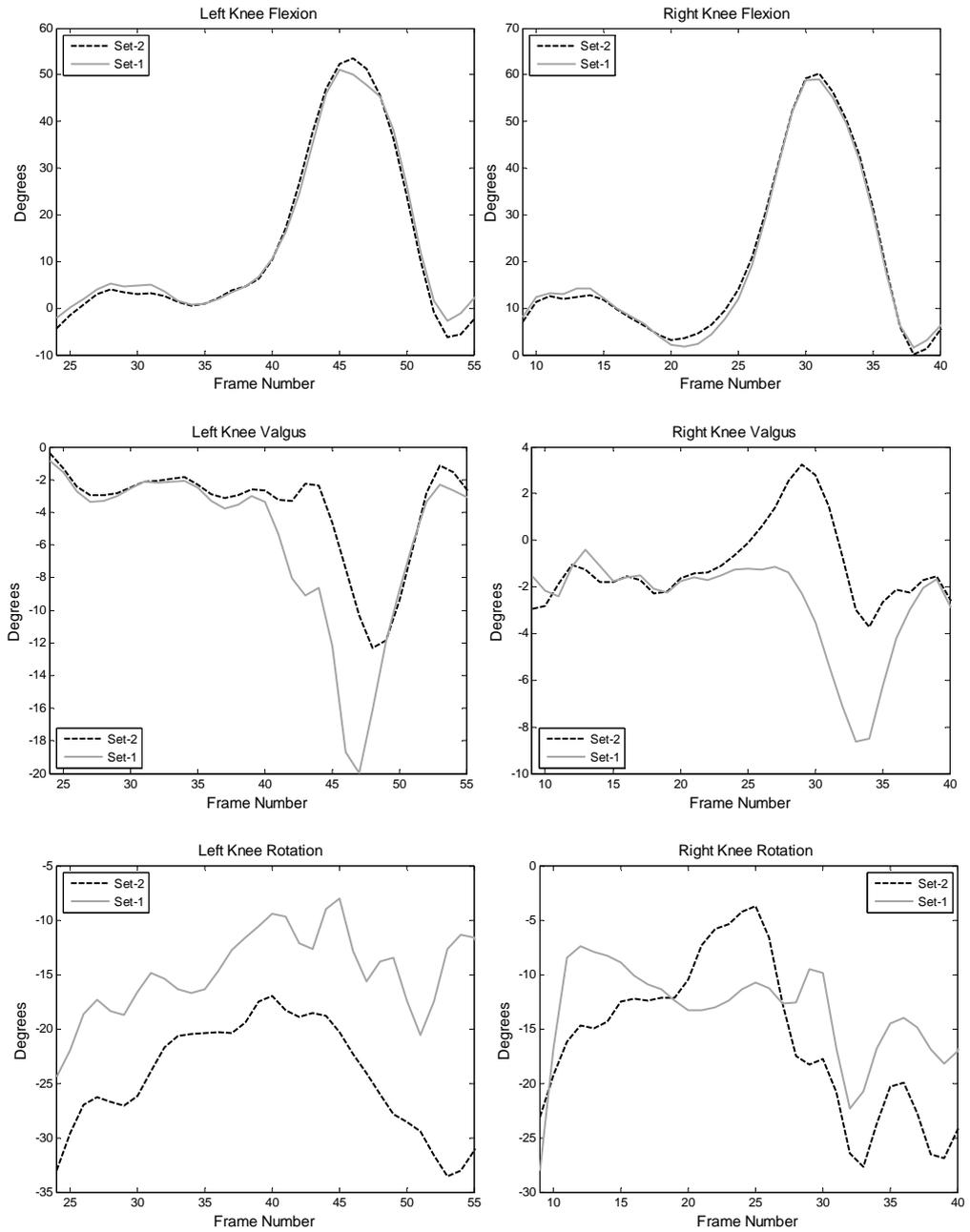
Knee Angles

Figure C.17 Knee Angles for 22nd Trial of Subject GK

Foot Angles
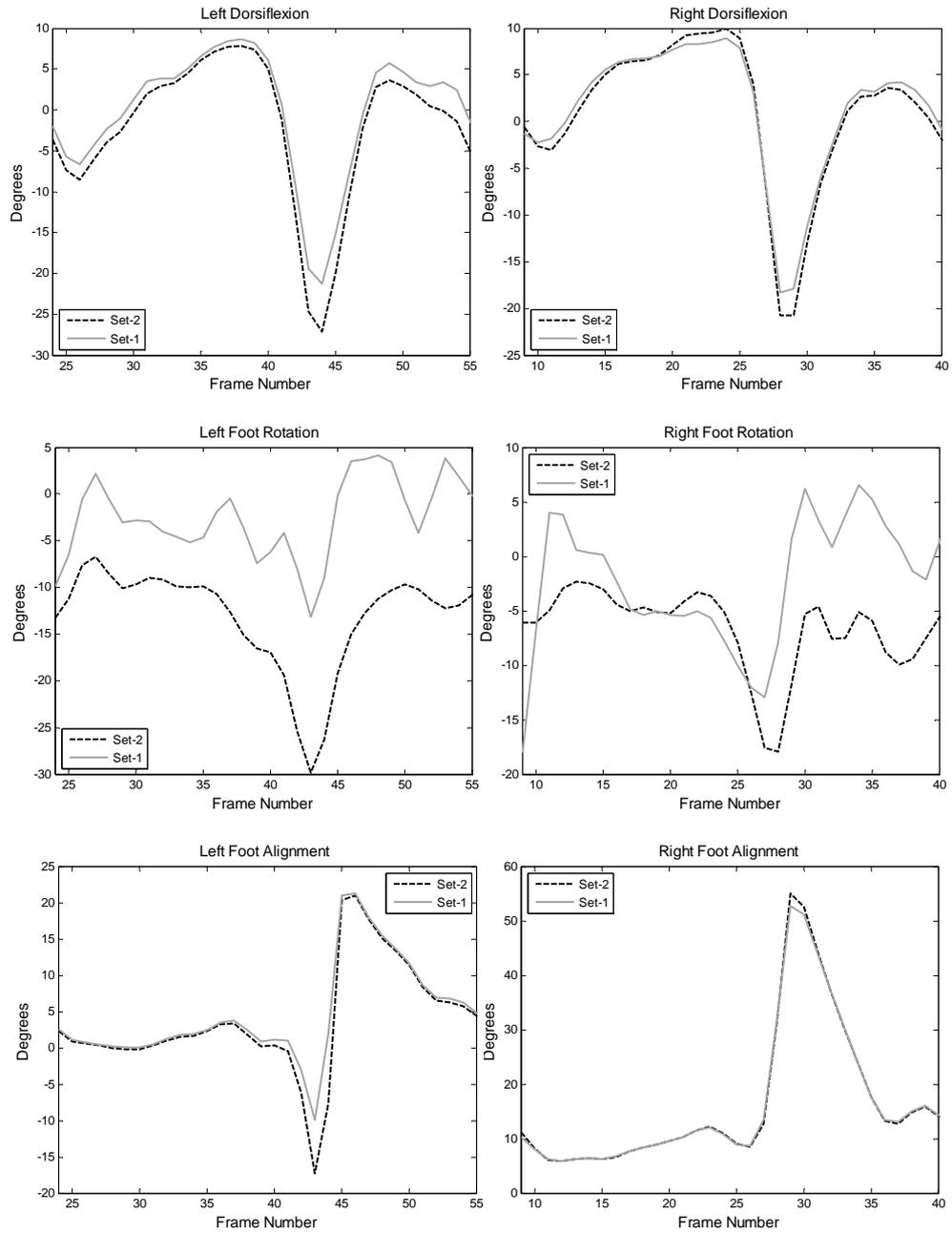
Figure C.18 Foot Angles for 22nd Trial of Subject GK

C.2.7 Subject KU, Trial 15

Hip Angles
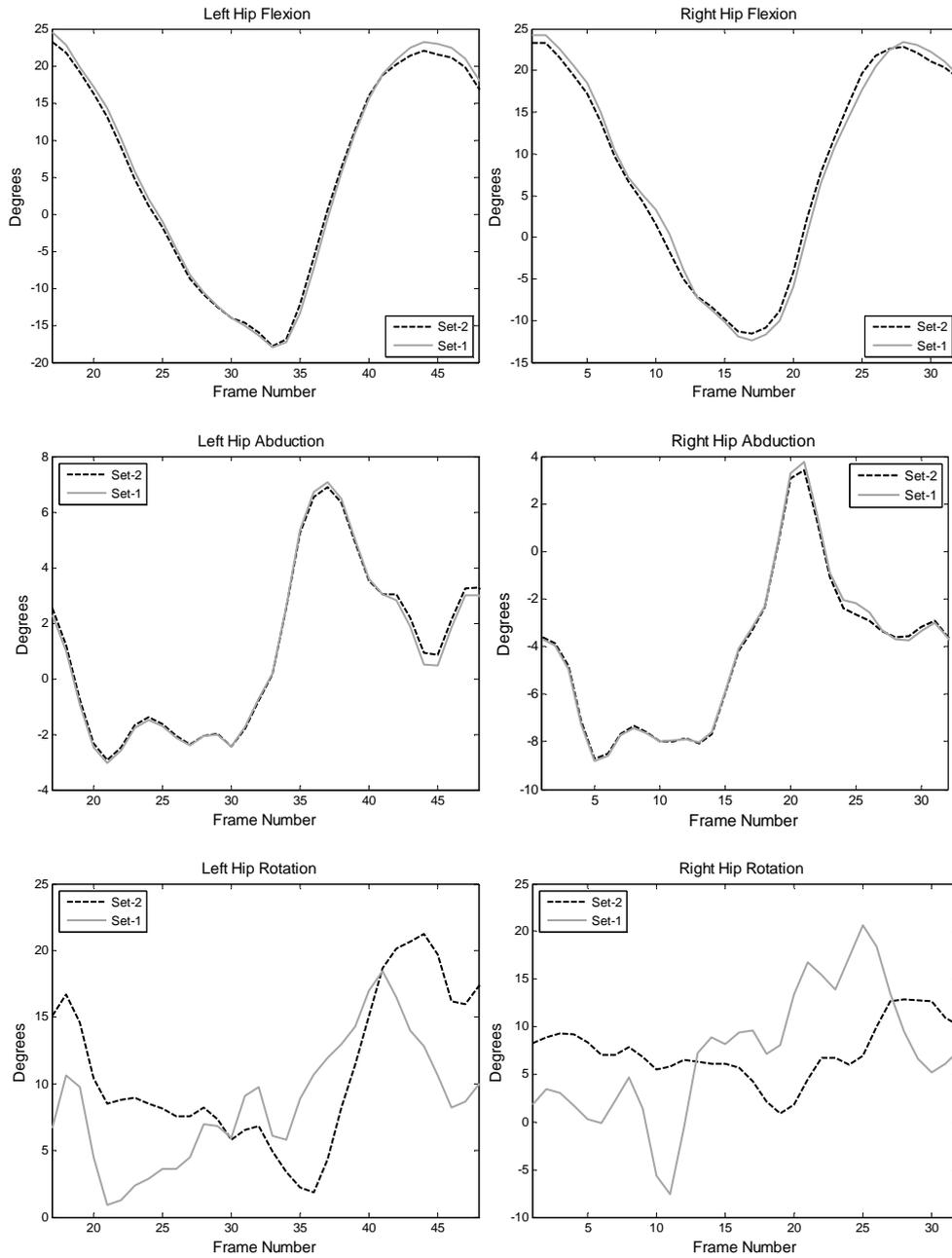
Figure C.19 Hip Angles for 15th Trial of Subject KU
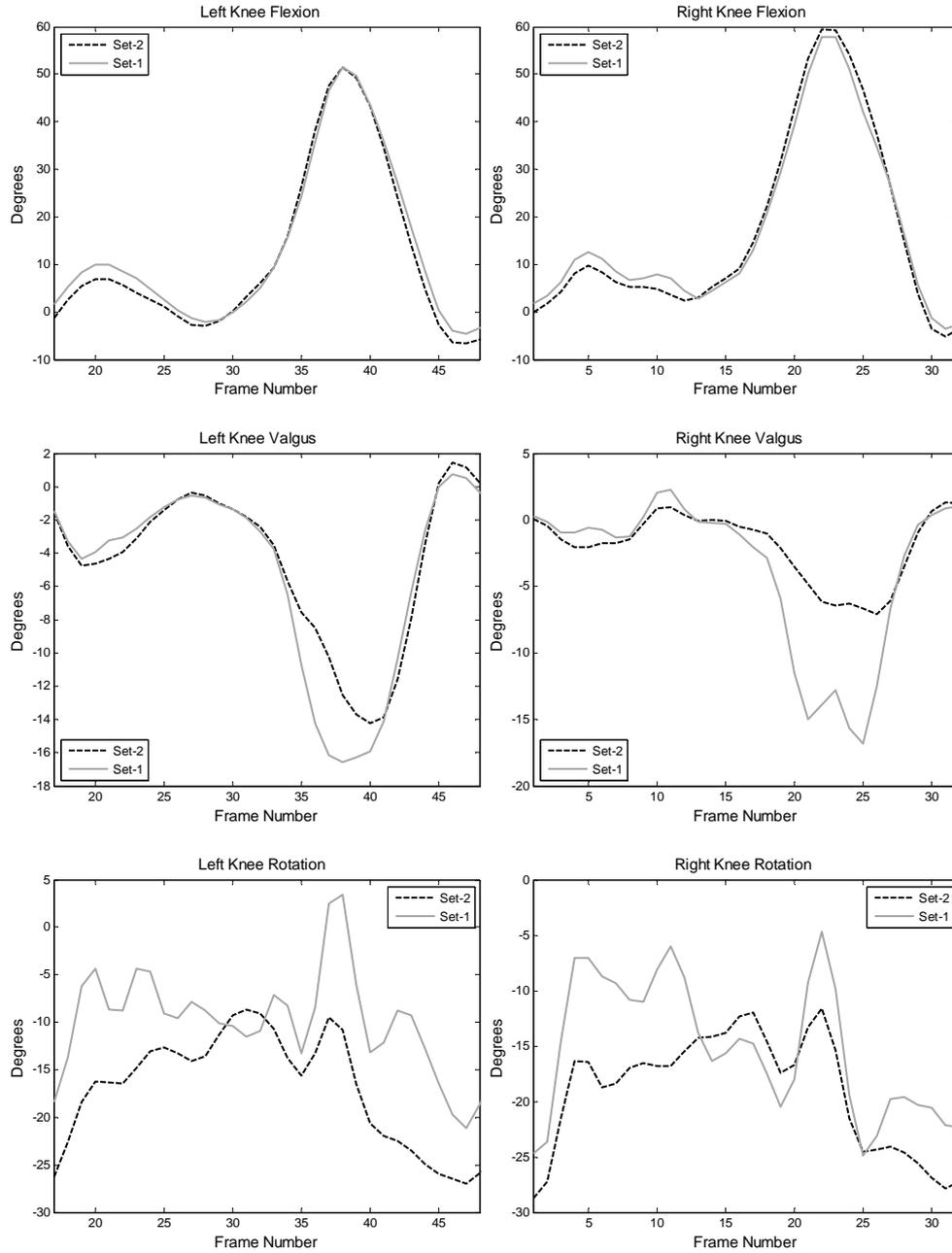
Knee Angles

Figure C.20 Knee Angles for 15th Trial of Subject KU
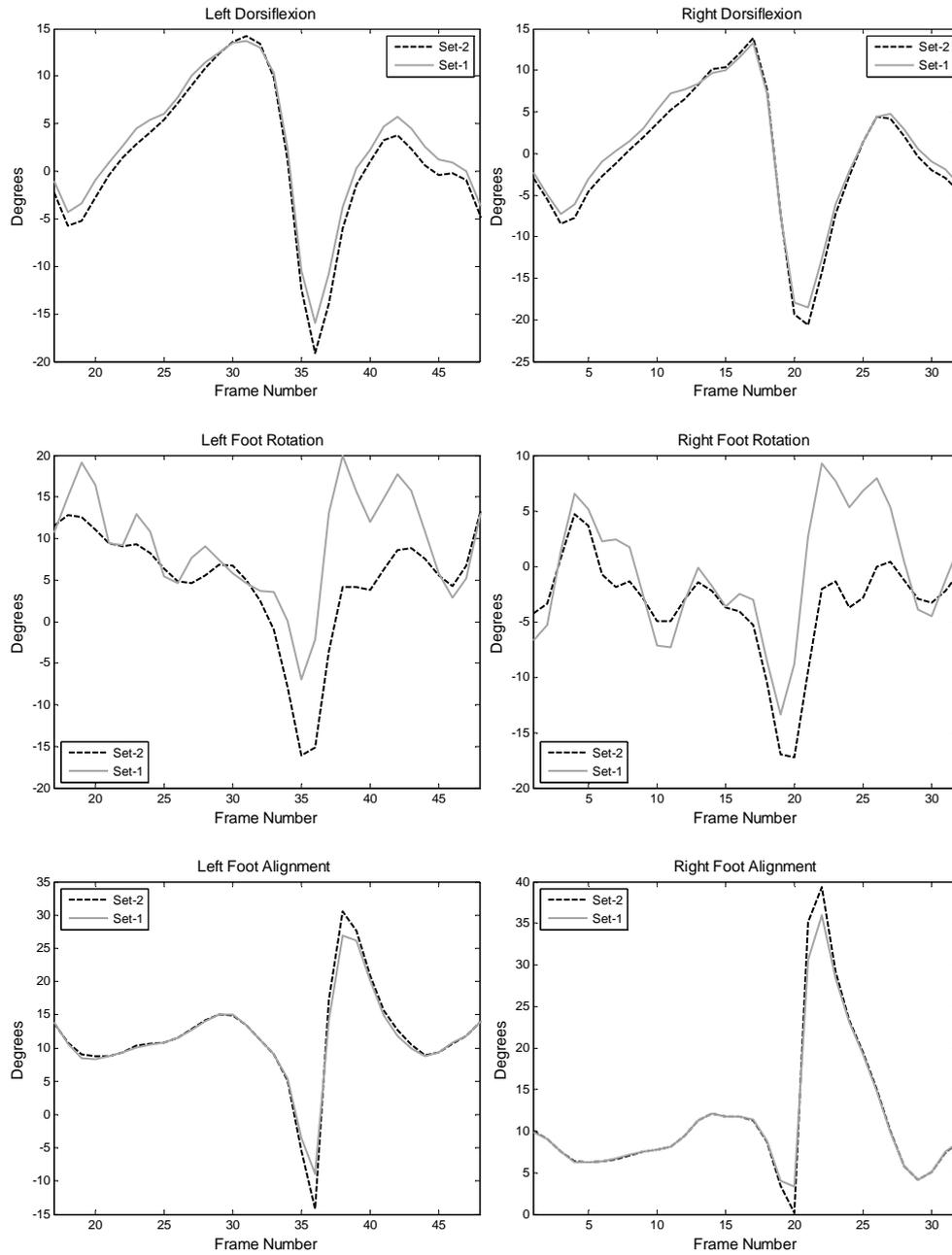
Foot Angles

Figure C.21 Foot Angles for 15th Trial of Subject KU

C.2.8 Subject KU, Trial 18

Hip Angles
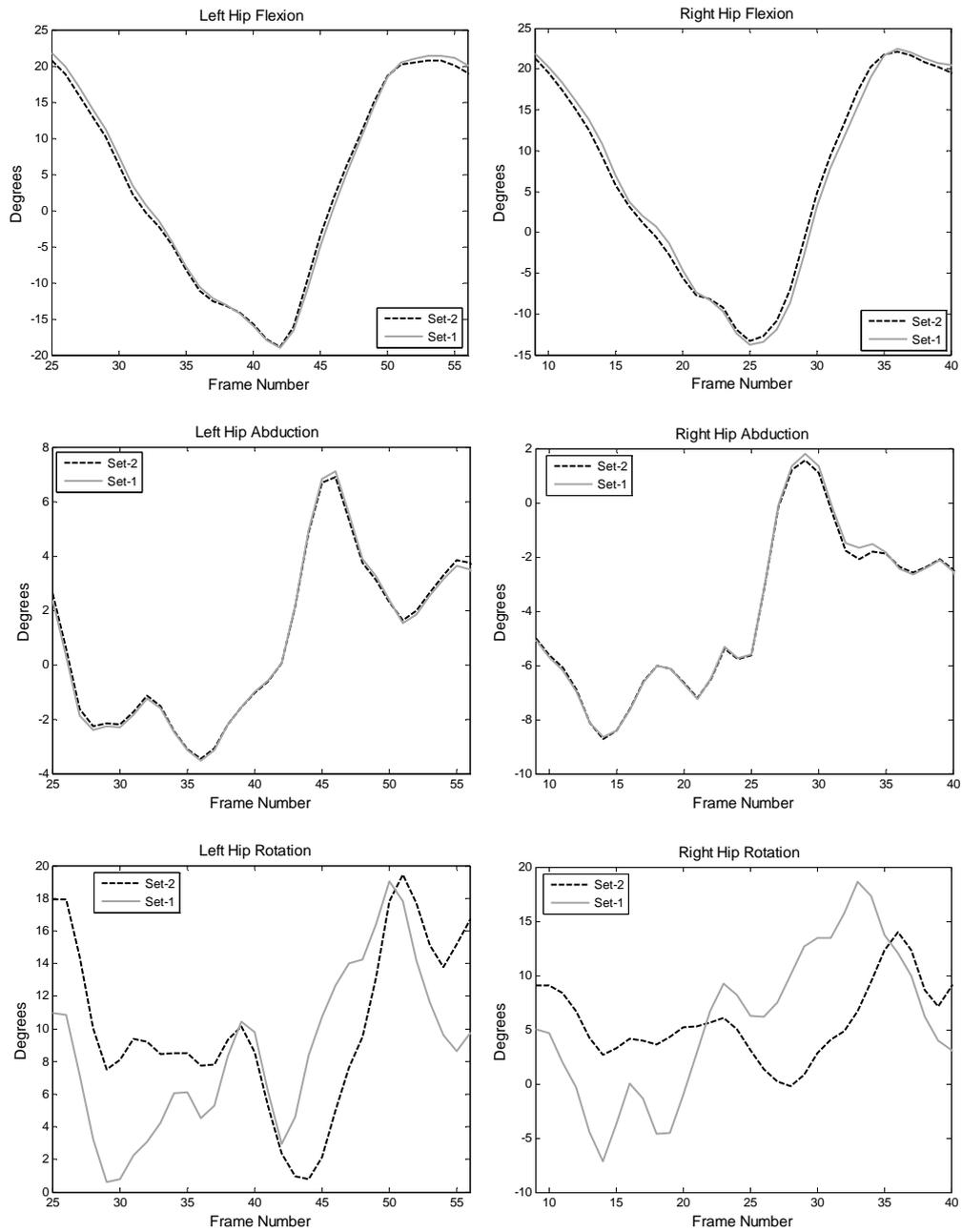
Figure C.22 Hip Angles for 18th Trial of Subject KU
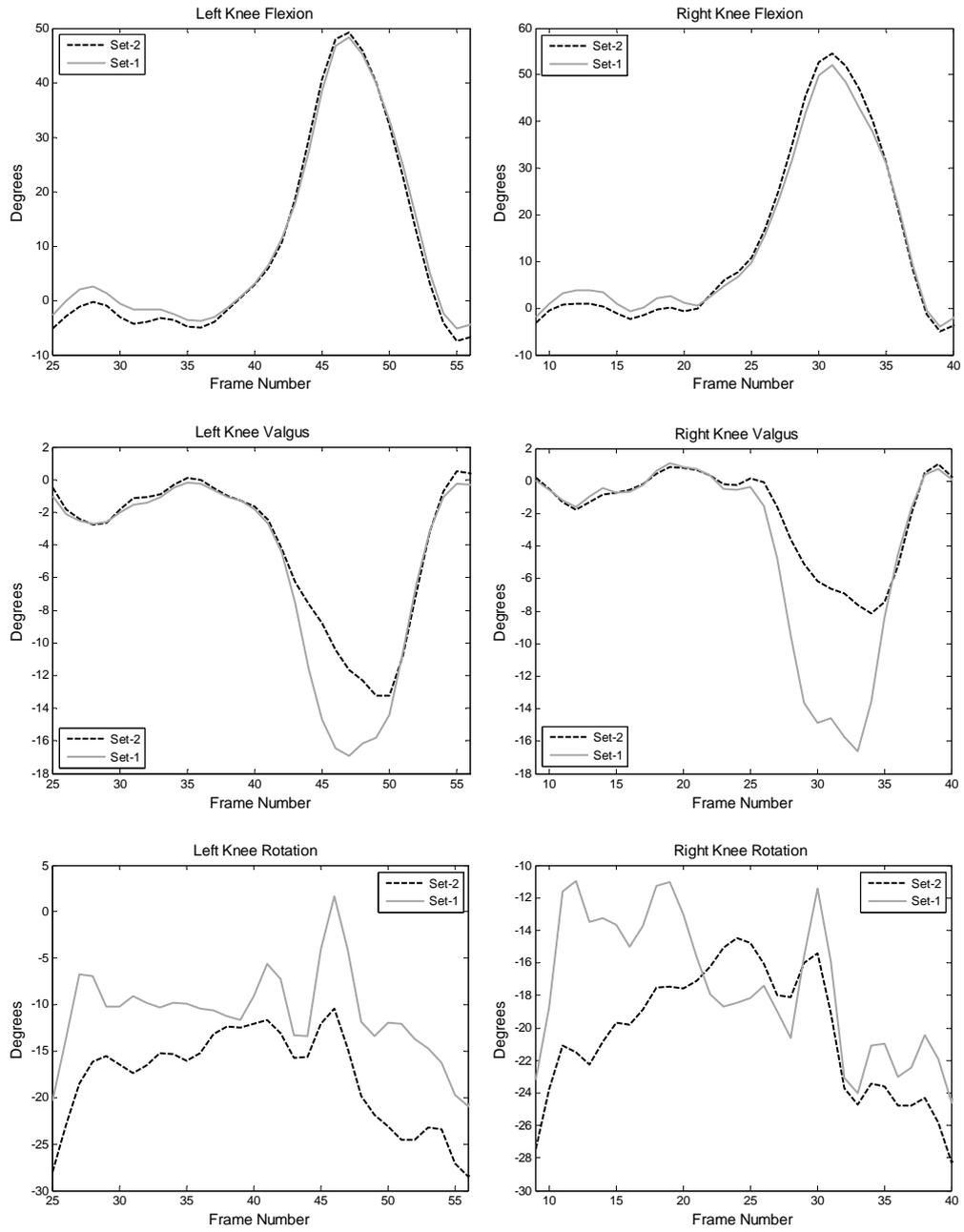
Knee Angles

Figure C.23 Knee Angles for 18th Trial of Subject KU

174
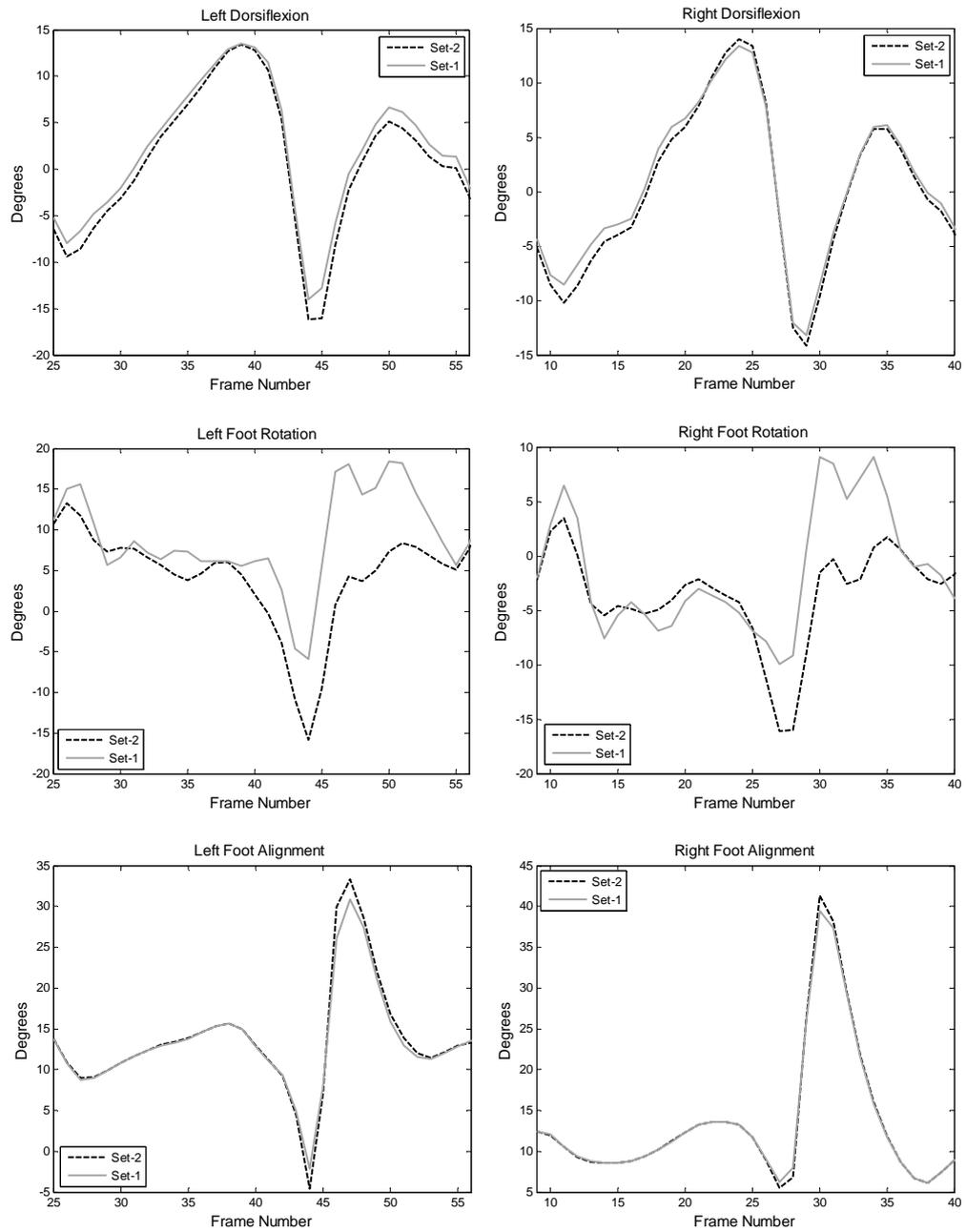
Foot Angles

Figure C.24 Foot Angles for 18th Trial of Subject KU

C.2.9 Subject KU, Trial 19

Hip Angles
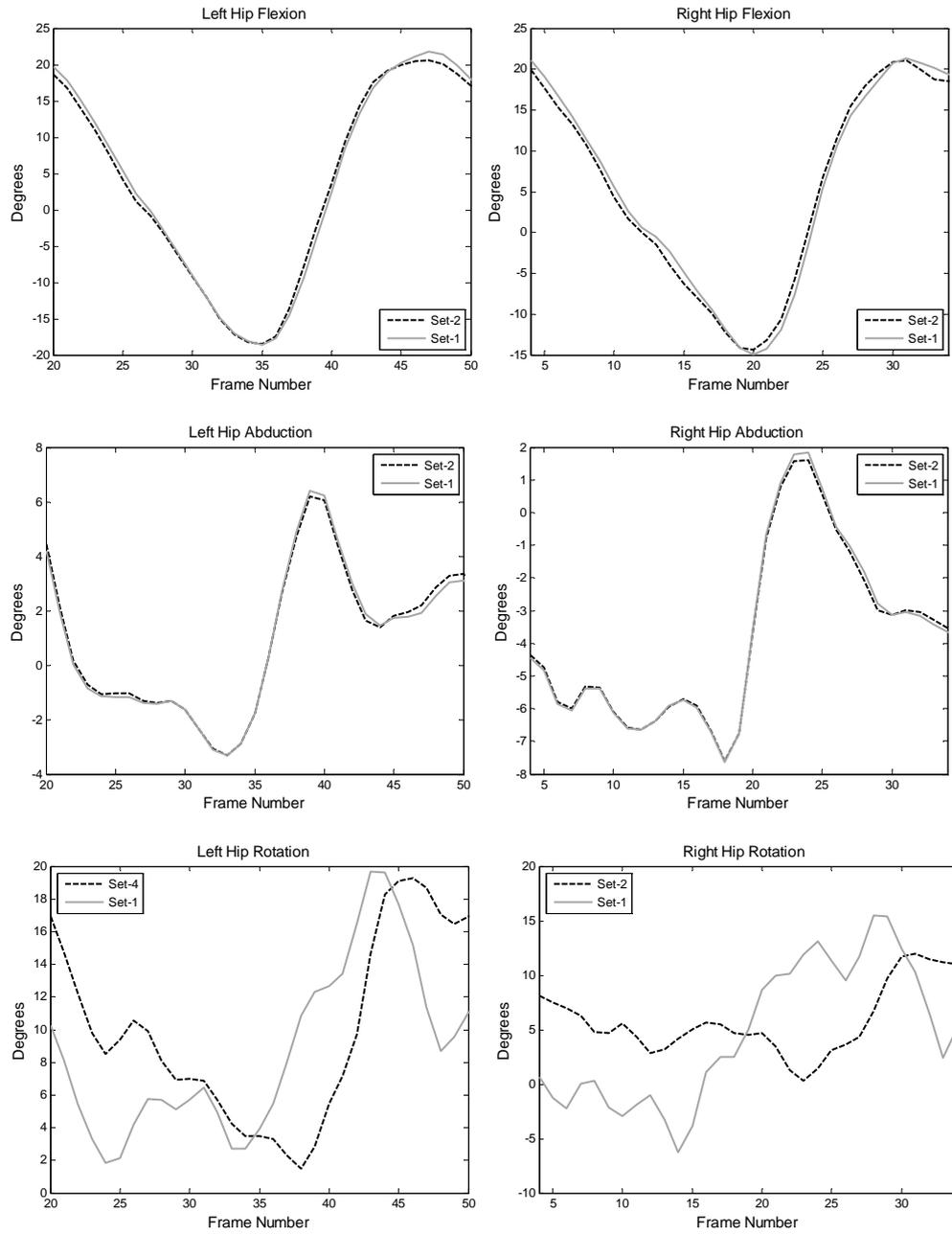
Figure C.25 Hip Angles for 19th Trial of Subject KU
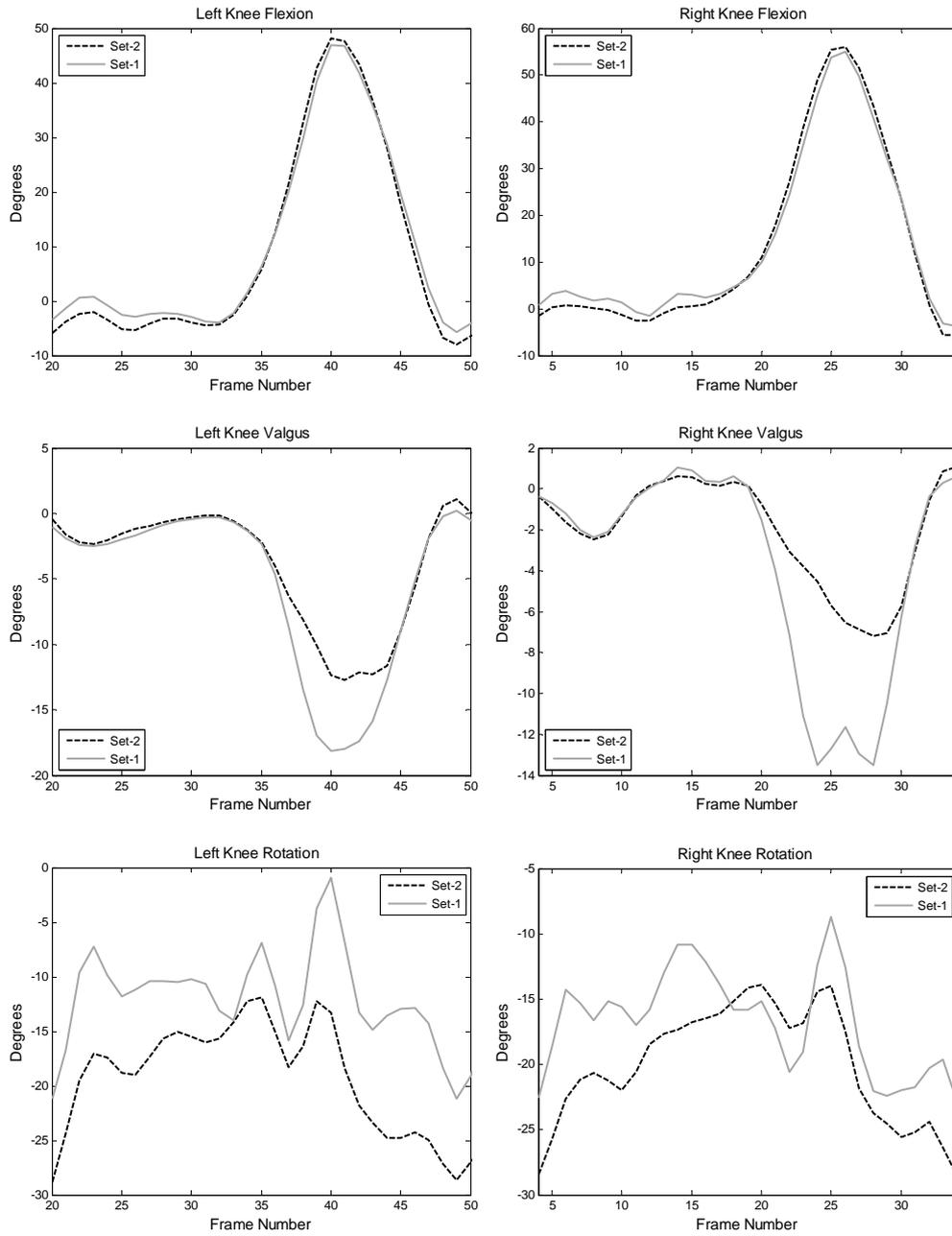
Knee Angles

Figure C.26 Knee Angles for 19th Trial of Subject KU
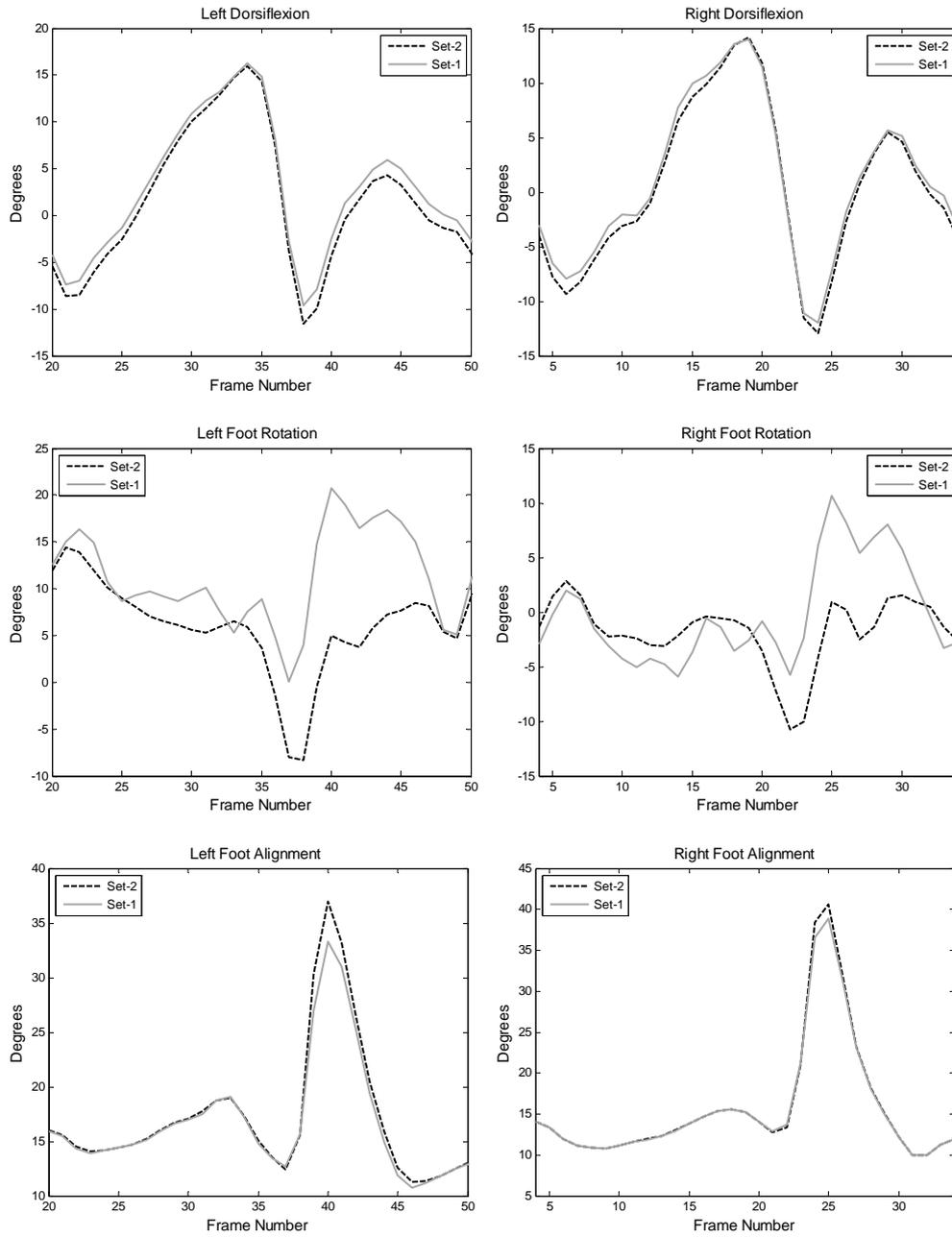
Foot Angles

Figure C.27 Foot Angles for 19th Trial of Subject KU

178

APPENDIX D

RAW KNEE VALGUS/VARUS PLOTS
WITH DIFFERENT DATA SETS

Knee valgus/varus angle plots of different data sets (Table 5.1) are presented in this section, for one selected trial of each subject.

D.1 Subject ED, Trial 18
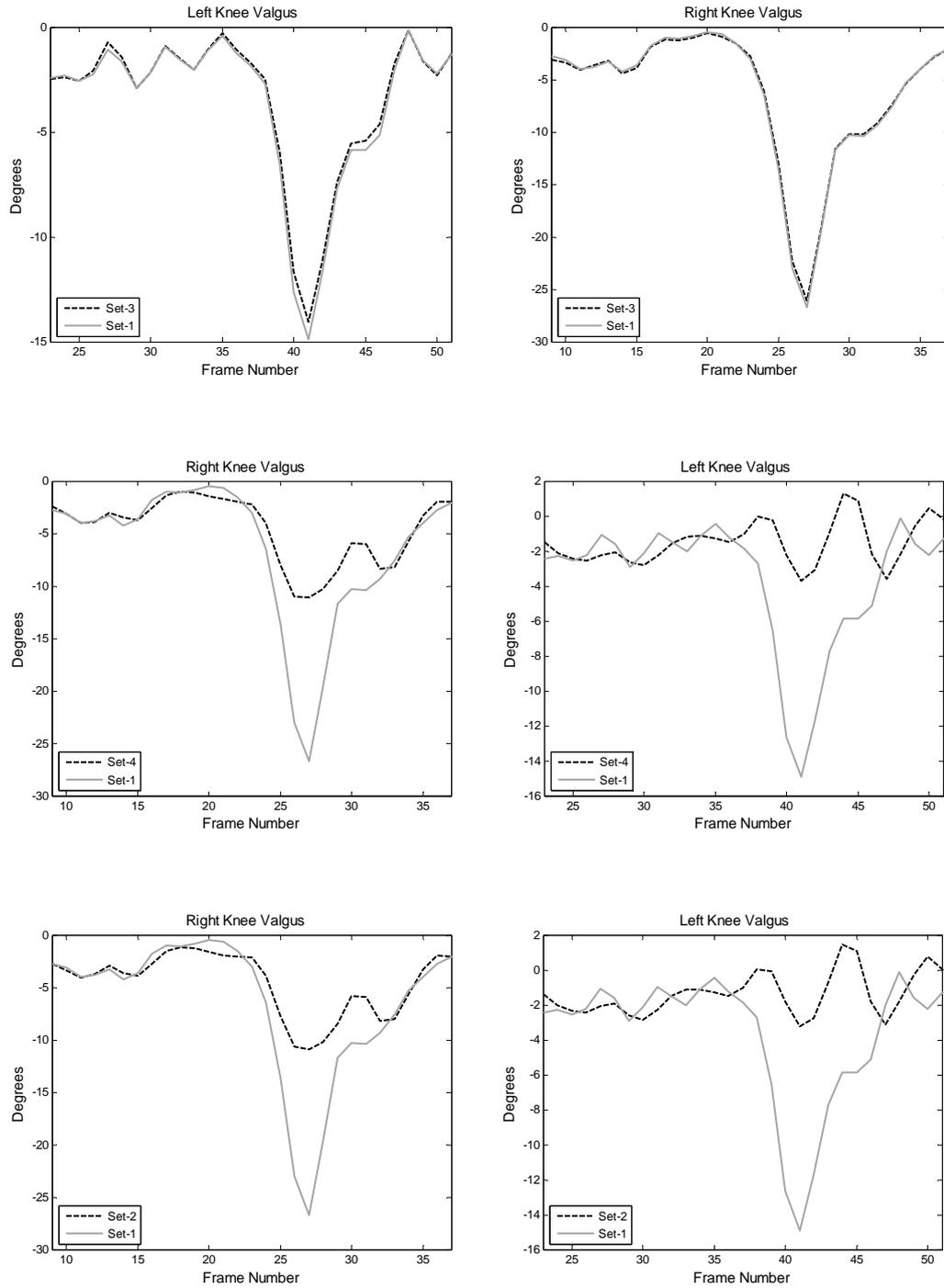
Figure D.1 Knee Valgus/Varus Angles for 18th Trial of Subject ED

D.2 Subject GK, Trial 22
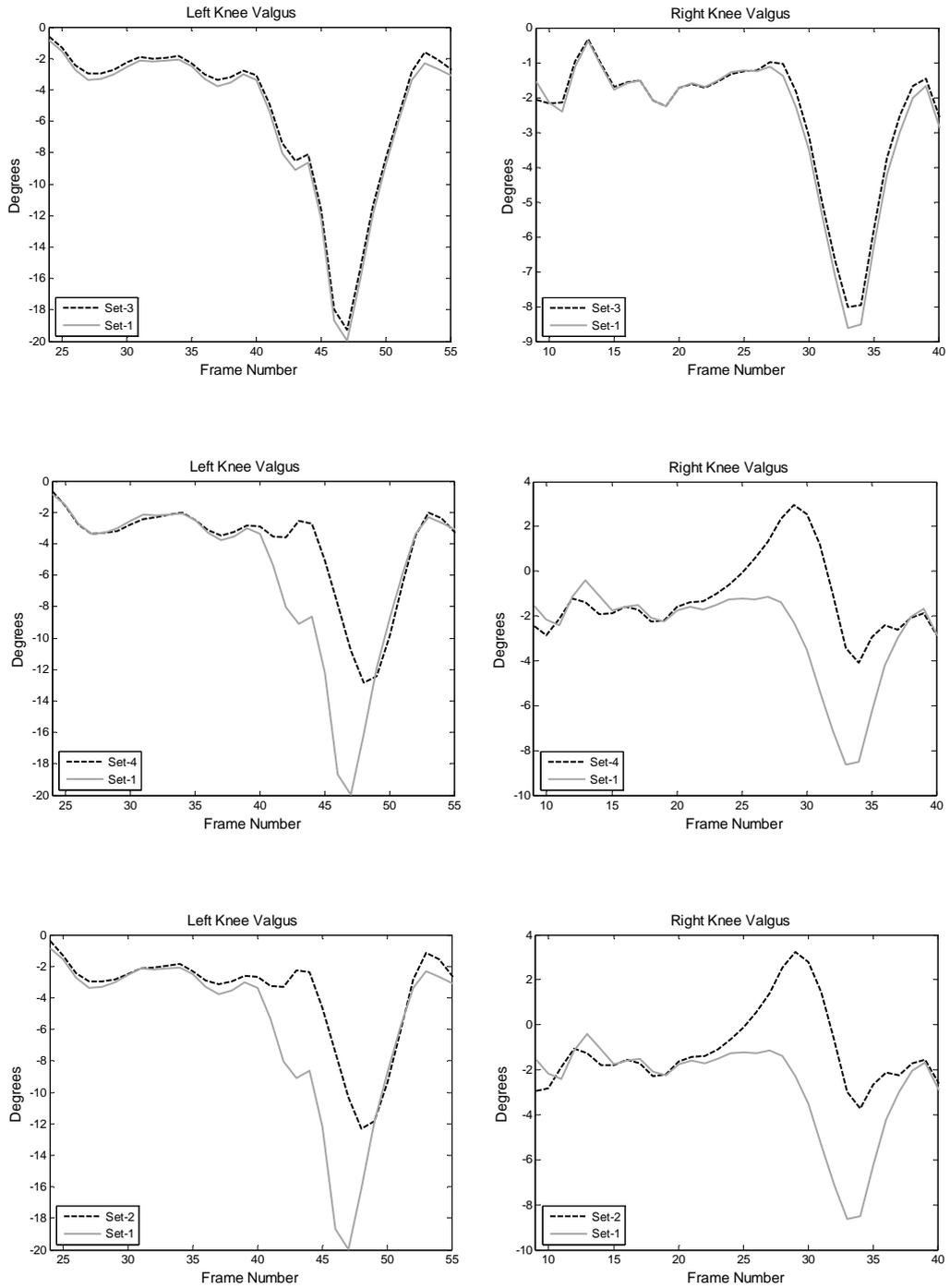
Figure D.2 Knee Valgus/Varus Angles for 22nd Trial of Subject GK

D.3 Subject KU, Trial 19
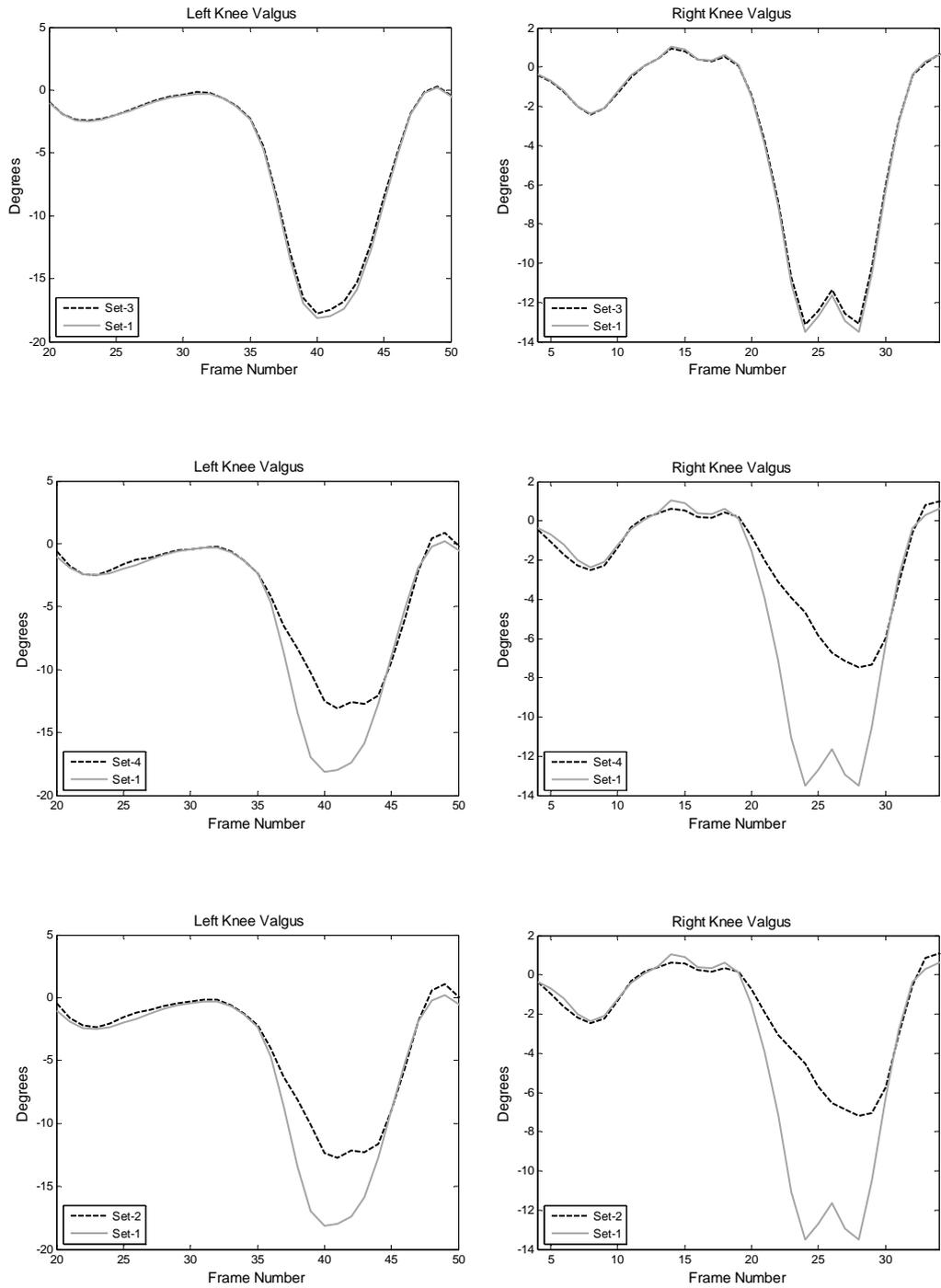
Figure D.3 Knee Valgus/Varus Angles for 19th Trial of Subject KU

APPENDIX E

SET-1 AND SET-4 RESULTS

Calculated root mean square errors of reference frames, knee-hip joint center distances and thigh segment α angles of data sets 1 and 4 are presented below for one selected trial of each subject.

E.1 Subject ED, Trial 18
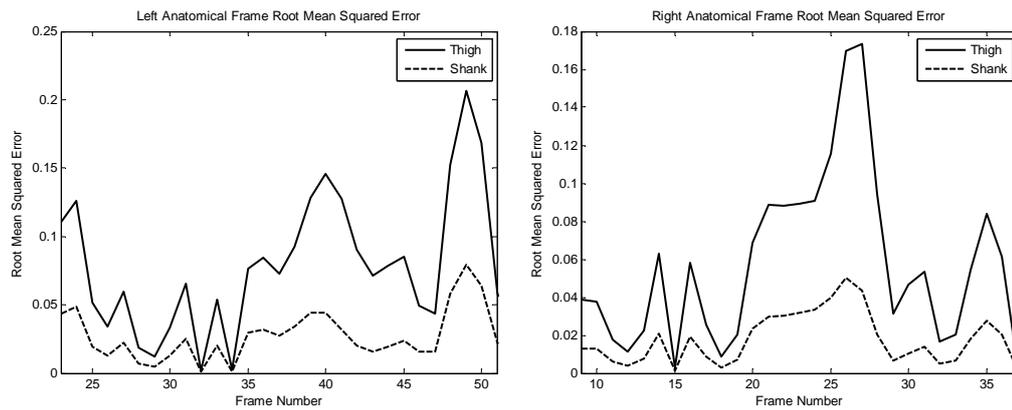
Figure E.1 Anatomical Frame Root Mean Squared Errors
for 18th Trial of Subject ED
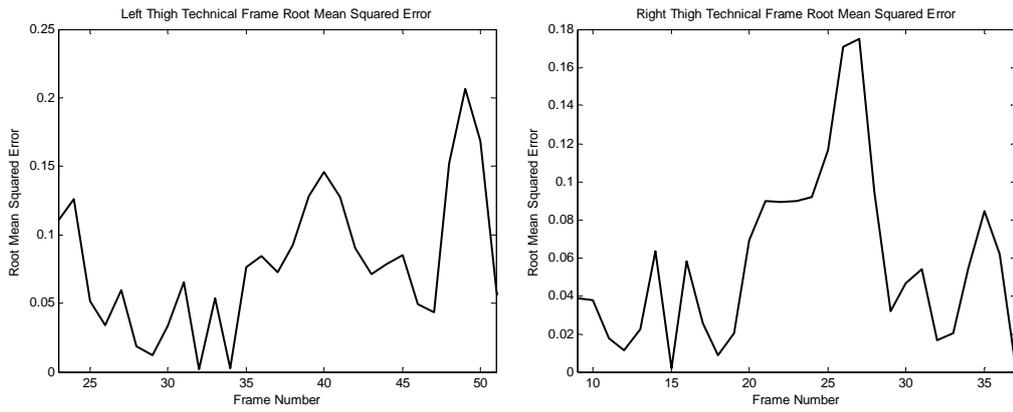
Figure E.2 Technical Frame Root Mean Squared Errors

for 18th Trial of Subject ED
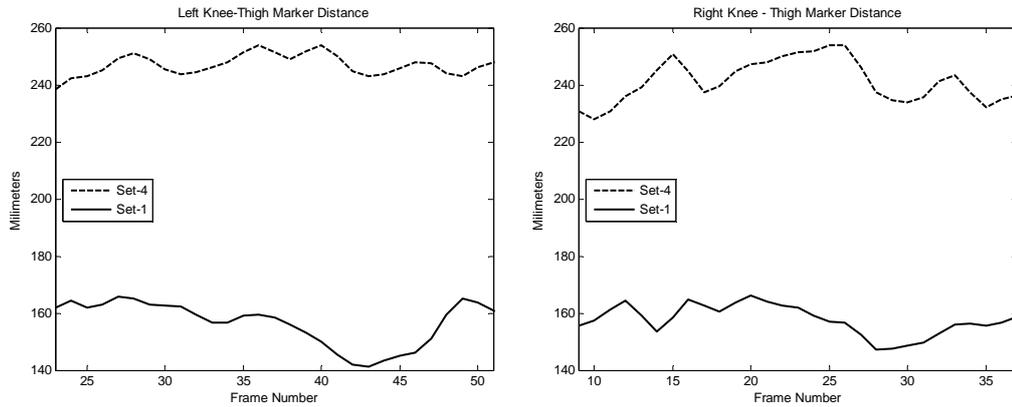
Figure E.3 Knee-Thigh Marker Distances for 18th Trial of Subject ED

184
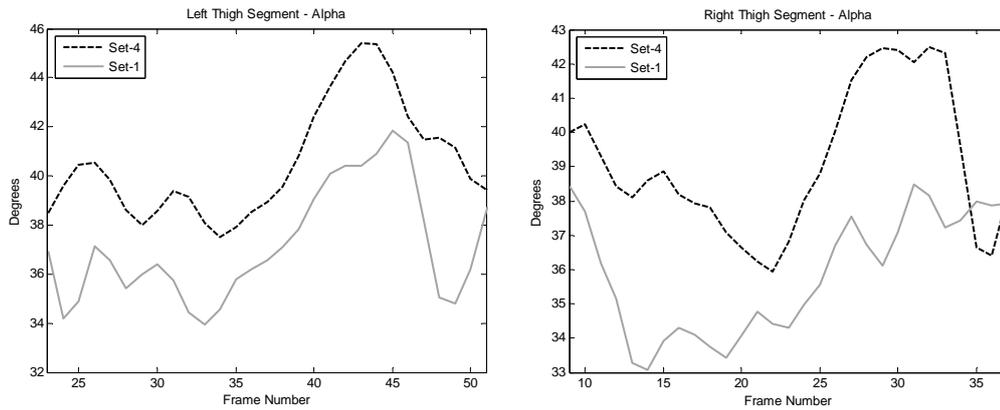
Figure E.4 Thigh Segment Angle, α for 18th Trial of Subject ED

Table E.1 Mean and Standard Deviation of Knee-Thigh Marker Distances for
18th Trial of Subject ED

Knee-Thigh Marker Distance	Mean (Millimeters)	Standard Deviation (Millimeters)
Right Segment, Set-1	157,50	5,21
Right Segment, Set-4	240,28	6,92
Left Segment, Set-1	156,00	7,93
Left Segment, Set-4	246,78	4,65

Table E.2 Mean and Standard Deviation of Thigh Segment Angle, α for 18th

Trial of Subject ED

Angle between knee-thigh and knee-HJC vectors , α	Mean (Degrees)	Standard Deviation (Degrees)
Right Segment, Set 1	35,75	1,82
Right Segment, Set 4	38,74	2,08
Left Segment, Set 1	37,23	2,06
Left Segment, Set 4	40,52	2,48

E.2 Subject GK, Trial 22
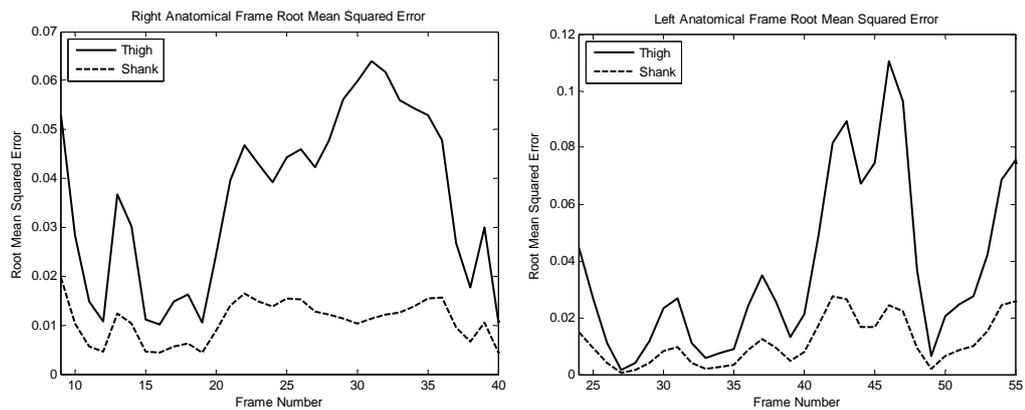
Figure E.5 Anatomical Frame Root Mean Squared Errors

for 22nd Trial of Subject GK
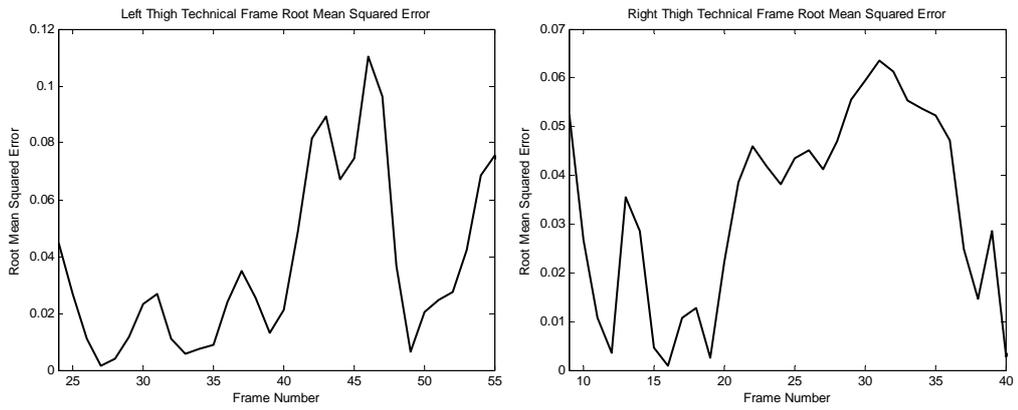
Figure E.6 Technical Frame Root Mean Squared Errors for 22nd Trial of Subject GK
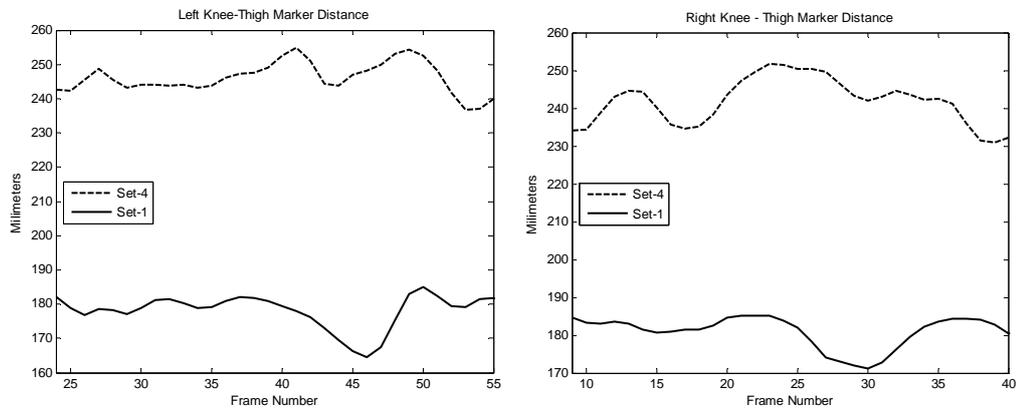
Figure E.7 Knee-Thigh Marker Distances for 22nd Trial of Subject GK
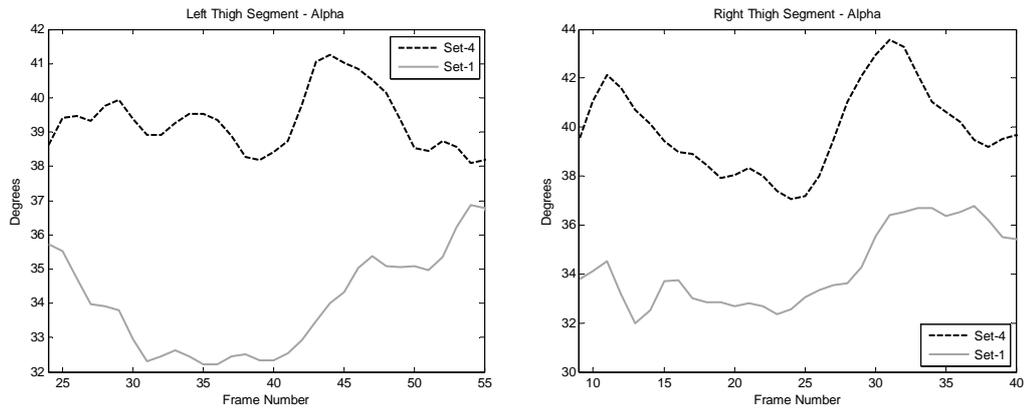
Figure E.8 Thigh Segment Angle, α for 22nd Trial of Subject GK

Table E.3 Mean and Standard Deviation of Knee-Thigh Marker Distances for
22nd Trial of Subject GK

Knee-Thigh Marker Distance	Mean (Millimeters)	Standard Deviation (Millimeters)
Right Segment, Set-1	181,27	3,93
Right Segment, Set-4	242,36	6,13
Left Segment, Set-1	178,48	4,73
Left Segment, Set-4	246,96	4,97

Table E.4 Mean and Standard Deviation of Thigh Segment Angle, α for 22nd Trial of Subject GK

Angle between knee-thigh and knee-HJC vectors , α	Mean (Degrees)	Standard Deviation (Degrees)
Right Segment, Set 1	34,1	1,81
Right Segment, Set 4	39,9	1,85
Left Segment, Set 1	33,83	1,32
Left Segment, Set 4	39,19	1,02

E.3 Subject KU, Trial 19
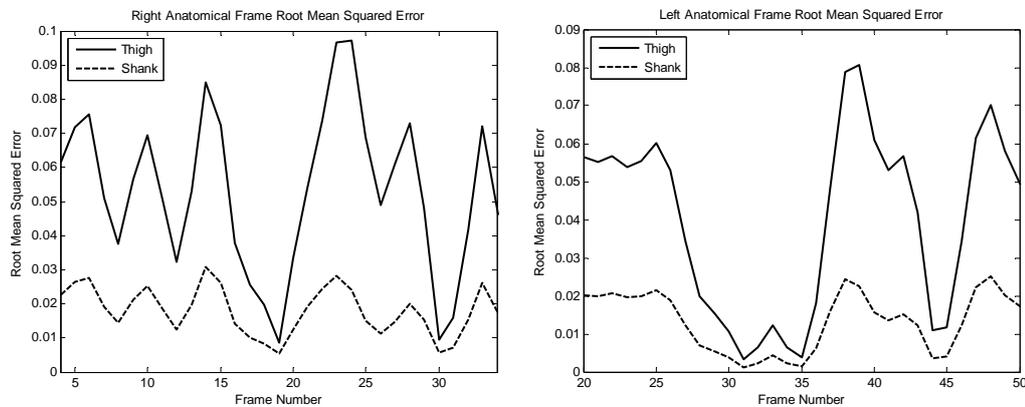
Figure E.9 Anatomical Frame Root Mean Squared Errors
for 19th Trial of Subject KU
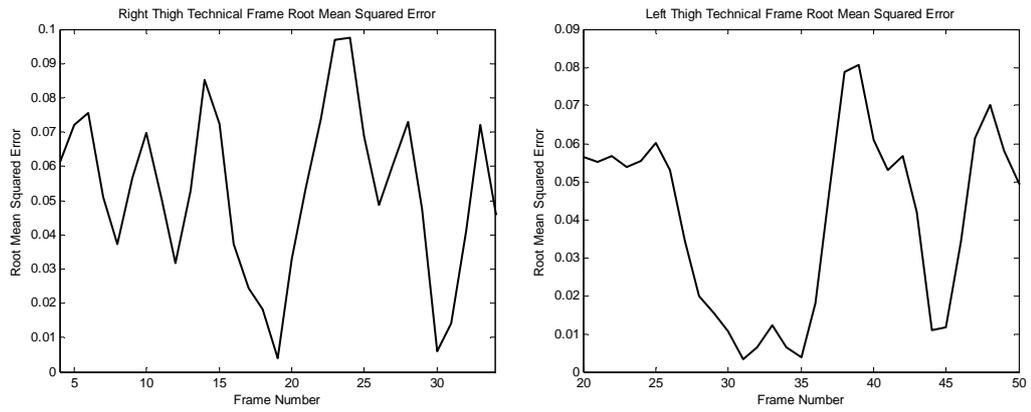
Figure E.10 Technical Frame Root Mean Squared Errors

for 19th Trial of Subject KU
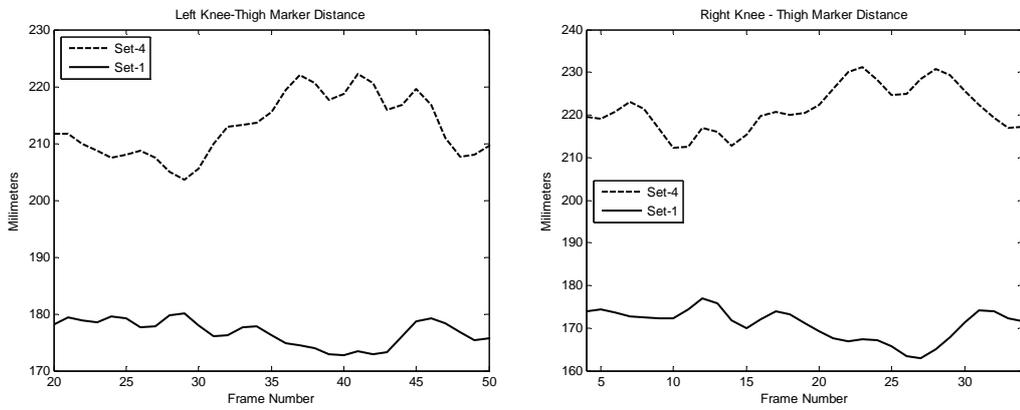
Figure E.11 Knee-Thigh Marker Distances for 19th Trial of Subject KU

190
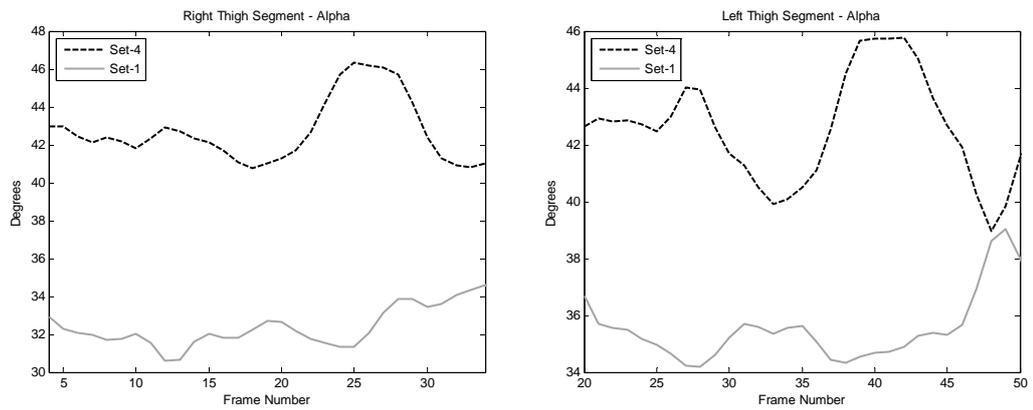
Figure E.12 Thigh Segment Angle, α for 19th Trial of Subject KU

Table E.5 Mean and Standard Deviation of Knee-Thigh Marker Distances for 19th Trial of Subject KU

Knee-Thigh Marker Distance	Mean (Millimeters)	Standard Deviation (Millimeters)
Right Segment, Set-1	170,35	4,03
Right Segment, Set-4	221,43	6,12
Left Segment, Set-1	177,03	2,45
Left Segment, Set-4	212,86	6,07

Table E.6 Mean and Standard Deviation of Thigh Segment Angle, α for 19th Trial of Subject KU

Angle between knee-thigh and knee-HJC vectors , α	Mean (Degrees)	Standard Deviation (Degrees)
Right Segment, Set 1	32,42	1,04
Right Segment, Set 4	42,69	1,75
Left Segment, Set 1	35,54	1,18
Left Segment, Set 4	42,65	1,72

APPENDIX F

GLOSSARY

Abduction	Movement away from midline of the body in frontal plane
Adduction	Movement towards midline of the body in frontal plane
Anterior	Towards the front of the body
ASIS	Anterior Superior Iliac Spine; most anterior superior point of ilium (upper part of hip bone)
Cadence	Number of steps per minute
Distal	Away from center of the body or point of attachment of limb to the body
Dorsiflexion	Downward movement of foot in sagittal plane
Extension	Movement at a joint that increases the angle between adjacent segments
External Rotation	Rotation away from midline of the body in transverse plane

Femoral epicondyle	Bony structure on the outer sides of knee
Femur	Long bone of the upper leg
Flexion	Movement at a joint that decreases the angle between adjacent segments
Frontal (Coronal) Plane	Plane that divides human body into front and back portions
Gait	Manner or style of human walking
Gait Analysis	Scientific description of human walking
Gait Cycle	Series of movements between two successive gait events of the same foot
Greater Trochanter	Bony area on the lateral and proximal end of femur
Heel Strike	Gait event denoting first contact of foot with the ground
Inferior	Away from the head or towards the lower part of the body
Internal Rotation	Rotation towards midline of the body in transverse plane

Lateral	Away from the midline; towards outer side of the body
Malleolus (pl. Malleoli)	Rounded projection on both sides of the ankle joint
Medial	Towards the center/midline of the body
Metatarsal	Any bone of foot between ankle and toes
Pelvis	Bony structure of hip area
Plantar Flexion	Upward movement of foot in sagittal plane
Posterior	Towards the back of the body
Proximal	Towards center of the body or point of attachment of limb to the body
Sacrum	Triangular bone at the base of the spine
Sagittal Plane	Plane that divides human body into right and left portions
Shank	Part of human leg between knee and ankle
Stance	Period of gait where foot is in contact with the ground

Step Length	Distance between successive heel strikes of opposite feet
Stereophotogrammetry	Motion capture
Stride Length	Distance between two successive heel strikes of the foot
Superior	Towards the head or upper part of the body
Swing	Period of gait where foot is not in contact with the ground
Thigh	Part of human leg between hip and knee
Tibia	Larger bone of the lower human leg
Toe-Off	Gait event denoting removal of foot from the ground
Transverse Plane	Plane that divides human body into upper and lower portions
Valgus	Turning outward away from midline of the body in frontal plane
Varus	Turning inward towards midline of the body in frontal plane